

## **General Disclaimer**

### **One or more of the Following Statements may affect this Document**

- This document has been reproduced from the best copy furnished by the organizational source. It is being released in the interest of making available as much information as possible.
- This document may contain data, which exceeds the sheet parameters. It was furnished in this condition by the organizational source and is the best copy available.
- This document may contain tone-on-tone or color graphs, charts and/or pictures, which have been reproduced in black and white.
- This document is paginated as submitted by the original source.
- Portions of this document are not fully legible due to the historical nature of some of the material. However, it is the best reproduction available from the original submission.

NSG-1467

(NASA-CR-162343) AN EXPERIMENTAL STUDY OF  
THE NOISE GENERATING MECHANISMS IN  
SUPERSONIC JETS Final Report, 15 Nov. 1977  
- 31 Oct. 1979 (Oklahoma State Univ.,  
Stillwater.) 67 p HC A04/MF A01

N79-33967

Unclas  
35893



# SCHOOL OF MECHANICAL AND AEROSPACE ENGINEERING

OKLAHOMA STATE UNIVERSITY

FINAL  
REPORT

AN EXPERIMENTAL STUDY OF THE NOISE  
GENERATING MECHANISMS IN  
SUPERSONIC JETS

by

Dennis K. McLaughlin

FINAL REPORT

To NASA Langley Research Center

October 31, 1979

AN EXPERIMENTAL STUDY OF THE NOISE  
GENERATING MECHANISMS IN SUPERSONIC JETS

FINAL REPORT  
TO NASA LANGLEY RESEARCH CENTER  
PERIOD: NOVEMBER 15, 1977 TO OCTOBER 31, 1979

by

Dennis K. McLaughlin

Principal Investigator

School of Mechanical and Aerospace Engineering  
Oklahoma State University  
Stillwater, Oklahoma 74074

NASA Technical Officer: Dr. J. M. Seiner  
Acoustics and Noise Reduction Division

NASA Grants Officer: Mr. F. S. Kawalkiewicz

## ABSTRACT

Flow fluctuation measurements with normal and X-wire hot-wire probes and acoustic measurements with a traversing condenser microphone were carried out in small air jets in the Mach number range from  $M = 0.9$  to  $2.5$ . One of the most successful studies involved a moderate Reynolds number  $M = 2.1$  jet. The major accomplishments of this part of the study included measurements to characterize the large scale turbulence properties in the jet, and near field microphone measurements to characterize the noise radiation. The measurements were interpreted in a manner which shed light on the physics of supersonic jet noise.

A parallel study involved similar measurements on a low Reynolds number  $M = 0.9$  jet. These measurements showed very clearly that there are important differences in the noise generation process of the  $M = 0.9$  jet in comparison with low supersonic Mach number ( $M \approx 1.4$ ) jets. Understanding these differences should improve our total understanding of both subsonic and supersonic jet noise. The measurements we performed provided experimental evidence which should help this understanding.

The final aspect of our experimental study involved performing X-wire measurements in low Reynolds number jets of  $M = 2.1$  and  $2.5$ . Although there were some problems with these measurements (primarily involving poor probe resolution) which have yet to be resolved some valuable experience was obtained with the X-wires. Preliminary measurements indicate that the X-wire technique will be invaluable in obtaining data to help theoreticians formulating a comprehensive analysis of the instability development and its associated radiated noise.

In addition to the measurements outlined above, some facility development in installing a surplus vacuum pump was undertaken. Some continued effort is needed on this project to render the pump operational for experiments. When operational the increased vacuum pump capability will allow larger jets to be run, and probe resolution difficulties will be reduced.

## TABLE OF CONTENTS

ABSTRACT	
I. INTRODUCTION	1
1.1 Summary list of major activities proposed	1
1.2 List of facility improvement projects proposed	1
1.3 Summary of goal reorientation based on early progress and results of NSF research	1
II. SUMMARY OF SUCCESSFUL INVESTIGATIONS	3
2.1 Moderate REynolds number $M = 2.1$ jet study	3
2.2 Low Reynolds number $M = 0.9$ jet study	4
2.3 X wire measurements in low Reynolds number $M = 2.1$ and $2.5$ jets.	4
III. PROGRESS ON FACILITY IMPROVEMENT	7
IV. CONCLUSIONS	8
4.1 Publications	8
4.2 Presentations	9
REFERENCES:	10
Attachment #1	
Attachment #2	
Attachment #3	

## I. INTRODUCTION

Listed below are the major experimental activities proposed as well as the facility development planned to be undertaken with the NASA grant sponsorship.

### 1.1 Major experimental activities proposed:

- 1) Flow fluctuation measurements in low to moderate Reynolds number  $M = 1.5$  to  $2.5$  jets.
- 2) Noise radiation measurements in the near field of the jets.
- 3) Flow visualization using smoke tracer and high speed motion photography.

### 1.2 Facility Improvement proposed:

- 1) Install and initiate operation of surplus Ingersoll Rand vacuum pump to increase pumping capability of system.
- 2) Construct high Reynolds number jet facility to serve as a test bed for flow visualization experiments.

### 1.3 Summary of Goal Reorientation:

During the early stages of the research results were obtained which indicated the advisability of shifting some of the priorities for the NASA sponsored research program. Some of the results were generated by experiments conducted with the National Science Foundation (NSF) grant support. The NSF grant terminated on April 15, 1978; all activity in our laboratory from that time on was supported by the current NASA grant monies.

The major shift of priorities came with our discovery that the noise generation mechanisms in low Reynolds number subsonic jets is remarkably different from the mechanisms in slightly supersonic jets (ie  $M = 1.4$ ). Since this discovery opened the potential for improved understanding of both subsonic and supersonic jet noise generation mechanisms we decided to

dedicate a portion of our time and NASA support towards completing the preliminary investigation of the  $M = 0.9$  jet.

In shifting priority to the  $M = 0.9$  jet experiments we decided to lower the priority of the flow visualization experiments. This decision was based upon two factors. First, the complications of establishing the correct lighting and the ideal amount of smoke tracer during the few seconds during which the high speed motion picture camera was to operate meant that a very substantial amount of experimental time would be required to produce photographs of reasonable quality. We were hard pressed to find this time in view of the other commitments in the research. Second, Sarohia and Massier (1) at the JPL (California Institute of Technology) had considerable recent success with high-speed Schlieren motion pictures of high speed air jets. Since Sarohia successfully identified the large scale organized structure in the jets, and related the observed structure to simultaneous nearfield noise measurements, the need for us to perform similar measurements greatly diminished.

## II. SUMMARY OF SUCCESSFUL INVESTIGATIONS

### 2.1 Moderate Reynolds Number $M = 2.1$ Jet Study.

The early parts of this study (prior to April, 1978) were supported by NSF, and the latter parts were supported by the present NASA grant. In our view, this study was completely successful, and produced experimental results which will have a far reaching impact on the aerodynamic noise field.

The study represented the first time anyone had probed a supersonic, turbulent jet with a hot-wire. In the moderate Reynolds number  $M = 2.1$  jet it was determined that the radiated noise is similar in sound pressure level, directivity and spectral content to conventional high Reynolds number turbulent jets (at  $M = 2$ ). However, in our case we were able to probe the flowfield with a normal hot-wire probe in order to measure many of the flow fluctuation properties which have a direct bearing on the noise generation process. Using this general technique, the dominant noise generation mechanism in the jet, involving the disintegration of the large scale coherent instability was identified and explored. The results of the experiments have greatly increased our understanding of the processes involved in the generation of supersonic jet noise. In addition, critical comparisons with the latest prediction method of the noise generated by large scale turbulence structure by Morris and Tam (2) were made. Such comparisons are essential to the further development of the promising jet noise analyses.

A copy of the manuscript "Measurements on the Flow and Acoustic Properties of a Moderate Reynolds Number Supersonic Jet" by T. R. Troutt and D. K. McLaughlin which has been submitted for publication to the Journal of Fluid Mechanics is attached to this report. This paper provides the details on the objectives and results of the moderate Reynolds number  $M = 2.1$  jet study.

## 2.2 Low Reynolds Number $M = 0.9$ Jet Study.

As mentioned earlier, preliminary measurements in a low Reynolds number  $M = 0.9$  jet demonstrated that the noise generation process is quite different from that of the low Reynolds number  $M = 1.4$  jet. Since this provided an opportunity to gain more understanding of noise generation processes in general we completed a preliminary study of the  $M = 0.9$  jet. The results of our measurements on the dominant noise generation process in the low Reynolds number  $M = 0.9$  jet were consistent with a vortex interaction model for subsonic jet noise first suggested by Laufer et al.(3). The predominant vortices are both helical and axisymmetric in shape and the acoustic field retains an azimuthal character consistent with the two types of vortical interactions. It appears that the dominant helical instability in the  $M = 0.9$  jet does not directly radiate noise through the growth and decay process as was determined to be the case in the low Reynolds number  $M = 1.4$  jet. Hopefully, this experimental information will be important to theoreticians devising analyses of jet noise in the low supersonic Mach number regime.

A copy of the AIAA paper "Flowfield and Acoustic Properties of a Mach Number 0.9 Jet at a Low Reynolds Number" by J. L. Stromberg, D. K. McLaughlin and T. R. Troutt is also attached to this report. This paper summarizes the important aspects of our low Reynolds number  $M = 0.9$  jet noise experiments.

## 2.3 X-Wire Measurements in Low Reynolds Number $M = 2.1$ and $2.5$ Jets.

This portion of our research was conducted wholly with NASA sponsorship. The goals of this part of the research were very ambitious. X-wires were to be used to measure the cross stream velocity fluctuations  $v'_{rms}$  as well as the major component of Reynolds stress  $\bar{\rho} \overline{u'v'}$ . (Our techniques using single normal hot wires to measure  $(\rho u)'_{rms}$  have been well established).

Suspecting that poor probe resolution would be one of the most serious difficulties we might encounter, we also planned on installing and making operational a surplus Ingersol Rand vacuum pump we had acquired for the purpose of increasing our pumping capability. As discussed in more detail later the pump did not meet the pumping requirement needs immediately. Consequently we proceeded with the X-wire measurements in the small jets, using our previously established vacuum pump. We felt it more important to perform the preliminary X-wire measurements in the small jets to establish the experience of using them in the low Reynolds number supersonic flow regime.

The X-wire measurements in the small jets have been very valuable to the progress of our research on supersonic jet noise. First a calibration procedure was developed which worked well in practice. Second, distributions of  $(\rho u)'_{rms}$ ,  $v'_{rms}$  and  $\bar{\rho} \overline{u'v'}$  were obtained at several axial locations in the  $M = 2.1$  and  $2.5$  jets (at low Reynolds numbers). The shapes of all three distributions are similar to those obtained in subsonic jets (by Bradshaw et al. (4)), however, the absolute levels are considerably lower. A considerable number of repetitive diagnostic measurements were undertaken which convinced us that the source of error in our measurements is probe resolution.

Despite the inherent error of our measurements several conclusions were apparent. First, the Reynolds stresses play an important role in the disintegration of the large scale organized instability of the supersonic jets. Our measurements showed that the Reynolds stresses grow very rapidly ahead of the region where the coherent structure disintegrates near the end of the potential core of the jet. This is extremely important in the diagnostics of jet noise because it is this region where the dominant noise production occurs, in the low Reynolds number supersonic jets. Second, our measurements indicated that the Reynolds stresses are made up primarily of broad-banded spectral components (turbulence) even in regions of the jet where the large

scale instability is very discrete. More detailed information of this type should be invaluable to theoreticians formulating a comprehensive analysis of the instability development and its associated radiated noise. Finally, our measurements concluded that the probe resolution problem must be solved, either by using larger jets or smaller probes, before the detailed measurements which are badly needed can be obtained. Such activity will be pursued in our next year's research effort.

Attachment No. 3 to this final report is a copy of the M.S. thesis "Crossed Hot-Wire Measurements in Low Reynolds Number Supersonic Jets" by Jerry D. Swearingen. This thesis reports on all X-wire measurements undertaken in this research project.

### III. PROGRESS ON FACILITY IMPROVEMENT

The major project in our facility improvement program was the installation of the surplus Ingersol Rand vacuum pump. We completed the foundation work and electrical, water and lubrication connections were made in a reasonably timely manner. Unfortunately, upon initiation of operation of the pump numerous serious leaks were discovered in the pump. Rather than expend all our efforts to repair all the leaks we decided to move ahead with the X wire measurements in the smaller jet to obtain the much needed experience with the techniques which were new to us.

In the meantime we have been working on repairing the Ingersol Rand vacuum pump leaks. We have replaced the main shaft seal and are in the process of diagnosing other necessary action. We must be aware however, that the pump, being surplus, is over 30 years old. There is the possibility that ring damage or main cylinder scoring has occurred which would make the complete rebuilding prohibitively costly. We will endeavor to determine our status with this pump as soon as possible. In the meantime we have proposed a series of experiments for next year's research that does not require the large jets or the larger pumping requirement which goes with it.

As mentioned in an earlier progress report, we have also constructed a small high Reynolds number jet facility. We have used this facility to make subsonic Mach number X-wire measurements as a check on some of our techniques. These measurements are reported in the MS thesis of Swearingen which is attachment #3 herewith.

This facility was originally intended as a test bed for flow visualization experiments. As discussed earlier these experiments were not carried out primarily because their need was greatly reduced upon the good quality work of Sarohia and Massier (1). This decision may be reevaluated depending upon future developments.

#### IV. CONCLUSIONS

Although not all objectives of the original proposal were met (primarily because of difficulties we encountered with the surplus vacuum pump) a substantial amount of the proposed experiments were conducted. The moderate Reynolds number  $M = 2.1$  jet study provided valuable information on both the large scale structure as well as the noise generation processes. This part of the study was undoubtedly the most successful. The Mach number 0.9 jet study provided some extremely interesting results on the dominant noise generation mechanism. The measurements demonstrated differences in the  $M = 0.9$  jet noise generation in comparison with previous  $M = 1.4$  jet measurements that conventional jet noise theories would not predict. The most important aspect of the results of this study is the identification of a physical effect for which we previously had little understanding.

With regard to our crossed hot-wire experiments in the supersonic jets, our work can be termed a partial success. We established calibration procedures and developed much needed experience with the techniques. Perhaps, most important, we established the magnitude of our probe resolution problems which must be resolved before more measurements of this type are attempted.

Finally, a list of publications and presentations is included which covers research conducted partially or wholly with the support of this research grant.

##### 4.1 Publications

- 1) "Flowfield and acoustic properties of a Mach number 0.9 jet at a low Reynolds number." by J. L. Stromberg, D. K. McLaughlin and T. R. Troutt. Submitted for publication to the Journal of Sound and Vibration, October 1979.

- 2) "Experiments on the flow and acoustic properties of a moderate Reynolds number supersonic jet." by T. R. Troutt and D. K. McLaughlin. Submitted for publication to the Journal of Fluid Mechanics, October 1979.

#### 4.2 Presentations

- 1) "Measurements on the Flow and Acoustic Properties of a Moderate Reynolds Number Supersonic Jet." by T. R. Troutt and D. K. McLaughlin. Paper No. EE2, American Physical Society, Division of Fluid Dynamics Meeting, November 1978.
- 2) "Crossed Hot-Wire Measurements in Low to Moderate Reynolds Number Supersonic Jets." by J. D. Swearingen, D. K. McLaughlin and T. R. Troutt. Paper No. EE3, American Physical Society, Division of Fluid Dynamics Meeting, November 1978.
- 3) "Flowfield and Acoustic Properties of a Mach Number 0.9 Jet at a Low Reynolds Number." by J. L. Stromberg, D. K. McLaughlin and T. R. Troutt. AIAA Paper No. 79-0593, March 1979.

#### REFERENCES

- 1) Sarohia, V., and Massier, P. F. "Experimental Results of Large-Scale Structures in Jet Flows and Their Relation to Jet Noise Production" AIAA Journal, Vol. 16, 1978, pp. 831-835.
- 2) Morris, P. J., and C. K. W. Tam. "Near and Far Field Noise From Large-Scale Instabilities of Axisymmetric Jets." AIAA Paper No. 77-1351, 1977.
- 3) Laufer, J., R. E. Kaplan, and W. T. Chu. "On the Generation of Jet Noise." AGARD Conference Proceedings No. 131 on Noise Mechanisms, 1973.
- 4) Bradshaw, P., D. H. Ferriss, and R. H. Johnson. "Turbulence in the Noise Producing Region of a Circular Jet." J. of Fluid Mech., Vol. 19, 1964, pp. 591-624.

EXPERIMENTS ON THE FLOW AND ACOUSTIC PROPERTIES OF A  
MODERATE REYNOLDS NUMBER SUPERSONIC JET

by T. R. Troutt and D. K. McLaughlin  
Oklahoma State University, Stillwater, Oklahoma

**Abstract:** An experimental investigation of the flow and acoustic properties of a moderate Reynolds number ( $Re=70,000$ ) Mach number  $M=2.1$  axisymmetric jet has been performed. The primary motivation behind these measurements was to extend the experimental studies conducted previously in this laboratory on low Reynolds number high speed jet noise to a higher Reynolds number regime where the flow and acoustic processes were found to be considerably more complex. In fact, mean flow and acoustic properties of this jet were determined to be closely comparable to high Reynolds number jet properties.

The major results of the flow field measurements demonstrate that the jet shear annulus is unstable over a broad frequency range. The growth rates and wavelengths of these instabilities as measured by a hot-wire were found to be in reasonable agreement with linear stability theory predictions. In remarkable agreement with subsonic jet results, the potential core of the jet was found to be most responsive to excitation at frequencies near a Strouhal number of  $St=0.3$ . The development of organized disturbances around  $St=0.3$  seems to agree in general with theoretical predictions by Morris and Tam.

The acoustic near field was characterized in terms of sound pressure

---

Preliminary copy: Submitted for publication to the Journal of Fluid Mechanics, October 1979.

level and directivity for both natural and excited (pure tone) jets. In addition, propagation direction and azimuthal character of dominant spectral components were also measured. It was determined that the large scale flow disturbances radiate noise in a highly directional pattern centered about  $30^\circ$  from the jet axis. The noise from these disturbances appears from simple ray tracing to be generated primarily near the region of the jet where the coherent fluctuations begin to decay. It was also determined that the large scale components of the acoustic field are made up predominately of axisymmetric ( $n=0$ ) and helical ( $n=\pm 1$ ) modes. The dominant noise generation mechanism appears to be a combination of Mach wave generation and a process associated with the saturation and disintegration of the large scale instability. The further development of a wave guide model of noise generation of the instability type appears to hold considerable promise.

## I. INTRODUCTION

Experiments on low Reynolds number high speed jets conducted previously in our laboratory by McLaughlin, Morrison and Troutt (1975, 1977), and Stromberg, McLaughlin and Troutt (1979) have shown that large scale discrete instabilities dominate the flow fluctuations upstream of the end of the potential core. For the case of the supersonic jets ( $M = 1.3$  to  $M = 2.5$ ), these large scale instabilities were determined to be directly responsible for a major portion of the noise radiated by the jets. This noise was found to have similar scaled amplitudes and directivity distributions as published results from high Reynolds number jets of equivalent Mach numbers (Dosanjh and Yu, 1968; Yu and Dosanjh, 1973). These results experimentally established the ability of large scale flow instabilities to efficiently produce noise.

The potential of organized large scale disturbances for producing noise was initially suggested by Mollo-Christensen (1960, 1967) with later contributions by Sedel'nikov (1967), Michalke (1969) and Bishop, Ffowcs Williams, and Smith (1971). The existence of these large structures in low speed jets has been demonstrated by a number of experimental studies most notably Crow and Champagne (1971), Lau, Fisher and Fuchs (1972), and Chan (1974). However, for high speed turbulent jets direct flow measurements are difficult to obtain. Indirect observations using flow visualization techniques (Lowson and Ollerhead, 1968; Potter, 1968; and Salant, 1973), however, have indicated the presence of large scale wave-like disturbances in turbulent supersonic jets.

One of the first attempts to produce a mathematical representation of jet noise generation by organized disturbances was presented by Tam (1972). Tam's model at that time used a linearized spatial stability theory to

develop an eigenvalue relation between the complex wave number and the frequency of the unstable wave. This stability theory followed the same general methods as were employed by Sedel'nikov (1967) and Michalke (1969). Since Tam's model assumed infinitesimally thin shear layers and a parallel mean flow, his results indicated that a monotonic increase in wave growth rate with increasing frequency would occur near the nozzle exit. In order to align his theoretical results with the large scale structure observed in the downstream region of the jet, Tam imposed a selection mechanism on the instability results. Tam's hypothesized mechanism used the order induced on the supersonic jet by the wave-cell structure to accomplish this selection. Unfortunately, recent evidence in low Reynolds number supersonic jets over a substantial Mach number range obtained by Morrison (1977) fail to support this mechanism.

Subsequent work on more advanced jet stability and noise prediction models has been performed by a number of investigators including Tam (1975), Chan (1974), Merkin and Liu (1975), Morris (1977), and Morris and Tam (1977). The primary concern of these works has been to develop more realistic flow models, which include some nonlinear effects, as well as more accurate mean flow profiles. Since acoustic measurements indicate that the dominant noise generation region is near the end of the potential core, nonlinear effects are no doubt quite important. The exact method of best incorporating these effects into mathematical models though is a controversial point. Morris and Tam (1977) apparently feel that the use of empirical mean flow profiles coupled with local linear stability calculations adequately models the coherent wave behavior. Although, as was pointed out by Morris (1977) himself, the actual importance of nonlinear terms in the calculations is simply not known at the present time.

The formulation of the nonlinear effects in the stability analysis is one of the major problems facing the researchers developing analytical jet noise models. Another major problem is the effect of non parallel flow (flow divergence). For incompressible flow, Crighton and Gaster (1976) have developed a method incorporating the flow divergence effects. In the supersonic jet, Morris and Tam (1977) have performed a similar analysis, however, the exact accuracy of some of their mathematics is suspect (Morris and Tam, 1979).

No doubt the progress of the theoretical models could be greatly aided by experimental studies on the coherent structures in turbulent high speed jets, but involved flow measurements in supersonic jets are most difficult to make. The most reliable turbulence instrument, the hot-wire anemometer, cannot be used in conventional high speed air jets because the dynamic pressures are too great for the fragile probes. This problem can be alleviated by reducing the density of the flow. This practice was followed in the earlier work, mentioned previously, conducted in our laboratory. At the low Reynolds numbers of these measurements, the flow fluctuations of the supersonic jets were found to be dominated by discrete large scale instabilities for approximately the entire length of the potential core. And as mentioned earlier the low Reynolds number experiments were important in establishing the noise radiation potential of the large scale instability waves in the jet.

In order to achieve an experimental condition more closely approaching a turbulent flow, the present study was carried out at a Reynolds number of  $Re = 70,000$  which is approximately 10 times greater than that of the previous low Reynolds number studies. This moderate Reynolds number was chosen as an attractive compromise between the increasingly more difficult experimental conditions and the increasingly more interesting and more in-

involved flow and acoustic phenomena encountered at higher Reynolds numbers. At the chosen Reynolds number, both the flow and acoustic properties were found to be considerably more complex than in the low Reynolds number condition. In fact, based on comparisons of mean flow and acoustic results presented here with high Reynolds number measurements, considerable support can be found for extrapolating many of the present results.

The goal of the present research was to characterize experimentally the dominant flow fluctuation properties in a  $M = 2.1$  moderate Reynolds number jet, and to investigate the related noise generation process. The experiments included measurements on both natural and artificially excited jets. The artificially excited measurements were used to illuminate properties of the coherent flow structure and its radiated noise.

## 2. EXPERIMENTAL APPARATUS AND PROCEDURES

### 2.1 Apparatus

These experiments were conducted in the free jet test facility shown schematically in Figure 1. This facility has been described in a previous reference (McLaughlin, Morrison and Troutt, 1977), so that only a brief description will be given here.

An axisymmetric supersonic nozzle with an exit diameter  $D$  of 10mm was used to produce the air jet. The nozzle contour was designed by the method of characteristics following Johnson and Boney (1975). The nominal  $M = 2$  air jet exhausts into a low pressure test chamber of dimensions  $1.1 \times 0.76 \times 0.71$  meters. The chamber is lined with acoustic foam which absorbs over

90% of the incident radiation for frequencies  $f$  above 1kHz. (The characteristic frequency of the jet was  $U_0/D = 50$  kHz, where  $U_0$  is the jet exit velocity.)

A three dimensional probe drive system was used to position the Pitot pressure, hot-wire and microphone probes employed in the research. The Pitot probe was a standard blunt end type with an outside diameter of 0.53mm. The hot-wire probes used were DISA 55A53 subminiature probes mounted on brass wedges. The 5 micron diameter wires were positioned perpendicular to the axial direction. DISA 55M constant temperature electronics were used to operate the probes. The frequency response of the anemometer was found to be flat within  $\pm 3$ dB up to 60kHz ( $St = \frac{fD}{U_0} = 1.4$ ) based on square wave response tests. A Bruel and Kjaer 3.175 mm diameter condenser microphone was used for the acoustic measurements. The microphone was assumed to have an omni-directional response for frequencies up to 80 kHz based on factory specifications. For overall level measurements both the microphones and hot-wire signals were band-passed filtered from  $St = 0.03$  to  $St = 1.3$  to remove chamber and electronic resonances. Frequency spectra of the sensor signals were obtained using a Tektronix 7L5 analyzer. For the spectra presented from the present measurements, a resolution window of 3kHz and a sweep speed of .05 sec/kHz were used.

The jet was artificially excited for some measurements using a glow discharge device consisting of a single point tungsten electrode positioned approximately 2mm from the nozzle exit which was reported earlier (McLaughlin et al. 1975).

## 2.2 Procedures

For all measurements in this study, the stagnation temperature of the jet was room temperature, approximately 294K, and the jet exit pressure  $p_c$  was maintained slightly above the test chamber pressure,  $p_c$  (approximately  $1.03 p_c$ ). The test chamber pressure for these measurements was approximately .05 atmospheres and the Reynolds number based on exit conditions was approximately 70,000.

Correlations and phase averages of sensor signals were measured using a Saicor 43A analyzer. The phase average of a fluctuating signal is here defined as:

$$\langle q(t) \rangle = \lim_{N \rightarrow \infty} \frac{1}{N} \sum_{n=0}^N q(t+n\tau)$$

where  $\tau$  is the period of the coherent disturbance and  $N$  is the number of disturbance cycles averaged over and  $t$  is time. The application of this function allows the recovery of the periodic portion of the fluctuating signal where a general representation of the signal is given by:

$$q(t) = \bar{q} + \tilde{q}(t) + q''(t)$$

Here  $\bar{q}$  is the mean component with the fluctuating component divided into two parts,  $\tilde{q}$  the periodic portion and  $q''$  the random contribution.

For flow fluctuation amplitude measurements, the hot-wire bridge voltage fluctuation  $e'$  was assumed to be related to the fluctuation in the flow quantity axial mass velocity ( $\rho u$ ) by the relation  $\frac{e'}{e} = A_m \frac{(\rho u)'}{\rho u}$  where the sensitivity coefficient,  $A_m$ , was determined through direct cali-

bration following the methods of Rose (1973) and Ko, McLaughlin and Troutt (1976). The above relation is applicable when total temperature fluctuations are assumed negligible. For the present measurements the total temperature fluctuations were found to account for less than 2% of the voltage fluctuation.

Sound pressure levels (in decibels, dBs) were scaled to the ambient test chamber pressure using the relation

$$\text{SPL} = 20 \log_{10} [p'_{\text{rms}} / (p_c p_{\text{ref}} / p_a)]$$

where  $p'_{\text{rms}}$  is the root mean square of the fluctuating sound pressure,  $p_a$  is atmospheric pressure and  $p_{\text{ref}} = 2 \times 10^{-5} \text{ N/m}^2$ .

### 3. EXPERIMENTAL RESULTS

#### 3.1 Natural Jet

##### 3.1a Mean Flow Field

Centerline Mach numbers for the present  $Re = 70,000$  jet are shown in Figure 2. The Mach numbers are calculated from Pitot and static pressure probe measurements using standard compressible flow relationships. The average centerline Mach number from  $x/D = 1$  to  $x/D = 8$  was found to be 2.12 with variations of  $\pm 4\%$  due to the weak shock cell structure of the jet. These measurements indicate the potential core length of the jet to be between 8 and 10 diameters. The sonic point in the jet is reached between 18 and 20 diameters downstream of the nozzle exit. Radial Mach number pro-

files for  $x/D = 1, 5, 10$  and  $15$  are shown in Figure 3. These measurements show that the mean flow changes from a profile with a central region of uniform velocity to an approximately Gaussian profile by  $x/D = 10$ .

The centerline Mach number distribution and the Mach number profiles are similar to the data obtained by Dutt (1977) and by McLaughlin *et al.* (1979) for cold air jets of Mach number 2.0 and Reynolds numbers in excess of  $Re = 10^6$ . However, a more careful look at the shear layer development yields some differences. To do this we have used a curve fit for the velocity profiles similar to the one used by Laufer, Kaplun and Chu (1973) for subsonic jets. It takes the form of a half-Gaussian:

$$\frac{\bar{u}(\eta)}{U} = \exp[-2.773(\eta + 0.5)^2] \quad \text{for } \eta > -0.5$$

$$= 1 \quad \text{for } \eta \leq -0.5$$

where  $\eta = \frac{r-r(.5)}{\delta}$ ,  $U$  is the velocity on the centerline of the jet at the given axial ( $x$ ) location,  $r(.5)$  is the radial location where the velocity is  $0.5 U$  and  $\delta$  is the local shear layer thickness. Downstream of the end of the potential core  $\delta = 2r(.5)$  and  $\eta$  reduces to  $\eta = \frac{r}{\delta} - \frac{1}{2}$  where  $\delta$  is now  $1/2$  the local jet diameter. (The jet diameter is taken to be the diameter of the locus of points where the mean velocity is .01 times the local centerline velocity.) Morris and Tam (1977) have also shown the above half-Gaussian to be a convenient curve fit for supersonic jet velocity data, particularly for input into the stability analysis of the jet.

Figure 4 includes mean velocity data of the four axial locations corresponding to the Mach number data of Figure 3. This figure demonstrates that the half-Gaussian is a reasonable representation for the mean velocity data both upstream and downstream of the end of the potential core. The

local shear layer thickness,  $\delta$ , and the  $r(.5)$  parameter used to generate the best curve fits are plotted in Figure 5 as a function of the axial coordinate. Included on the figure are the data for the same parameters determined by measurements made by McLaughlin et al. (1979) in a Mach number 2.0,  $Re = 5.2 \times 10^6$  jet. There is a reasonable similarity in the development of the present moderate Reynolds number jet in comparison with its high Reynolds number counterpart. However, the shear layer, in the potential core region of the jet does not display the linear growth dependence typical of fully turbulent shear layers. This slow initial growth rate indicates that the jet shear layer is in transition from laminar to turbulent flow in the moderate Reynolds number jet. Hot-wire measurements presented subsequently demonstrate that the laminar to turbulent transition in the shear layer occurs over the first 2 or 3 jet diameters. This contrasts to the extensive length of transitional flow found in the low Reynolds number ( $Re = 7900$ ) jet as measured by Morrison (1977). The low Reynolds number jet parameters are also shown in Figure 5 for comparison.

### 3.1b Fluctuating Flow Field

Frequency spectra of the hot-wire fluctuation signal obtained at the radial position of maximum voltage fluctuation (which is approximately the center of the jet shear layer) are shown in Figure 6 for several  $x/D$  locations. Beyond  $x/D = 8$  the probe was located on the centerline of the jet. These spectra show that high frequency flow fluctuations centered around a Strouhal number of approximately 0.6 grow rapidly and dominate the spectra for the first three diameters downstream of the jet exit. At  $x/D = 4$ , although the high frequency fluctuations still dominate the spectra, a marked increase in the amplitude of low frequencies (below  $St = 0.25$ ) can be seen. From  $x/D = 4$  to  $x/D = 6$  the high frequency fluctuations steadily decay,

transferring energy into intermediate frequencies around  $St = 0.30$ .

Spectral energy transfer to intermediate frequencies continues from  $x/D = 6$  to  $x/D = 8$  resulting in a fully developed turbulent spectrum at  $x/D = 8$ . Beyond  $x/D = 8$ , the fluctuation spectra continuously shift towards lower frequency content with downstream location as indicated by the spectrum at  $x/D = 10$ . The general shape and development of these spectra is quite similar to spectra measured by Miksad (1972) in an incompressible free shear layer. However, the spectra differ considerably from the low Reynolds number supersonic jet spectra (Morrison, 1977) which were found to be dominated by a narrow frequency band near  $St = 0.2$  for the first 10 jet diameters.

Figure 7 shows radial profiles of the mass velocity fluctuations in the jet for several downstream positions. The measurements are reported in terms of rms mass velocity fluctuations,  $(\rho u)'_{rms}$ , non-dimensionalized by the mean mass velocity at the centerline of the nozzle exit  $(\overline{\rho u})_0$ . The radial peak of the fluctuation amplitude moves toward the center of the jet and the width of the shear layer increases with downstream location. By  $x/D = 9$  it is apparent that large amplitude fluctuations have reached the jet centerline indicating the end of the potential core region. This result is consistent with the mean flow measurements which showed a decrease in Mach number beginning in this region.

Flow fluctuation amplitude measurements as a function of  $x/D$  are shown in Figure 8. Prior to the end of the potential core these measurements were obtained with the hot-wire located in the center of the shear layer. After the end of the potential core the hot-wire was positioned on the jet centerline to avoid Mach number effects in the data reduction. The measurements show that the amplitude of the fluctuations grows approximately exponentially for the first 3 downstream diameters. The amplitude of the fluctuations then oscillates from  $x/D = 4$  to  $x/D = 7$  before begin-

ning a steady decline at  $x/D = 8$ . Also shown in the figure for comparison are measurements obtained by Morrison (1977) in the low Reynolds number jet. Associated with the increasing Reynolds number is an increase in the growth rate of the fluctuations accompanied by an upstream shift in the location of maximum fluctuation level in the jet. The upstream shift is consistent with the faster development of the mean flow profiles, as illustrated earlier in Figure 5.

Amplitude measurements of spectral components of the hot-wire signal in the jet shear layer are shown in Figure 9. An active bandpass filter with the cut-off frequencies set to 20% above and below the center frequency of interest was used to obtain these measurements. The attenuation characteristic of the filter was 24 dB/octave.

The data demonstrate that each spectral component grows approximately exponentially for 2.5 to 3 downstream diameters with the higher frequencies growing faster. Assuming this initial region of fluctuation growth to be governed by classical linear stability theory, the mathematical representation for the fluctuating flow properties is given by

$$q(x, r, \theta, t) = \hat{q}(r) e^{-k_i x} (k_r x + n\theta - \omega t)$$

For a parallel flow  $M = 2.0$  jet with a top hat velocity profile, Tam (1972) has predicted the axial growth rate  $k_i$  as a function of frequency  $\omega$ . A non-dimensional plot of Tam's predictions with the present data is shown in Figure 10. The trend of the experimental growth rates, increasing growth with increasing Strouhal number, agrees with Tam's theoretical prediction. Moreover, the experimental growth rates and theoretical values are quite close for the two intermediate Strouhal numbers. Beyond  $x/D = 2 \frac{1}{2}$ , after the high frequency fluctuations have grown to approximately 3% of the mean exit mass-velocity nonlinear effects become apparent. These effects show up in the decreasing growth rates of the two higher frequencies, in increasing

growth rates at the lower frequencies and in simultaneous development of the mean velocity profiles as demonstrated by the data of Figure 5.

Between  $x/D = 3 \frac{1}{2}$  and  $x/D = 5 \frac{1}{2}$  the amplitudes of the  $St = 0.09$  and  $St = 0.76$  components saturate and then oscillate. The  $St = 0.38$  component, however, goes through a region of slow growth between  $x/D = 3 \frac{1}{2}$  and  $5 \frac{1}{2}$ . This region of secondary growth for intermediate frequencies was also observed in the spectral results. Beyond  $x/D = 9$  all spectral components show a continual decline in amplitude. The beginning of this region occurs approximately at the end of the potential core region as indicated by the mean flow measurements.

### 3.1c Acoustic Field

Sound pressure level (SPL) contours of the overall near field noise are shown in Figure 11. The near field contours are similar to high Reynolds number measurements in amplitude levels and general shape (Yu and Dosanjh, 1972 and McLaughlin *et al.* 1979). The contours are also similar in shape and amplitude to the noise contours Morrison and McLaughlin (1979) measured for the low Reynolds number jet at the same Mach number. (The low Reynolds number contours are shown in dashed lines on the figure.) However, one important difference between the low Reynolds number results and the present measurements is obvious. The low Reynolds number contours are displaced downstream 6 to 10 jet diameters from the high Reynolds number contours. This displacement is most probably related to the fact that the flow fluctuations amplitudes saturate further downstream in the low Reynolds number jet.

Figure 12 shows the sound pressure level as a function of the angle from the jet axis. These measurements were made at a constant radius of 40 jet diameters from the nozzle exit. Also shown on the figure are comparison data from a  $M = 2.0$  jet at a high Reynolds number obtained by

McLaughlin et al. (1979) and low Reynolds number data from Morrison and McLaughlin (1979). This figure shows that for all jets the highest levels of generated noise occur at angles around  $30^\circ$  to the jet axis.

Spectral analysis of the microphone signal obtained at several locations along a constant radial coordinate are presented in Figure 13. These spectra show a shift towards increased lower frequency content as downstream position is increased. This trend has been noted in high Reynolds number jet noise measurements by previous investigators (Yu and Dosanjh, 1973; Laufer et al. 1976). This trend is also in general agreement with hot-wire spectral results mentioned earlier.

To demonstrate the effect of Reynolds number on the acoustic frequency content, spectra from three different jets are presented in Figure 14. These spectra were measured near the angle of maximum noise emission of the three jets. The bottom spectrum is from the low Reynolds number jet measured by Morrison & McLaughlin (1979), the middle spectrum is from the present measurements, and the top spectrum was reported by Laufer et al. (1976) for a  $Re = 2.6 \times 10^6$ ,  $M = 2.0$  jet. At the low Reynolds number condition, the flow is dominated by a narrow band of frequencies and the noise spectrum is similar. At the two higher Reynolds number conditions, the spectra are quite full, however, both have a broad peak around  $St = 0.2$  which coincides approximately with the low Reynolds number peak.

SPL contours of the near field noise band passed around two different spectral components ( $St = 0.19$  and  $St = 0.38$ ) are shown in Figure 15. These frequencies encompass a large portion of the broad peak of the major noise production spectrum. Two important general features of these contours should be noted. One is the downstream lobes which are apparent at both frequencies. The other feature is a bulge located in the upstream region of the contours. This upstream bulge is barely apparent in the higher

Strouhal number contours, but becomes more obvious in the lower Strouhal number plot. For the lower Strouhal number contours, a definite separation between the two regions is evident. These two regions have been noticed before by prior investigators Laufer et al. (1976) and Yu and Dosanjh (1973). However, the upstream bulge is accentuated in the present measurements.

### 3.1d Summary of Natural Jet Results

The mean flow measurements show that the jet has an initial central region of uniform velocity which transitions to an approximately Gaussian profile by  $x/D = 10$ . The average Mach number of the jet was found to be 2.12 in the potential core region and the sonic point was reached between 18 and 20 diameters downstream. These mean flow results are similar to high Reynolds number measurements at equivalent Mach numbers.

A more quantitative measure of the mean flow development was obtained by plotting  $\delta$ , the local shear layer thickness as a function of the axial coordinate  $x$ . This plot showed that the moderate Reynolds number jet developed somewhat slower initially than high Reynolds number jets. This difference was attributed to the initial region of transitional flow near the nozzle exit.

The flow fluctuation measurements demonstrate that high frequency fluctuations grow at a constant exponential rate for the first  $2\frac{1}{2}$  to 3 downstream diameters. Beyond  $x/D = 3$  nonlinear effects become apparent and by  $x/D = 5$ , the flow fluctuation spectra are quite broad and the total fluctuation amplitude attains a saturated condition. By  $x/D = 8$  the spectra are fully developed. Beyond  $x/D = 8$  the amplitude of the flow fluctuations decreases, and the spectral content of the fluctuations shifts progressively to lower frequencies.

These results differ considerably from low Reynolds number measurements at the same Mach number. The lower Reynolds number fluctuations were found

by Morrison (1977) to be dominated by a narrow band of frequencies near  $St = 0.2$  for the first 10 diameters downstream of the jet exit. Growth rates of the flow fluctuations in the low Reynolds number jet are much slower and the fluctuation level does not saturate until  $x/D = 10$ .

Acoustic spectra demonstrate that the noise produced by the moderate Reynolds number jet has a broad frequency content. The content of the acoustic spectra was observed to move to lower frequencies as the microphone was moved downstream. These features are similar to published high Reynolds number results.

SPL contours of the overall acoustic field were found to be similar in shape and level to both low and high Reynolds number measurements. However, the low Reynolds number contours are displaced by approximately 6 to 10 jet diameters downstream. This displacement was attributed to the observed shift in the location of the amplitude saturation region of the flow fluctuations. Since apparently the major effect of changing the overall flow fluctuation growth rate upon the noise contours was simply to shift the contours axially and not to change their shape or amplitude significantly, it can be inferred that the major noise production mechanism is largely independent of fluctuation growth rate. It seems more plausible in light of these results to suppose that the major noise generation mechanisms may be characteristic of phenomena which occur downstream of the initial region of unstable fluctuation growth.

The results of acoustic measurements also indicate that two localized regions of major noise production are present in the acoustic field of the jet. This feature has been noted previously in a number of high Reynolds number investigations. It was also noted that the angle with respect to the jet axis of the dominant noise radiation decreases with decreasing

frequency. This result had also been noted by several investigators of high Reynolds number jet noise.

### 3.2 Artificially Excited Jet

#### 3.2a Effects of Excitation

In order to develop an understanding of the nature of the coherent fluctuations within the jet, an artificial disturbance was input at the nozzle exit using the glow discharge device. As discussed in an earlier paper (McLaughlin et al 1975) the excitation device is similar to one used first by Kendall (1967). It consists of a tungsten electrode near the nozzle exit to which a 700 volt peak to peak a.c. signal is applied with a 400 volt negative bias. Because there is a breakdown voltage of approximately 600 volts, this method actually introduces a glow of ionized air which turns on and off at the excitation frequency. Such an excitation, in contrast to a sinusoidal excitation, possesses considerable harmonic content.

Figure 16 shows an example of the frequency spectra at several downstream locations in the center of the shear layer with the jet excited at  $St = 0.38$ . The spectra show that the exciter generates a disturbance initially concentrated at the fundamental forcing frequency and its second harmonic. Over the first six downstream diameters the amplitude of the fundamental grows slightly while the harmonic decays. Beyond  $x/D = 6$  the fundamental rapidly decays until by  $x/D = 10$  its presence is barely distinguishable. These spectra are typical of excitation spectra for frequencies over the range studied ( $St = 0.09 - 0.8$ ), the only major difference being that at lower excitation frequencies more higher harmonic content becomes apparent. Several previous investigators of free shear flows

(Browand 1966; Crow and Champagne 1971; Miksad 1972 and Kibens 1979) have also found that artificial excitation causes the fluctuation spectra to become discretized in a similar manner.

Although the input disturbance from the exciter dominates the flow fluctuation spectra near the nozzle, its effect is initially localized within the thin shear layer of the jet. This fact can be seen in Figure 17 which shows a radial profile of the overall mass velocity fluctuations at  $x/D = 1$  for a jet excited at  $St = 0.19$ . As a consequence of the excitation the initial region of low amplitude exponential growth on the shear layer is bypassed.

The effect of the excitation on the jet centerline mass-velocity fluctuations for four excitation frequencies is shown in Figure 18. These measurements were bandpass filtered  $\pm 1$  kHz around the excitation frequency. An interesting result is evident from this figure. Apparently the jet core is much more responsive to excitation at the intermediate frequencies of  $St = 0.19$  and  $St = 0.38$ . This result is closely analogous to results obtained by Crow and Champagne (1971) in a turbulent subsonic jet which was found to be most responsive to a  $St = 0.3$  excitation.

More recent subsonic jet measurements by Chan (1974), Moore (1977) and Hussain and Zaman (1975) have also noted this selectivity. The exact mechanism by which the jet selects these frequencies is still poorly understood but it apparently exists in both subsonic and supersonic jets.

It is also important to determine the effect of the excitation on the mean flow as well as on the jet turbulent structure. Troutt (1978) presented mean flow profiles which show that the development of the present jet occurs

over a shorter distance in the excited jet compared with the natural jet. As demonstrated earlier, the shear layer thickness parameter  $\delta$  is a more sensitive measure of the jet development than are the profiles. Therefore the parameters  $\delta$ , and  $r(.5)$  corresponding to the excited and natural jets are presented in Figure 19 to demonstrate the effect of excitation. This figure clearly indicates that the excited disturbances enhance the mean flow development. This result implies that naturally occurring organized large scales may also be efficient mixing agents.

SPL contours of the overall near field for the jet excited at  $St = 0.19$  are shown in Figure 20. The shapes and positions of these contours are approximately the same as the natural jet contours shown in Figure 11. However, an increase in the noise level at corresponding locations in the acoustic field is apparent. A directivity plot generated from these contours is shown in Figure 21. For comparison the natural jet measurements are also shown on the plot. This plot shows that the directivity of the noise radiation in the two cases is almost identical although the amplitude is approximately 2 to 3 db higher in the excited case.

SPL contours filtered around the fundamental excitation frequency are shown in Figure 22 for the  $St = 0.19$  and  $0.38$  spectral components. The contours are remarkably similar in shape to the corresponding ones measured for the same spectral components of the natural jet. The directivities of the major noise emission at each frequency comparing the natural and excited jets are also almost identical. Corresponding directivity plots in Figure 23 show this clearly. As would be expected due to the concentrated nature of the excited acoustic spectra, there is a considerable increase in the SPL for a given angle. However, surprisingly there seems to be very little change in the directivity of the noise radiation. This result implies that the arti-

ficial disturbances may well generate noise by the same mechanism responsible for the downstream noise emission pattern in the natural jet. This implication makes it of considerable interest to determine some of the important characteristics of the artificially excited disturbance and its noise radiation.

### 3.2b Excited Flow Disturbance Measurements

Measurements of the axial wavelength of excited disturbances in the jet were made by cross-correlating the hot-wire signal with the excitation signal and measuring the change in the time lag of the peak of the correlation curves for various downstream positions. An example of these measurements for a typical disturbance is shown in Figure 24. The results of the wavelength measurements, presented in terms of non-dimensional wave number  $k_r D$  as a function of disturbance Strouhal number, are shown in Figure 25. These measurements show an approximately linear relationship between  $k_r$  and  $St$ . This type of relation was predicted by Tam (1972) in an early stability study of the supersonic jet and has been measured in subsonic jets by Chan (1974). Tam's prediction for a spiral-mode instability ( $n = \pm 1$ ) in a  $M = 2.1$  jet is also shown in Figure 25. The fact that Tam's predicted values are somewhat lower in terms of wavenumber should not be viewed too critically, since he used a simple non-diverging top hat mean velocity profile in his stability model.

Multiplying the axial wavelength by the frequency of the disturbance gives the axial phase velocity of the disturbance. Figure 26 shows the axial phase velocity as a function of Strouhal number. For most of the Strouhal number range the phase velocity is approximately constant, however, the phase velocity decreases considerably at the low frequency end of the spectrum. This trend of phase velocity variation for low frequency disturbances

was also noted by Chan (1974) for azimuthal modes  $n = 1$  and  $n = 2$  in a subsonic jet. It is also notable that the average convection velocity for disturbances between  $St = 0.28$  and  $St = 0.48$  is approximately  $0.80 U_0$  which is in close agreement with the value measured by Dutt (1977) from laser Schlieren cross-correlations in a high Reynolds number  $M = 2.0$  jet.

An important point to note in addition is that disturbances traveling faster than  $0.65 U_0$  will be traveling supersonically with respect to the air outside the jet. Supersonically traveling waves have the ability to radiate Mach wave like sound emission (Phillips 1960; Ffowcs Williams 1963). Morrison & McLaughlin (1979) have shown that the noise radiation has different propagating characteristics when the phase velocity of the instability waves exceeds the ambient acoustic velocity.

Morris and Tam (1977) claim that only waves with supersonic phase velocities will radiate to the far field. The instability waves in the  $M = 1.4$  and  $2.1$  jets at low Reynolds number studied by Morrison (1977) travel subsonically (with respect to the surrounding air) but they nevertheless radiate efficiently to the far field. Morris and Tam (1977), Liu (1974) and Tam (1971) alledge that because the waves are growing they actually posses supersonic phase components. This argument is reasonable for the growing portion of the waves, but as will be seen later, the decay- ing portion of the waves also radiate very efficiently. Morris and Tam (1979) have pointed out that this is one area of the stability analysis noise genera- tion model which needs considerable attention.

Figure 27 shows the axial development of the coherent mass-velocity fluctuation amplitude in the center of the jet shear layer for the two intermediate frequencies,  $St = 0.19$  and  $St = 0.38$ . Due to the strong radial dependence of the hot-wire measurement near the nozzle exit there is consider- able scatter. However, faired curves through the data indicate the general

growth and decay of the wave amplitude. Unfortunately, direct comparisons with the measured data and Tam's 1975 theory for the evolution of his coherent noise generation term are not possible due to differences in the definitions of the theoretical and measured terms. It should be noted however, that the general pattern of growth and decay is similar for both the measured and theoretical quantities.

### 3.2c Acoustic Radiation from Artificially Excited Disturbances

By phase averaging the microphone signal in the noise radiation field the fraction of the total signal directly caused by the excited flow disturbances was determined. Figure 28 shows the percentage of the phase averaged component as a function of downstream position for two excitation frequencies ( $St = 0.19$  and  $0.38$ ). These measurements were recorded at a constant radial location of 8 diameters. At low values of  $x/D$ , the noise at both Strouhal numbers shows a low percentage of the phase averaged component. However, at approximately  $x/D = 8$ , both frequencies show an increase in phase averaged components. The  $St = 0.38$  phase averaged component goes above 50% by  $x/D = 12$ , while the  $St = 0.19$  component reaches this value slightly farther downstream at  $x/D = 16$ . These points correspond approximately to the location of the inflection region in the filtered natural jet contours (Figure 15) indicating the beginning of the downstream lobed area. In agreement with these results several investigators (Dutt 1977; Dahan and Elias 1976; Maestrello 1976) of high speed jets have also noted high correlations for the noise at small spherical angles ( $\beta \leq 45^\circ$ ).

Measurements of the wavelengths of the acoustic radiation in the radial and axial directions were obtained for the same two frequencies ( $St = 0.19$  and  $St = 0.38$ ). These measurements were made by cross-correlating the

microphone signal with the exciter signal and measuring the time lag change for various positions in the acoustic field in a similar fashion to the flow wavelength measurements. The axial  $\lambda_a$  and radial  $\lambda_r$  wavelengths were used to calculate the acoustic wavelength normal to the wave fronts,  $\lambda_a$ . Table I shows the results of these measurements for the two frequencies. Also included in the table are the calculated angle of the wave propagation with respect to the jet axis  $\alpha$  and the corresponding calculated Mach wave angle,  $\mu$ , of the supersonic flow disturbance. A schematic depicting the relationship of the flow  $\lambda_d$  and acoustic wave lengths is shown in Figure 29. The acoustic phase speed,  $c_a$ , was calculated from the measured acoustic wavelength and the frequency. This speed is compared to the acoustic velocity  $a_0$  calculated from the temperature of the surrounding air. This comparison gives an indication of the measurement error.

It can be seen from the table that the faster flow disturbance ( $St = 0.38$ ) produces acoustic waves propagating close to the Mach angle computed from the disturbance speed. The slower disturbance ( $St = 0.19$ ) however, produces waves which are inclined at an angle considerably lower than the predicted Mach angle. This feature was also observed by Morrison and McLaughlin (1979) in low Reynolds number supersonic jet measurements for waves traveling just above and below the speed of sound.

Based on these results and Morrison and McLaughlin's measurements, it seems that a simple eddy Mach wave model for the major noise generation mechanism is not of sufficient complexity to explain all of the measured noise field properties. However, it does appear that a Mach wave component of noise radiation does occur for higher frequency and consequently higher phase velocity disturbances.

Mach wave type radiation has been noticed by other experimenters using flow visualization techniques (Salant 1973; Lowson and Ollerhead 1968).

Recently Dutt (1977) found that the angle of the Mach waves in his shadow-graphs implied a disturbance convection velocity which was in agreement with his Laser cross-correlation measurements.

To approximately locate the major noise sources in the jet, a simplified ray tracing technique was used. This technique involved drawing a line perpendicular to the acoustic wave front from a point approximately in the center of the contour lobes. The point of intersection of the perpendicular line with the jet then indicates the location of the major noise sources.

The results of this technique indicate that the major noise sources for  $St = 0.38$  noise radiation are located between 6 and 8 diameters downstream of the jet exit. The major noise sources for the  $St = 0.19$  noise radiation were found to be located between 8 and 10 diameters downstream. Flow fluctuation amplitude measurements have shown that both of these locations are downstream of the initial growth of the flow disturbances, and in the axial region where the disturbance saturates and begins to decay. This finding appears to support theoretical studies of Merkin and Liu (1975) in which they attribute a strong noise generation mechanism to the nonlinear disintegration of the coherent disturbance.

The azimuthal character of the acoustic radiation from excited disturbance at  $St = 0.19$  and  $St = 0.38$  was determined by measuring the phase relationship between the microphone and exciter signal for various angles of  $\theta$ . These measurements were made at an axial location of  $x/D = 12$  on a cylindrical radius of  $r/D = 3$ . The amplitude of the phase averaged signal was also recorded for each measurement position. The results of the measurements are shown in Figure 30. The amplitude measurements are nondimensionalized by the amplitude of the maximum phase averaged signal on the arc.

Numerical fits for the data were obtained by superposing three azimuthal modes of mode numbers  $n = 0, +1$ , and  $-1$ . (It is generally accepted that low mode numbers dominate axisymmetric flows.) These modes are mathematically represented by the equation

$$q_n = A_n e^{i(n\theta - \omega t + \alpha_n)}; \quad n = 0, +1, -1$$

where  $\alpha_n$  was used to represent a phase difference between modes at the axial measurement station. Before attempting to find  $A_n$  and  $\alpha_n$  for each mode it was assumed the  $A_1 = A_{-1}$  and that  $\alpha_1 = \alpha_{-1}$ . Since the flow is axisymmetric  $\alpha_1$  and  $\alpha_{-1}$  can be set to any  $\theta$ . For simplicity  $\theta = 0$  was chosen. The best fits for the data were found to be  $A_0/A_1 = 1.4$  with  $\alpha_0 = 130^\circ$  for the  $St = 0.19$  disturbance and  $A_0/A_1 = 0.5$  with  $\alpha_0 = 90^\circ$  for the  $St = 0.38$  data. The indication that disturbances occur in both axisymmetric and antisymmetric modes is in agreement with Dutt's (1977) findings for a high Reynolds number  $M = 2.0$  jet.

It is of interest to note that the antisymmetric excitation device is apparently capable of exciting both antisymmetric and axisymmetric flow disturbances. This finding indicates that the excitation device does not necessarily dictate the downstream character of the artificial disturbance. Consequently, this result encourages somewhat greater confidence to be placed in the applicability of the results of excited measurements to natural jet phenomena.

### 3.2d Summary of Excited Jet Results

It was found that the artificial exciter generates a flow disturbance at the fundamental forcing frequency and its higher harmonics. For several diameters downstream of the nozzle exit, it was observed that the flow fluctuation spectral content in the jet shear layer is concentrated at the

excitation frequency and its harmonics. Further downstream the spectral content of the flow fluctuations disperses and the effect of the excitation on the flow spectra reduces until by  $x/D = 10$  it is finally unobservable. Centerline flow fluctuation measurements demonstrated that the jet core is most responsive to excitation at the intermediate Strouhal numbers ( $St = 0.19$  and  $St = 0.38$ ). Also, excitation at  $St = 0.19$  was shown to increase the mean flow spreading rate of the jet.

The acoustic field spectra near the nozzle exit are not noticeably affected by the excitation. Further downstream near the SPL contour lobes, peaks in the acoustic spectra appear at the fundamental forcing frequency and its harmonics. The relative strength of these peaks shifts to the lower harmonics and fundamental as downstream position increases.

Noise amplitude measurements indicate that a large portion of the noise from the excited disturbances propagates toward the downstream lobed region of the contours. Phase averaged acoustic measurements confirm this fact. The directivity of the noise from the excited disturbance was also found to be close to the natural case for the two Strouhal numbers observed ( $St = 0.19$  and  $St = 0.38$ ). These measurements indicate that organized flow disturbances are directly responsible for a major portion of the noise radiation produced by supersonic jets.

Flow measurements of the excited disturbances demonstrate that the disturbance wavelength decreases approximately linearly with increasing Strouhal number; a trend predicted by Tam (1972) using a linear stability theory. Phase velocity calculated from the measured wavelengths show an increase in velocity at low Strouhal numbers. Above  $St = 0.38$  up to  $St = 0.84$ , the phase velocity remains approximately constant with wave speeds between  $0.76 U_0$  to  $0.81 U_0$ .

Phase averaged amplitude measurements of excited flow fluctuations in the jet shear layer show that the  $St = 0.19$  and the  $St = 0.38$  disturbances peak in amplitude near  $x/D = 6$  however, the  $St = 0.38$  disturbance decays at a considerably faster rate than the  $St = 0.19$  disturbance in the region downstream of their peak. The trends of the coherent wave evolution were noted to be in general agreement with theoretical predictions by Tam (1975).

Phase front measurements of the acoustic radiation indicate that the  $St = 0.38$  disturbance radiates noise at approximately the Mach wave angle calculated from the phase velocity of the flow disturbance. The  $St = 0.19$  disturbance radiates noise with wave fronts inclined at an angle considerably less than the Mach wave angle. These results are in agreement with acoustic phase front measurements by Morrison and McLaughlin (1979) of noise radiated by subsonically and supersonically traveling instability waves in low Reynolds number jets.

By drawing a line perpendicular to the measured wave fronts at a point near the center of the acoustic lobes, the approximate location of the noise sources in the jet can be determined. The  $St = 0.38$  noise source was found to be centered between 6 and 8 diameters downstream of the nozzle exit. The  $St = 0.19$  noise source is centered between 8 and 10 diameters downstream of the nozzle exit. Both of these locations correspond to positions in the flow where the amplitude of the fluctuations at these frequencies saturate and begin to decay.

Azimuthal acoustic measurements indicate that the noise radiation from the  $St = 0.19$  and the  $St = 0.38$  disturbances includes both antisymmetric and axisymmetric modes. The lower frequency disturbance was found to contain a considerably larger portion of the axisymmetric mode than the higher frequency disturbance.

#### 4. CONCLUSIONS

Interpretations of natural jet phenomena based on the artificially excited results of this study should be made with care. Since it was shown that excitation not only causes dramatic changes in the initial flow fluctuation spectra, but also can cause changes in the mean flow spreading rate, the exact relationship between the artificially excited flow and the natural jet are debatable. However, it does not seem unreasonable to expect that measured properties of the excited disturbances such as wavelength, interaction with the core flow, and noise generation mechanics are also characteristic of naturally occurring organized disturbances. This type of assumption has been used by previous investigators in flows of this type (Crow and Champagne 1971; and Chan 1974) and its application is favored by the authors of the present study.

Proceeding in the above discussed view, a number of important conclusions can be drawn from the measurements. The growth rates of the initial jet instabilities and the wavelengths of the coherent disturbances are in reasonable agreement with linear stability theory predictions. The measured growth and decay evolution of the coherent wave amplitude seems to be in general agreement with recent advanced stability theories developed by Morris and Tam (1977). The noise generated by the coherent disturbances is propagated in a primarily downstream direction which indicates that the lobed pattern of the SPL contours is caused by noise generated from organized disturbances. The results of phase measurements in the acoustic field indicate that while Mach wave radiation may be present, other types of large scale noise generation mechanisms are also present. Since most of the noise generated by the organized disturbances seems to originate near the region of breakdown of the coherent wave energy, it is most likely that strongly

nonlinear processes associated with large scale fluctuations are responsible for a major portion of the generated noise.

One of the more interesting results obtained in this study was the finding that artificial disturbances at two intermediate frequencies ( $St = 0.19$  and  $St = 0.33$ ) were able to affect the jet core much more efficiently than the higher and lower frequencies studied. This result is quite similar to the result first noted by Crow and Champagne (1971) in a study of a subsonic jet and later observed by other experimentalists (Chan 1974; Moore 1977; and Hussain and Zaman 1975). The numerous areas of agreement between experiment and instability theory, together with the present absence of a comprehensive prediction method for the frequency selection phenomenon of axisymmetric jets, support the need for continued development of stability type theories with application to jet flows.

#### ACKNOWLEDGEMENT

This research was supported by the National Science Foundation under Grant No. ENG 75-21405 and the National Aeronautics and Space Administration under Grant No. NSG 1467. The suggestions and assistance of Ms. E. A. Bastion, Dr. G. L. Morrison, Dr. J. M. Seiner, Mr. J. L. Stromberg and Mr. J. D. Swearingen are gratefully acknowledged.

TABLE I  
ACOUSTIC WAVELENGTH MEASUREMENTS

St	$\frac{\lambda_d}{D}$	$\frac{\lambda_x}{D}$	$\frac{\lambda_y}{D}$	$\mu$ degrees	$\alpha$ degrees	$c_a$ m/sec	$a_o$ m/sec
0.19	3.85	4.35	4.87	63	48	324.	344.
0.38	2.11	2.10	3.15	54	56	342.	344.

## REFERENCES

- BISHOP, K. A., FLOWCS WILLIAMS, J. E. & SMITH, W. 1971 On the noise sources of the unsuppressed high-speed jet. *J. Fluid Mech.*, 50, 21-31.
- BROWAND, F. K. 1966 An experimental investigation of the instability of an incompressible, separated shear layer. *J. Fluid Mech.*, 26, part 2, 281-307.
- CHAN, Y. Y. 1974 Spatial waves in turbulent jets. *Physics of Fluids*, 17, 46-53.
- CRIGHTON, D. G. & GASTOR, M. 1976 Stability of slowly diverging jet flow. *J. Fluid Mech.*, 77, 397-413.
- CROW, S. C. & CHAMPAGNE, F. H. 1971 Orderly structure in jet turbulence. *J. Fluid Mech.*, 48, 547-591.
- DAHAN, P. C. & ELIAS, G. 1976 Source structure pattern in a hot jet by infrared-microphone correlation. AIAA Paper No. 76-542.
- DOSANJH, D. S. & YU, J. C. 1968 Noise from underexpanded axisymmetric jet flow using radial jet flow impingement. Proceedings, AFOSR-UTIAS Symposium on Aerodynamic Noise, Toronto, 169-188.
- DUTT, B. 1977 Role of large scale structures in the noise generation of a turbulent supersonic jet. Ph.D. Dissertation, University of Southern California.
- FLOWCS WILLIAMS, J. E. 1963 The noise from turbulence convected at high speed. *Phil. Trans. A* 255, 459.
- HUSSAIN, A. K. M. F. & ZAMAN, K. B. M. Q. 1975 Effect of acoustic excitation on the turbulent structure of a circular jet. Proceedings of the Third Interagency Symposium on University Research in Transportation Noise, University of Utah, Salt Lake City, Utah.
- JOHNSON, C. B. & BONEY, L. R. 1975 A method for calculating a real-gas two-dimensional nozzle contour including the effects of gamma. NASA TM X-3243, Langley Research Center, Hampton, Virginia.

- KENDALL, J. M. 1967 Supersonic boundary layer stability experiments. Proc. Boundary Layer Trans. Study Group, Meeting, II, Aerospace Rep. TR-0158 (S3816-63)-1.
- KIBENS, V. 1979 Discrete noise spectrum generated by an acoustically excited jet. AIAA Paper No. 79-0592.
- KO, C. L., MCLAUGHLIN, D. K. & TROUTT, T. R. 1978 Supersonic hot-wire fluctuation data analysis with a conduction end-loss correction. J. Phys. E: Sci. Instrum., 11, 488-494.
- LAU, J. C., FISHER, M. J. & FUCHS, H. V. 1972 The intrinsic structure of turbulent jets. J. Sound and Vibration, 22, 379-406.
- LAUFER, J., KAPLAN, R. E., & CHU, W. T. 1973 Acoustic modeling of the jet noise abatement problem. Proceedings of the Interagency Symposium on University Research in Transportation Noise, Stanford, California.
- LAUFER, J., SCHLINKER, R. S., & KAPLAN, R. E. 1976 Experiments on supersonic jet noise. AIAA Journal, 14, 489-497.
- LIU, J. T. C. 1974 Developing large-scale wavelike eddies and the near jet noise field. J. Fluid Mech., 62, 437-464.
- LOWSON, M. V., & OLLERHEAD, J. B. 1968 Visualization of noise from cold supersonic jets. J. Acoust. Soc. Am., 44, 624.
- MAESTRELLO, L. 1976 Two point correlation of sound pressure in the far field of a jet: Experiment. NASA TM-72835.
- MCLAUGHLIN, D. K., MORRISON, G. L. & TROUTT, T. R. 1975 Experiments on the instability waves in a supersonic jet and their acoustic radiation. J. Fluid Mech., 69, 73-95.
- MCLAUGHLIN, D. K., MORRISON, G. L. & TROUTT, T. R. 1977 Reynolds number dependence in supersonic jet noise. A.I.A.A. J., 15, 526-532.
- MCLAUGHLIN, D. K., SEINER, J. M. & LIU, C. H. 1979 On noise generated by large scale instabilities in supersonic jets. NASA Report, in preparation.

- MERKINE, L. O. & LIU, T. T. C. 1975 On the development of noise-producing large-scale wavelike eddies in a plane turbulent jet. *J. Fluid Mech.*, 70, 353-368.
- MICHALKE, A. 1969 Sound generation by amplified disturbances in free shear layers. Deutsche Luft-und Raumfahrt Rep. no. 69-90.
- MIKSAD, R. W. 1972 Experiments on the nonlinear states of free-shear-layer transition. *J. Fluid Mech.*, 56, 695-719.
- MOLLO-CHRISTENSEN, E. 1960 Some aspects of free shear-layer instability and sound emission. *Nato Report* 260.
- MOLLO-CHRISTENSEN, E. 1967 Jet noise and shear flow instability seen from an experimenter's viewpoint. *J. Applied Mech.*, 34, 1-7.
- MOORE, C. J. 1977 The role of shear-layer instability waves in jet exhaust noise. *J. Fluid Mech.*, 80, Part 2, 321-357.
- MORRIS, P. J. 1977 Flow characteristics of the large scale wavelike structure of a supersonic round jet. *J. Sound and Vibration*, 53, 223-244.
- MORRIS, P. J. & TAM, C. K. W. 1977 Near and far field noise from large-scale instabilities of axisymmetric jets. *A.I.A.A. Paper No.* 77-1351.
- MORRIS, P. J. & TAM, C. K. W. 1979 Private communication.
- MORRISON, G. L. 1977 Flow instability and acoustic radiation measurements of low Reynolds number supersonic jets, Ph.D. Dissertation. Oklahoma State University, Stillwater, Oklahoma.
- MORRISON, G. L. & MCLAUGHLIN, D. K. 1979 The noise generation by instabilities in low Reynolds number supersonic jets. *J. Sound and Vibration*, 65, 177-191.
- PHILLIPS, O. M. 1960 On the generation of sound by supersonic turbulent shear layers. *J. Fluid Mech.* 9, 1-28.
- POTTER, R. C. 1968 An investigation to locate the acoustic sources in a high speed jet exhaust stream. *Wyle Lab. Tech. Report* WR 68-4.

- ROSE, W. C. 1973 The behavior of a compressible turbulent boundary layer in a shock-wave-induced adverse pressure gradient. NASA TN D-7092.
- SALANT, R. F. 1973 Investigation of jet noise using optical holography. Department of Transportation Report No. DOT-TSC-OST-73-11.
- SEDEL'NIKOV, T. K. 1967 The frequency spectrum of the noise of a supersonic jet. Phy. Aero. Noise. Moscow: Nauka. (Trans. 1969 N.A.S.A. TTF-538, 71-75.)
- STROMBERG, J. L., MCLAUGHLIN, D. K., & TROUTT, T. R. 1979 Flowfield and acoustic properties of a Mach number 0.9 jet at a low Reynolds number. A.I.A.A. Paper No. 79-0593.
- TAM, C. K. W. 1971 Directional acoustic radiation from a supersonic jet generated by shear layer instability. J. Fluid Mech., 46, 757-768.
- TAM, C. K. W. 1972 On the noise of a nearly ideally expanded supersonic jet. J. Fluid Mech., 51, 69-95.
- TAM, C. K. W. 1975 Supersonic jet noise generated by large scale disturbances. J. Sound and Vibration, 38, 51-79.
- TROUTT, T. R. 1978 Measurements on the flow and acoustic properties of a moderate Reynolds number supersonic jet. Ph.D. Dissertation, Oklahoma State University, Stillwater, Oklahoma.
- YU, J. C. & DOSANJH, D. S. 1973 Noise field of supersonic Mach 1.5 cold model jet. J. Acoust. Soc. Am., 51, 1400-1410.

## LIST OF FIGURES

- Figure 1. (a) Schematic diagram of the jet test chamber.  
(b) Coordinate system.
- Figure 2. Distribution of mean Mach number on the jet centerline.
- Figure 3. Radial Mach number profiles.  $x/D$ : (a) 1, (b) 5, (c) 10, (d) 15.
- Figure 4. Mean velocity data.  $x/D$ :  $\square$  1,  $\bullet$  5,  $\Delta$  10,  $\square$  15.
- Figure 5. Axial distribution of mean velocity profile parameters.  
(a)  $M = 2.1$ ,  $Re = 70,000$ , (b)  $M = 2.0$ ,  $Re = 5,200,000$ , (c)  $M = 2.1$ ,  $Re = 7900$ . —  $\delta/2D$ ; ---  $r(.5)/D$ .
- Figure 6. Hot-wire spectra at several axial locations in the jet shear layer.  
 $x/D$ : (a) 1, (b) 2, (c) 3, (d) 4, (e) 5, (f) 6, (g) 8, (h) 10.
- Figure 7. Radial profiles of mass velocity fluctuation amplitude.  
 $x/D$ : (a) 1, (b) 3, (c) 6, (d) 9, (e) 12, (f) 15.
- Figure 8. Overall mass velocity fluctuation amplitude in the jet shear layer.  
 $Re$ :  $\bullet$  70,000,  $\square$  7900, Morrison (1977).
- Figure 9. Band-passed mass velocity fluctuation amplitude in the jet shear layer.  $St$ :  $\square$  0.09,  $\square$  0.19,  $\bullet$  0.38,  $\Delta$  0.76.
- Figure 10. Initial mass velocity fluctuation growth rates.  $\square$  present experiments; — Tam (1972) prediction.
- Figure 11. Overall sound pressure level contours. —  $Re = 70,000$ ;  
----  $Re = 7,900$ , Morrison and McLaughlin (1979).
- Figure 12. Directivity plot of overall sound pressure level,  $R/D = 40$ .  
 $\square$   $M = 2.1$ ,  $Re = 7900$ ,  $\bullet$   $M = 2.1$ ,  $Re = 70,000$ ,  $\square$   $M = 2.0$ ,  $Re = 5.2 \times 10^6$ .
- Figure 13. Microphone spectra,  $r/D = 8$ .  $x/D$ : (a) 4, (b) 8, (c) 12, (d) 16, (e) 20, (f) 24, (g) 28.

Figure 14. Acoustic spectra in the major noise emission direction.

(a)  $M = 2.0$ ,  $Re = 2.6 \times 10^6$ , (b)  $M = 2.1$ ,  $Re = 70,000$ ,

(c)  $M = 2.1$ ,  $Re = 7900$ .

Figure 15. Band-passed sound pressure level contours.

(a)  $St = 0.15 - 0.23$ , (b)  $St = 0.30 - 0.45$ .

Figure 16. Hot-wire spectra in jet shear layer; jet excited at  $St = 0.38$ .

$x/D$ : (a) 1, (b) 3, (c) 6, (d) 8, (e) 10.

Figure 17. Radial profile of mass velocity fluctuation amplitude,  $x/D = 1$ ;

jet excited at  $St = 0.19$ .

Figure 18. Band-passed mass velocity fluctuation amplitude on the jet

centerline. Excitation  $St$ :  $\square$  0.09,  $\circ$  0.19,  $\bullet$  0.38,  $\Delta$  0.57.

Figure 19. Axial distribution of mean velocity profile parameters.

$\circ$  —  $\square$ , natural jet;  $\bullet$  —  $\bullet$  excited jet.

Figure 20. Overall sound pressure level contours; jet excited at  $St = 0.19$ .

Figure 21. Overall sound pressure level directivity,  $R/D = 24$ .  $\circ$  natural jet;

$\bullet$  excited jet.

Figure 22. Band-passed sound pressure level contours for excited jet.

(a)  $St = 0.15 - 0.23$ , excited at  $St = 0.19$ ; (b)  $St = 0.30 - 0.45$ ,  
excited at  $St = 0.38$ .

Figure 23. Band-passed sound pressure level directivity plots.  $\circ$  Natural jet;

$\bullet$  Excited jet. Excitation  $St$ : (a) 0.19 (b) 0.38.

Figure 24. Flow disturbance phase angle; jet excited at  $St = 0.38$ .

Figure 25. Axial wavenumber of excited disturbance.  $\circ$  present experiment;

— Tam (1972) prediction.

Figure 26. Axial phase velocity of excited disturbance.

Figure 27. Coherent mass velocity fluctuation amplitude in jet shear layer.

$St$  component:  $\circ$  0.19,  $\bullet$  0.38.

Figure 28. Coherent sound pressure level;  $r/D = 8$ . St component: 0 0.19,  
● 0.38.

Figure 29. Schematic of the orientation of the flow disturbance and acoustic waves.

Figure 30. Coherent sound pressure fluctuation amplitude and phase angle as a function of azimuthal angle. 0, ● Experimental data,  
—— numerical curve fit. St component: 0 0.19, ● 0.38.

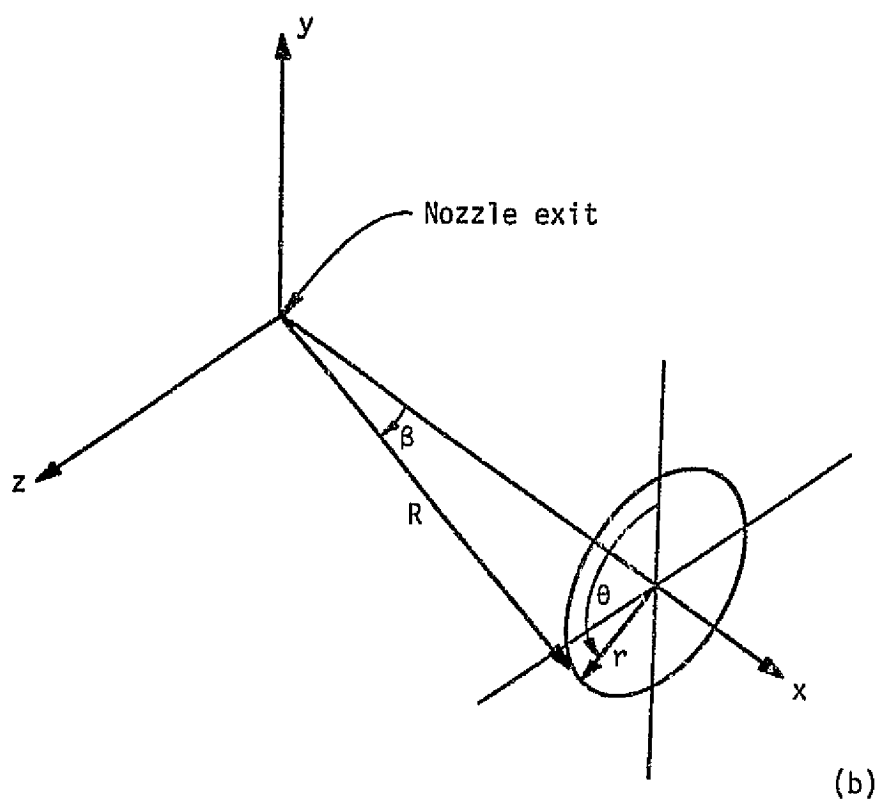
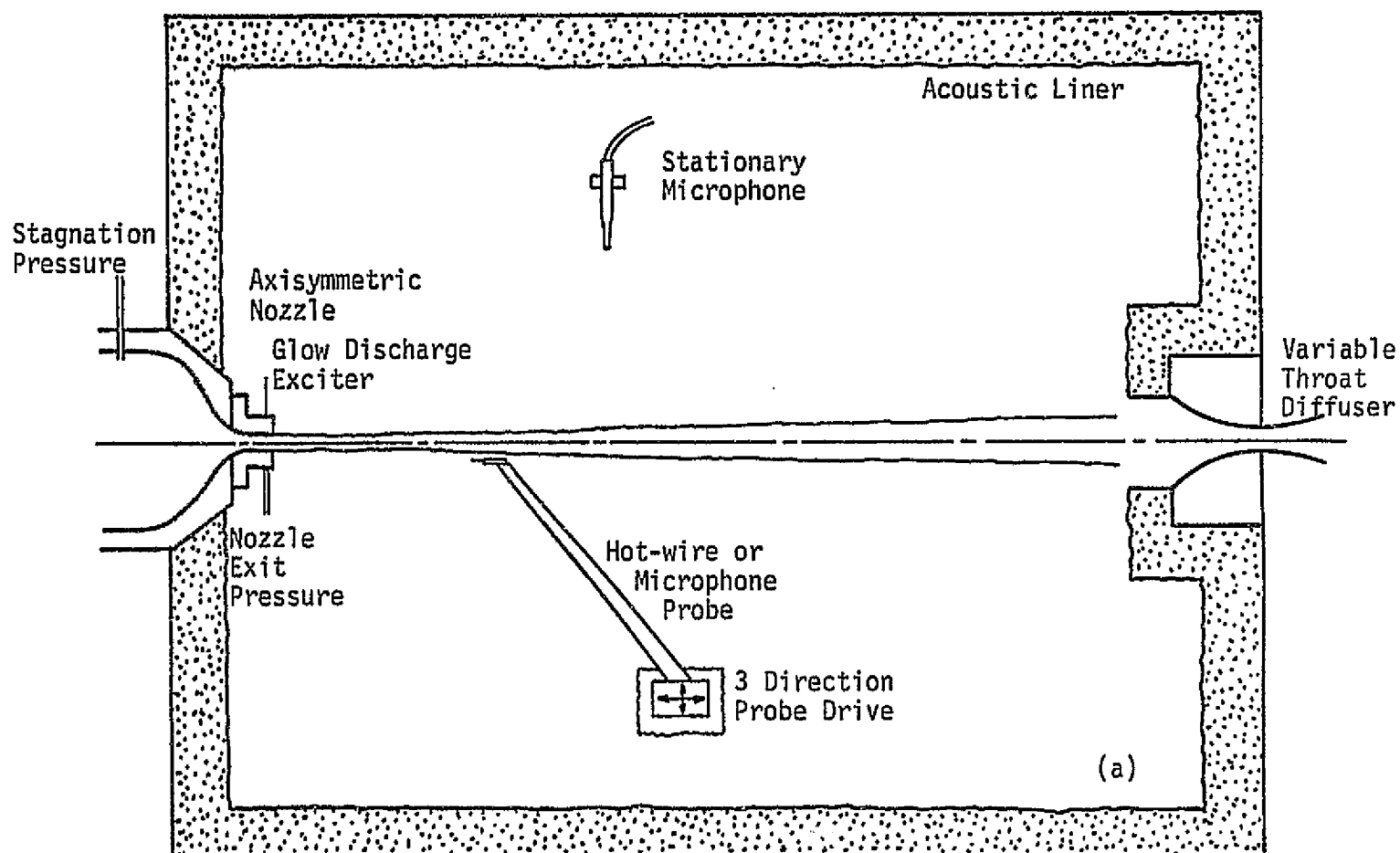


Figure 1. (a) Schematic diagram of the jet test chamber.  
(b) Coordinate system.

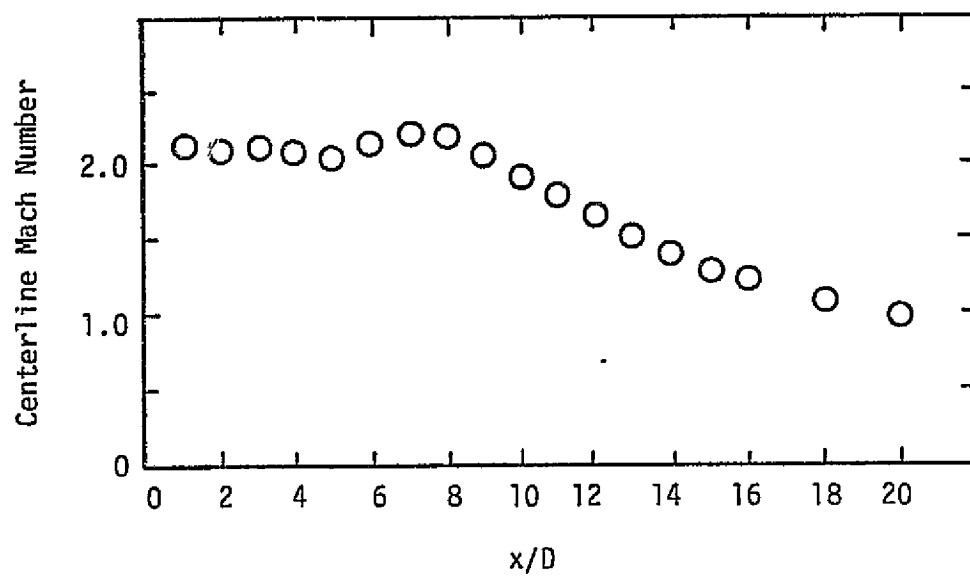


Figure 2. Distribution of mean Mach number on the jet centerline.

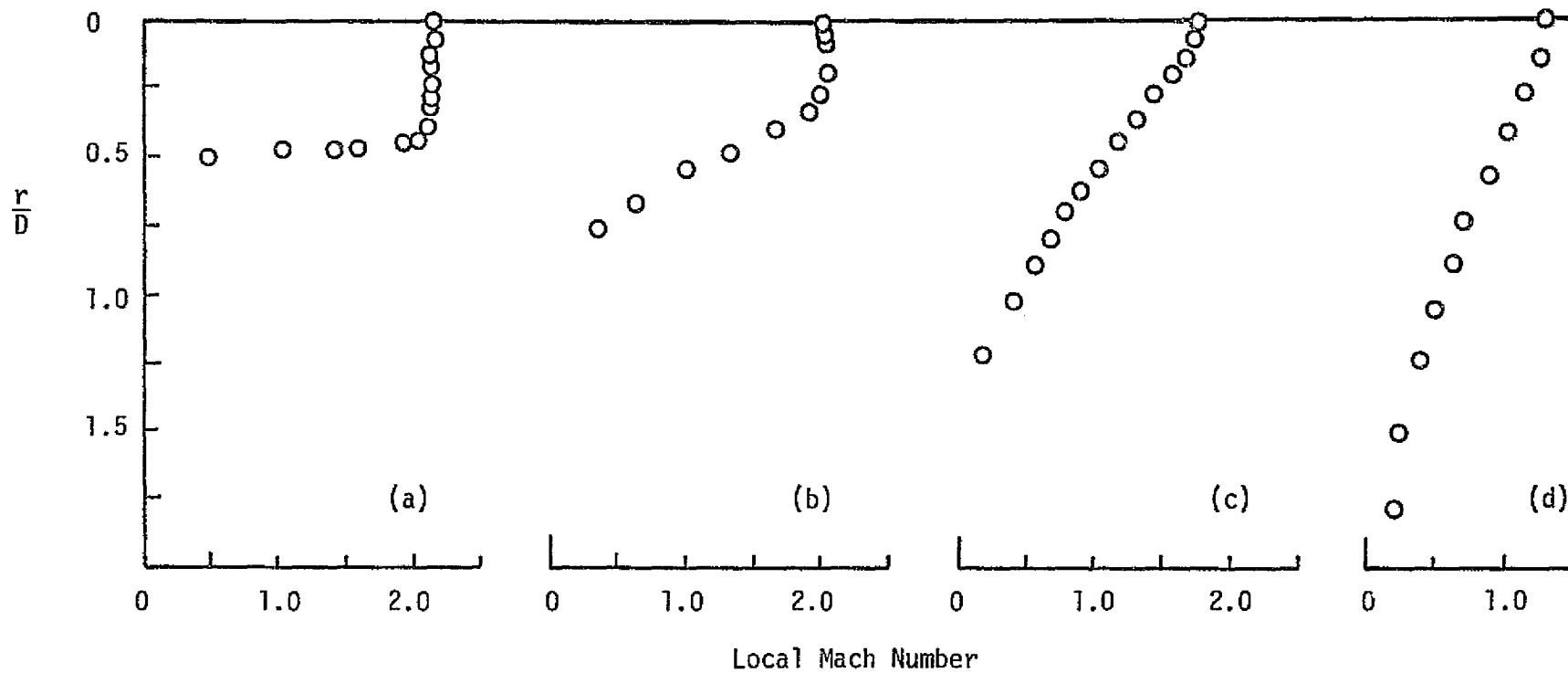


Figure 3. Radial Mach number profiles.  $x/D$ : (a) 1, (b) 5, (c) 10, (d) 15.

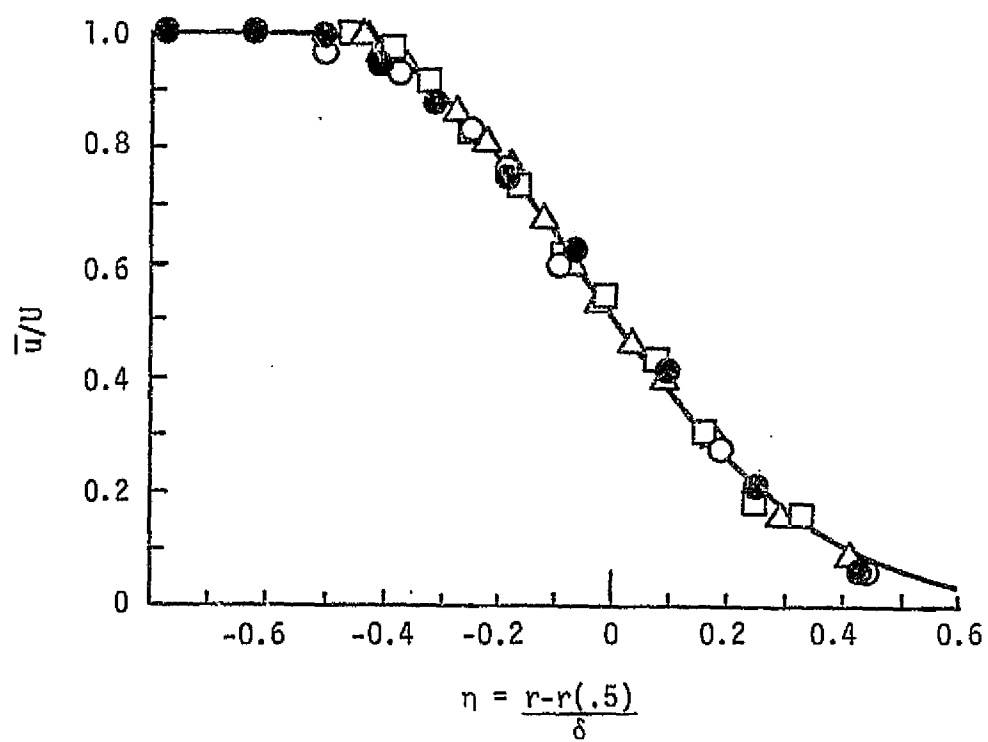


Figure 4. Mean velocity data.  $x/D$ : 0.1, 0.5,  $\Delta$  10, 15.

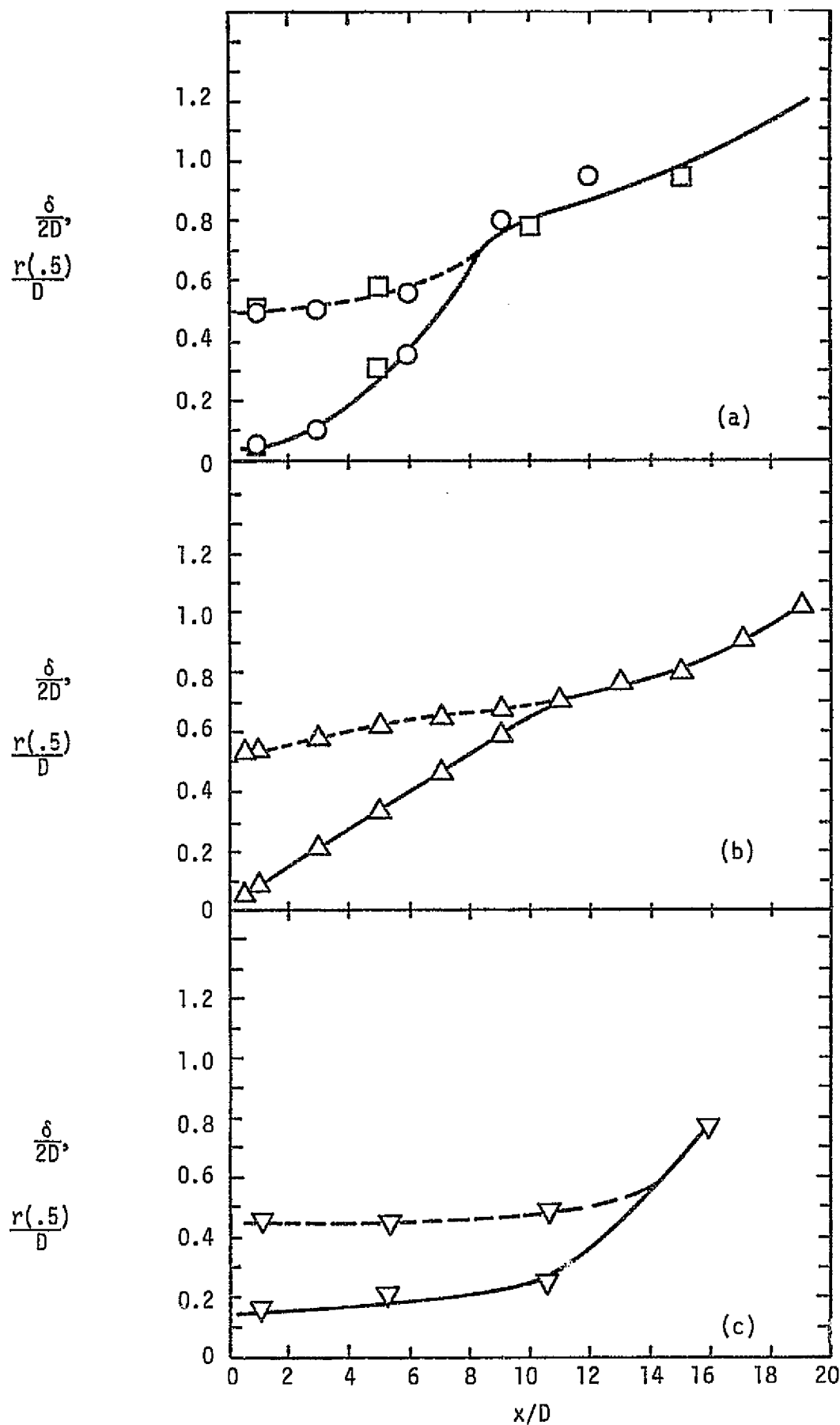


Figure 5. Axial distribution of mean velocity profile parameters.  
 (a)  $M = 2.1, Re = 70,000$ , (b)  $M = 2.0, Re = 5,200,000$ ,  
 (c)  $M = 2.1, Re = 7900$ . —  $\delta/2D$ ; ---  $r(.5)/D$ .

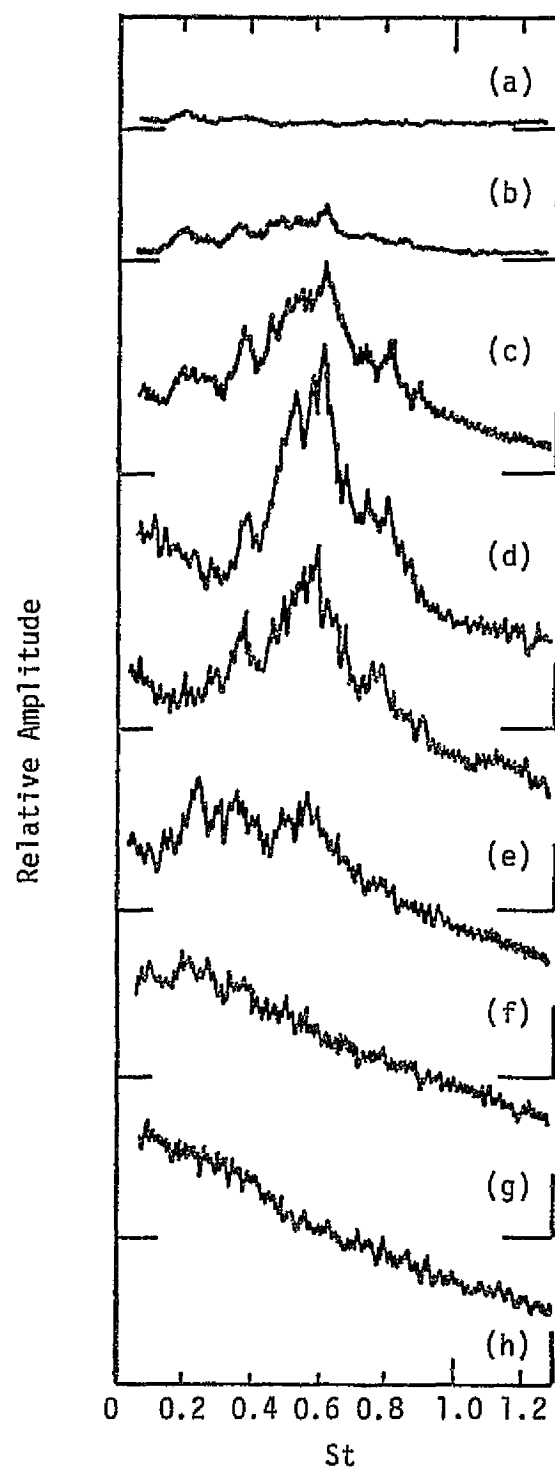


Figure 6. Hot-wire spectra at several axial locations in the jet shear layer.  $x/D$ : (a) 1, (b) 2, (c) 3, (d) 4, (e) 5, (f) 6, (g) 8, (h) 10.

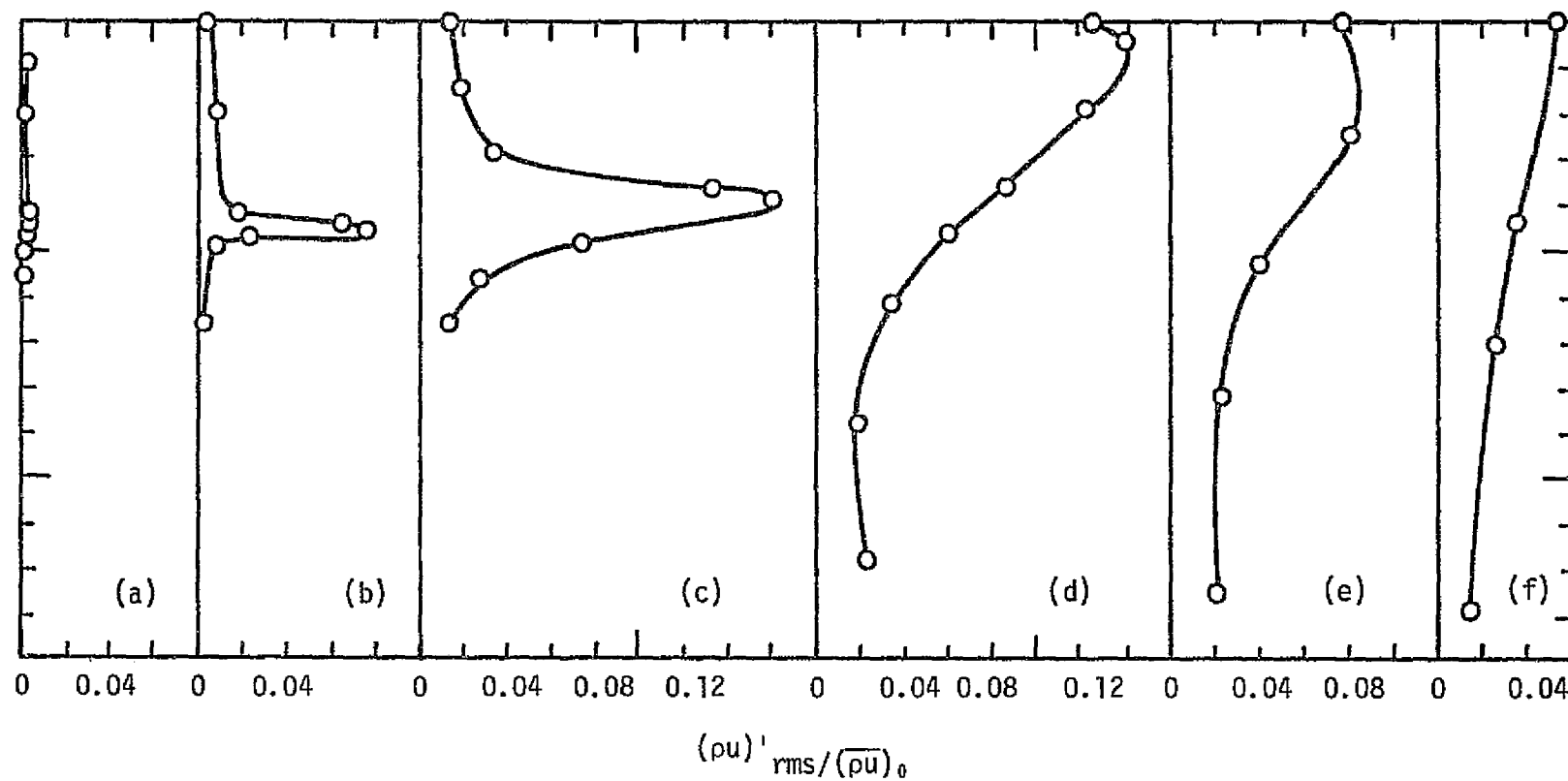


Figure 7. Radial profiles of mass velocity fluctuation amplitude.

$x/D$ : (a) 1, (b) 3, (c) 6, (d) 9, (e) 12, (f) 15.

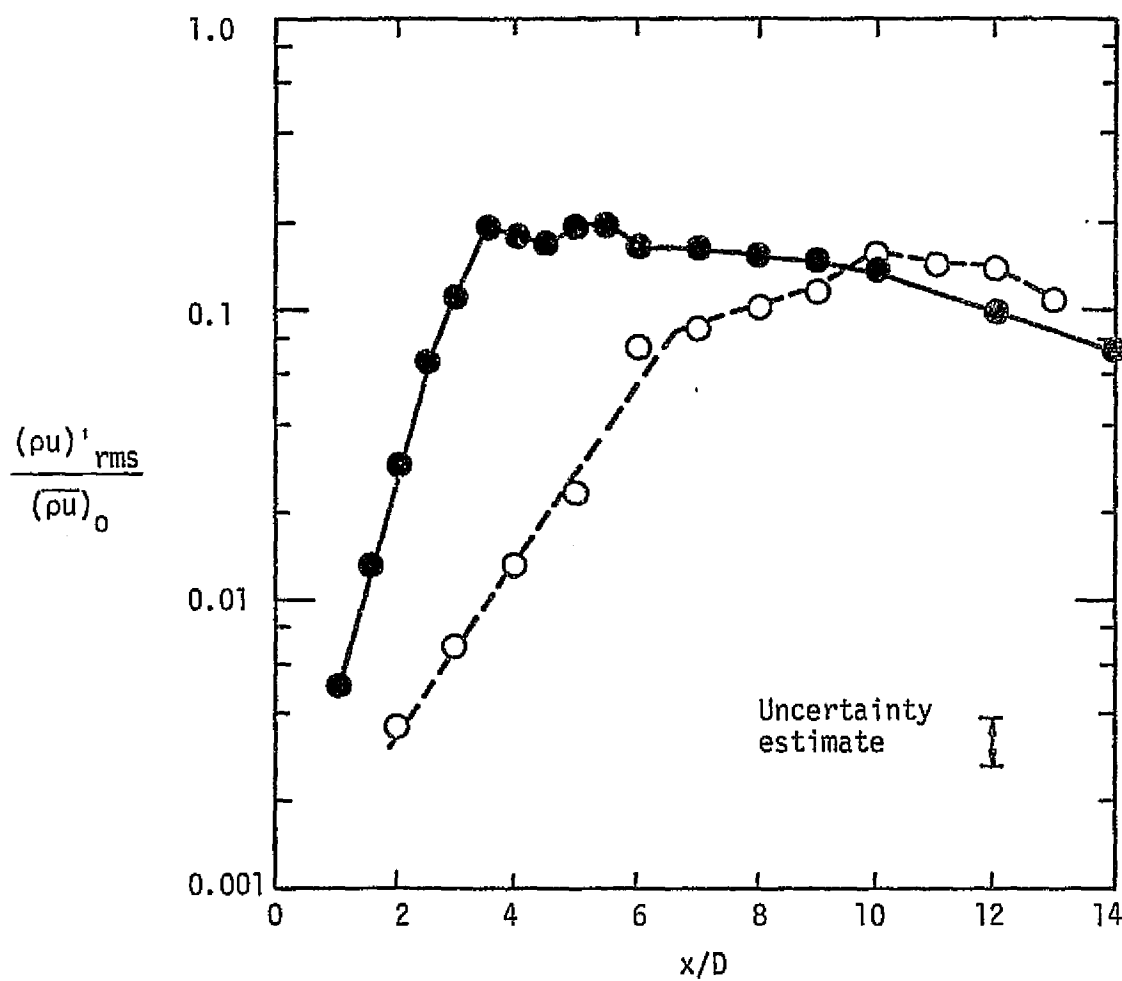


Figure 8. Overall mass velocity fluctuation amplitude in the jet shear layer. Re: 0 70,000, 0 7900, Morrison (1977).

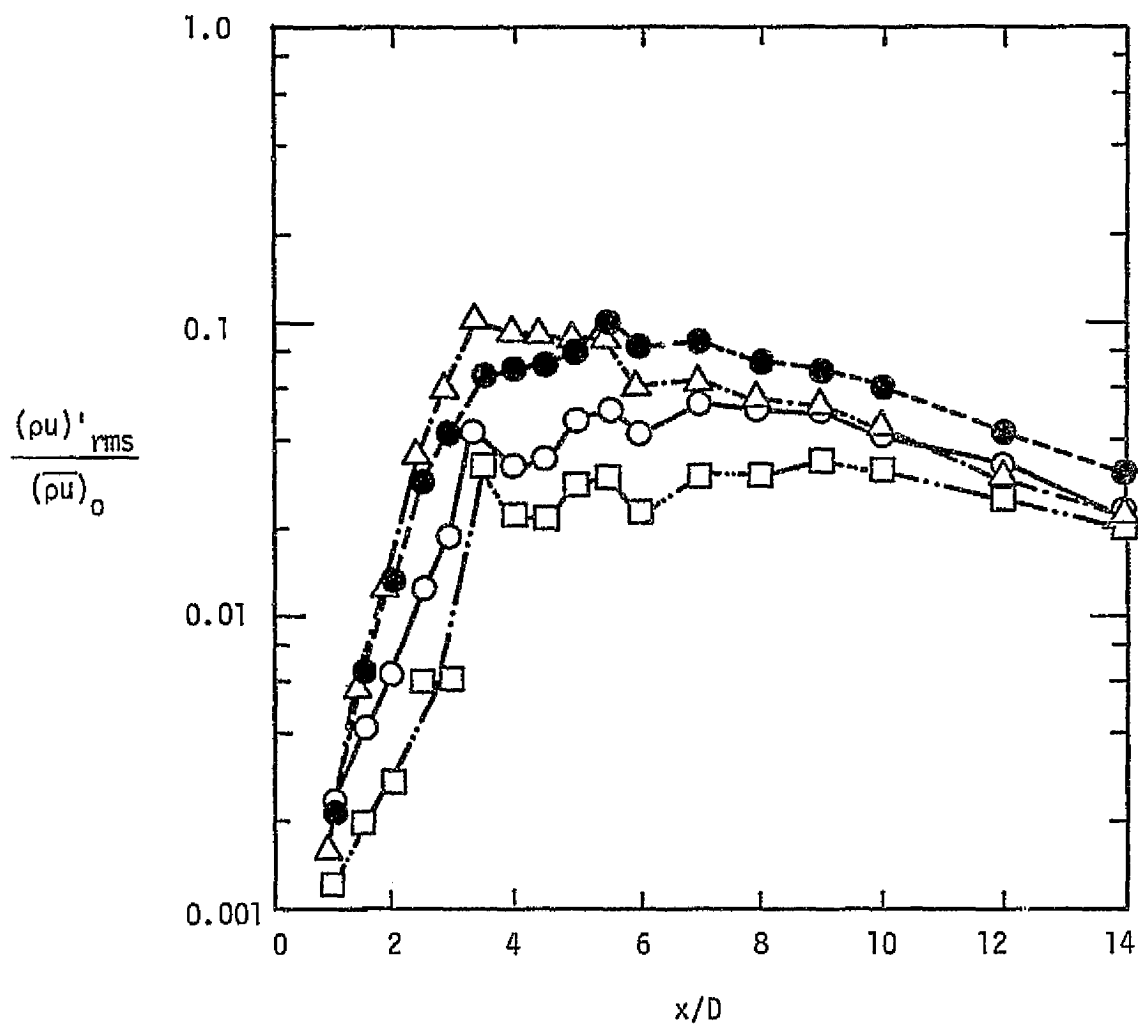


Figure 9. Band- passed mass velocity fluctuation amplitude in the jet shear layer. St:  $\square$  0.09,  $\circ$  0.19,  $\bullet$  0.38,  $\triangle$  0.76.

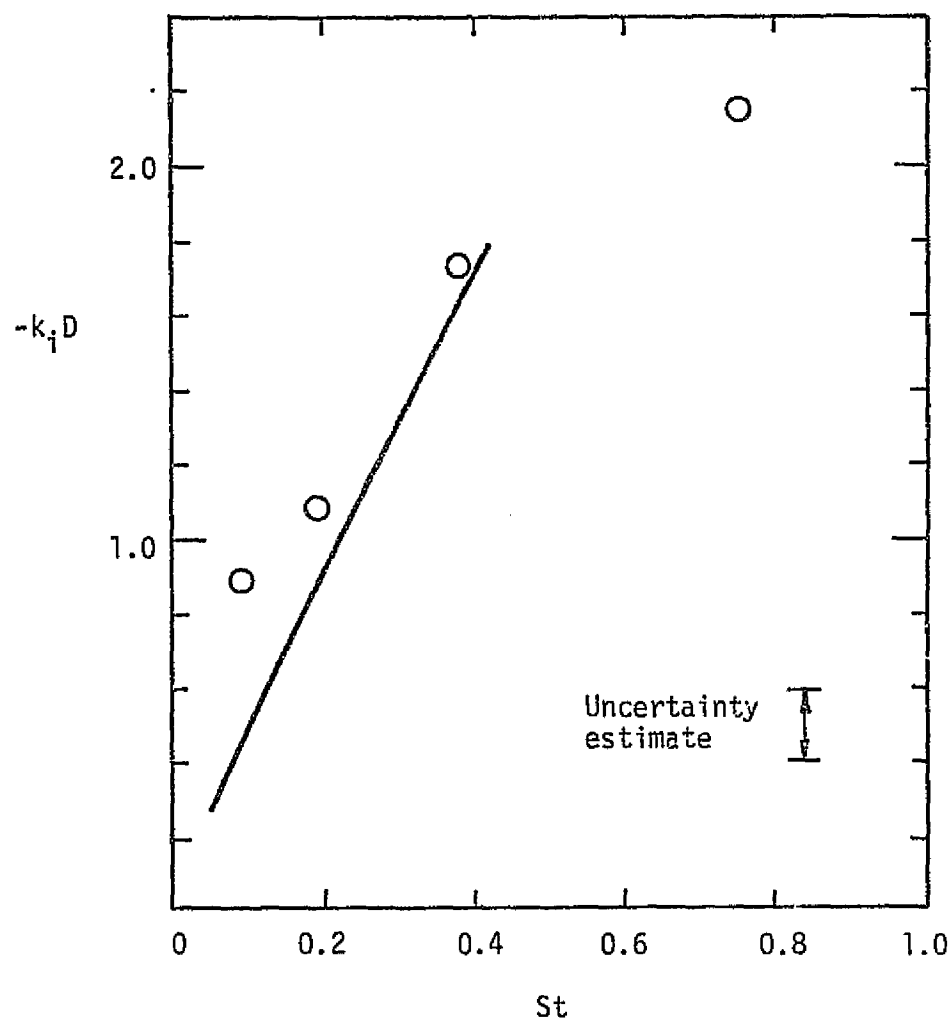


Figure 10. Initial mass velocity fluctuation growth rates.  
 O present experiments; — Tam (1972)  
 prediction.

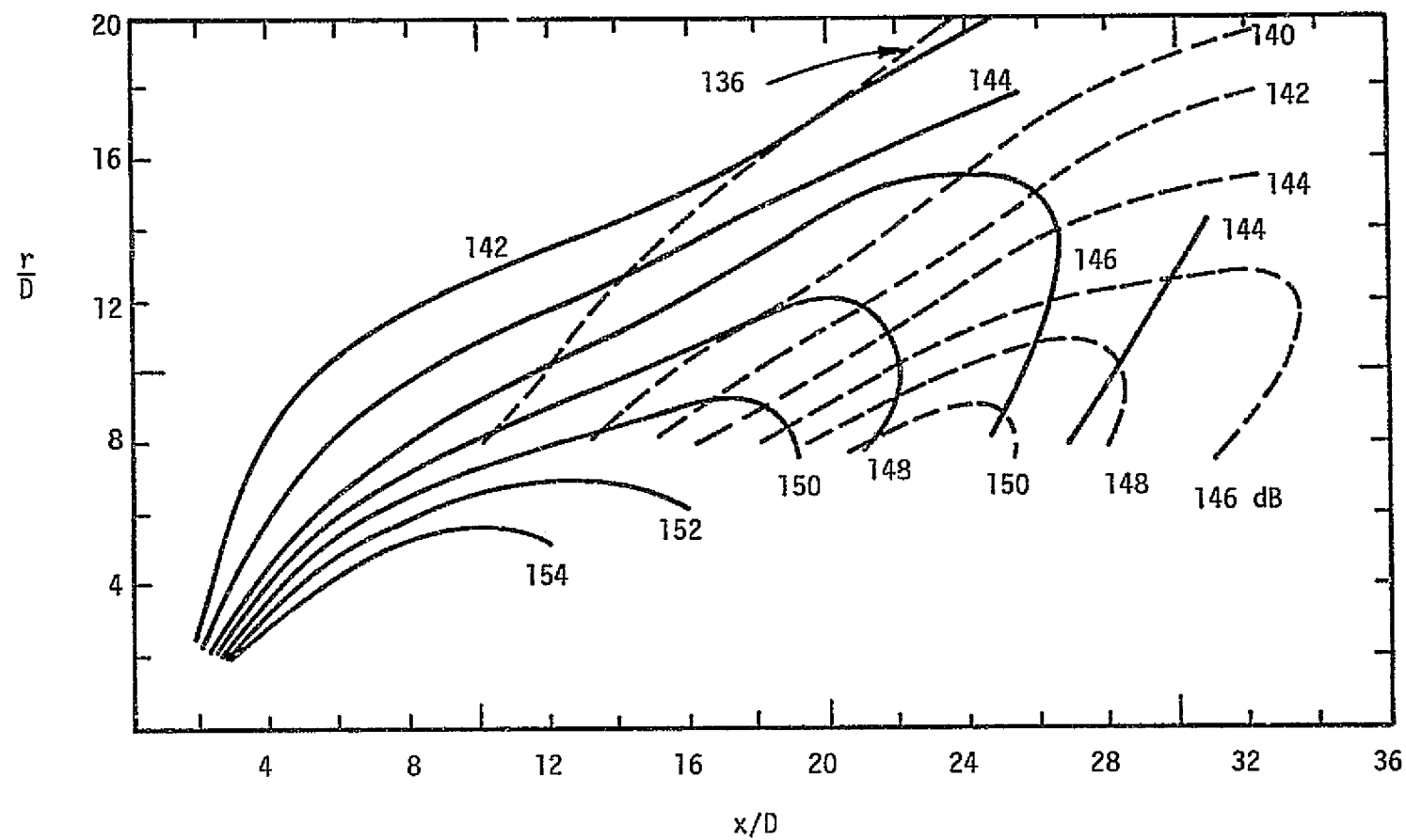


Figure 11. Overall sound pressure level contours. —  $Re = 70,000$ ; ---  $Re = 7900$ , Morrison and McLaughlin (1979).

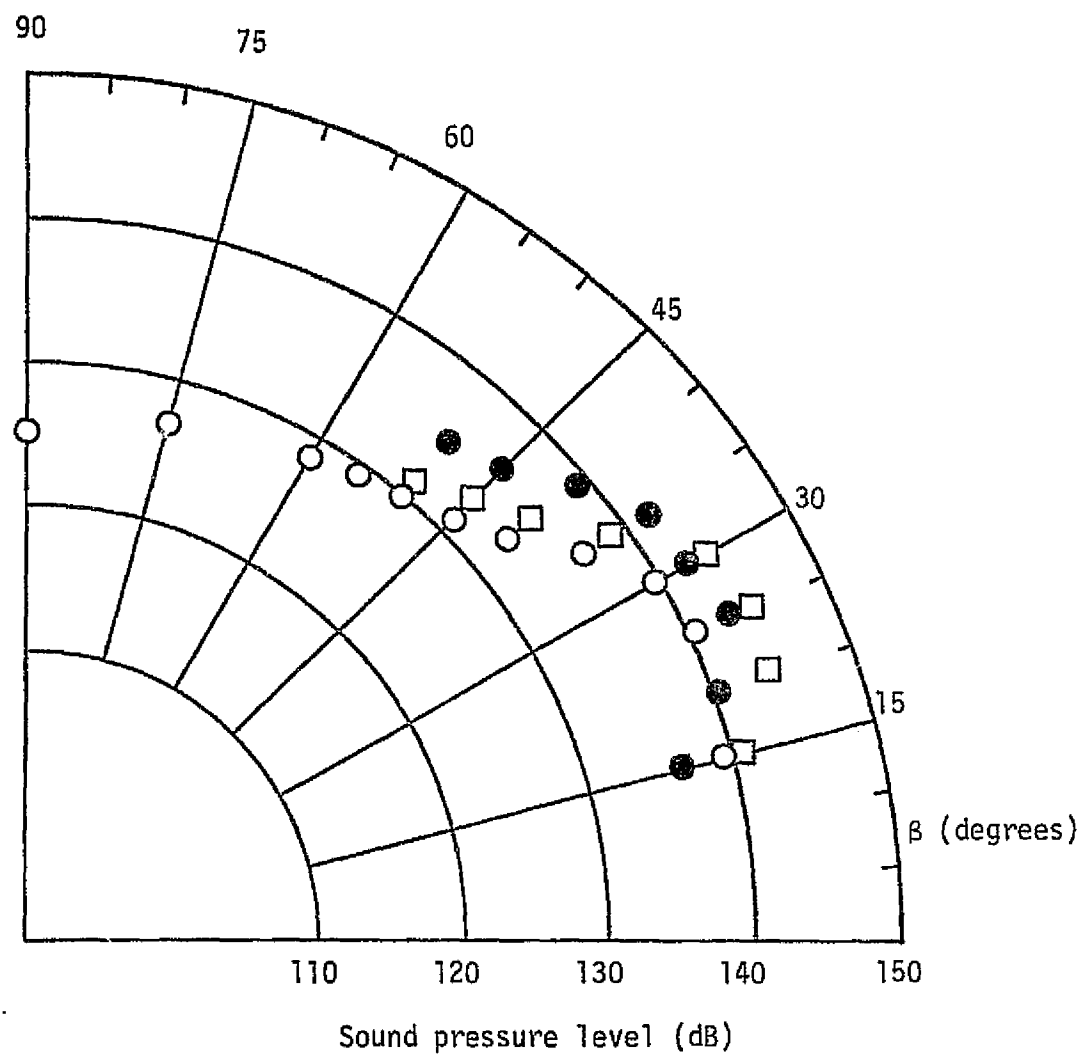


Figure 12. Directivity plot of overall sound pressure level,  
 $R/D = 40$ .  $\square$   $M = 2.1$ ,  $Re = 7900$ ,  $\bullet$   $M = 2.1$ ,  $Re = 70,000$ ,  
 $\circ$   $M = 2.0$ ,  $Re = 5.2 \times 10^6$ .

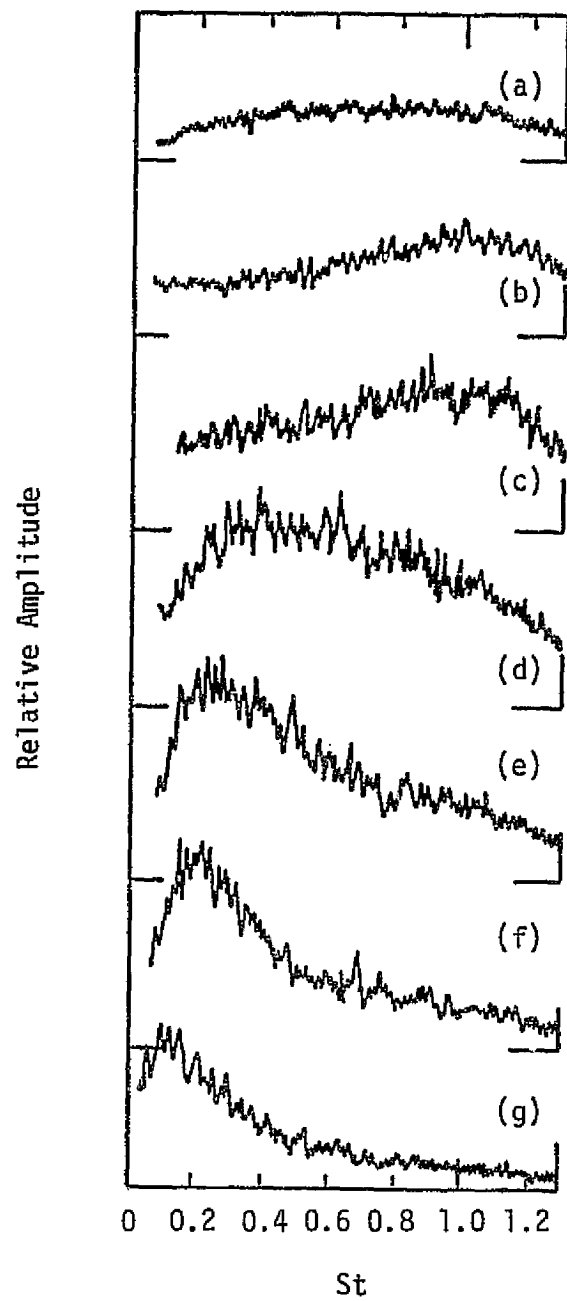


Figure 13. Microphone spectra,  $r/D = 8$ .

$x/D$ : (a) 4, (b) 8, (c) 12,

(d) 16, (e) 20, (f) 24, (g) 28.

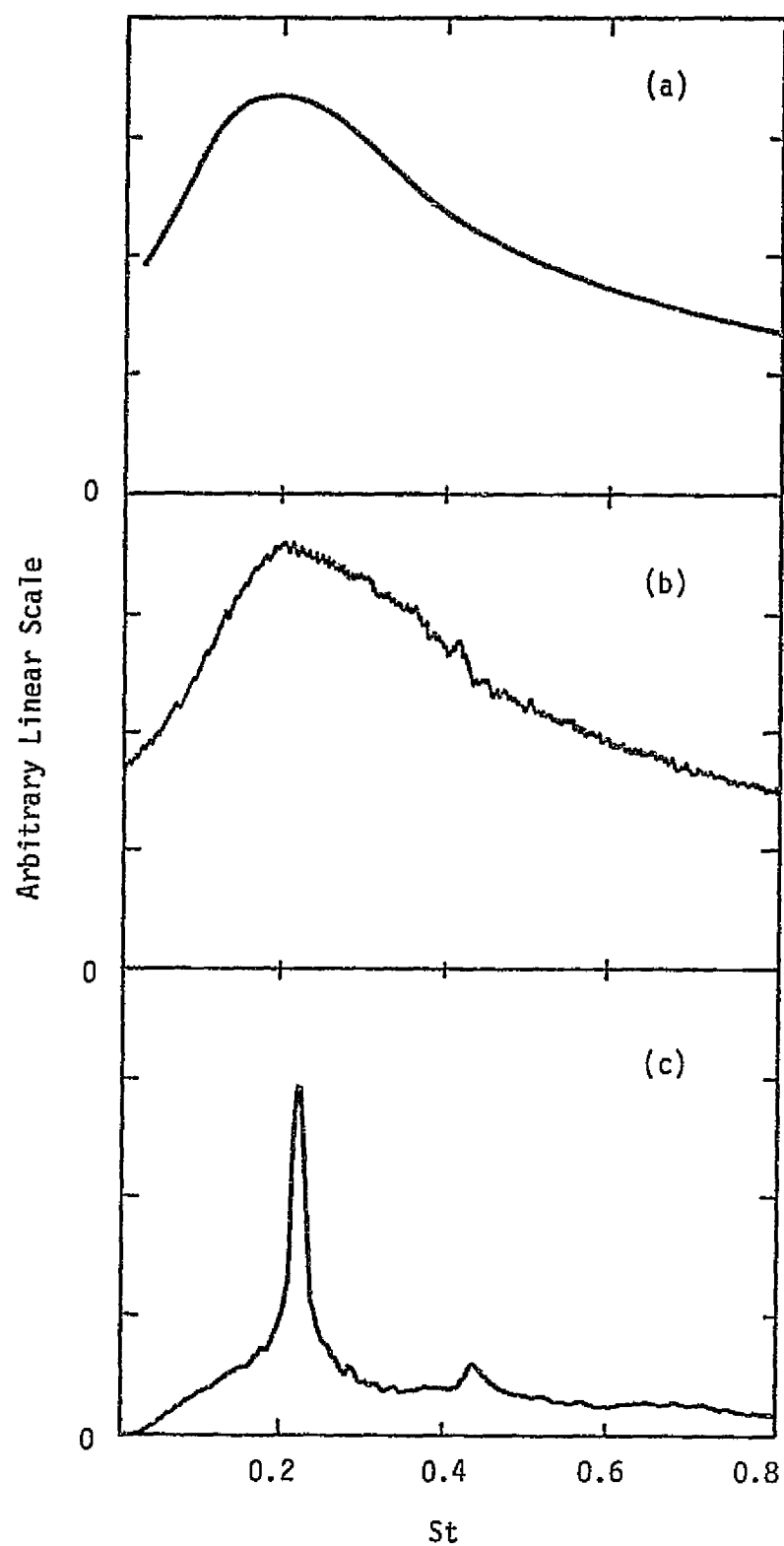


Figure 14. Acoustic spectra in the major noise emission direction. (a)  $M = 2.0$ ,  $Re = 2.6 \times 10^6$ , (b)  $M = 2.1$ ,  $Re = 70,000$ , (c)  $M = 2.1$ ,  $Re = 7900$ .

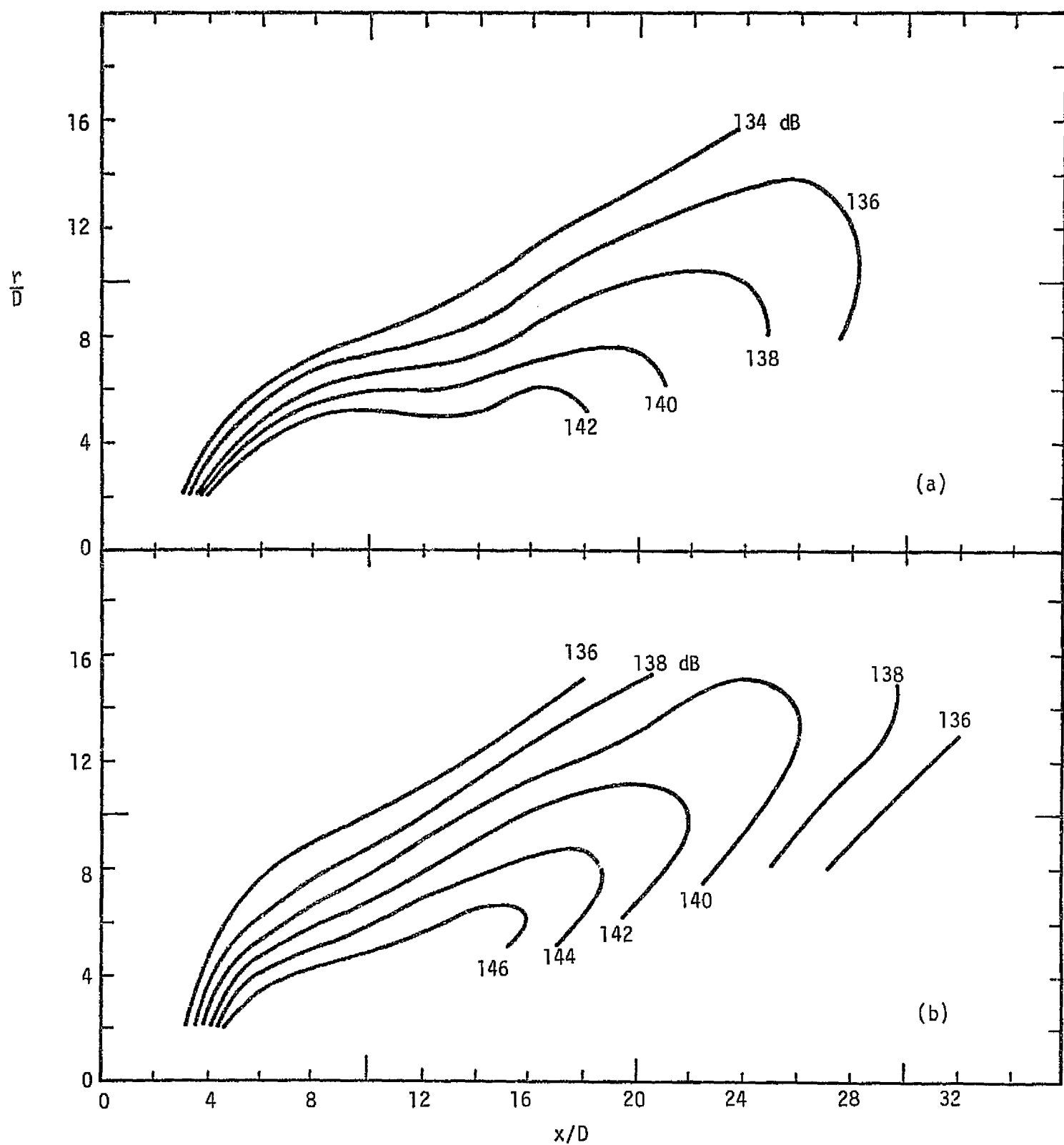


Figure 15. Band-passed sound pressure level contours. (a)  $St = 0.15 - 0.23$ ,  
(b)  $St = 0.30 - 0.45$ .

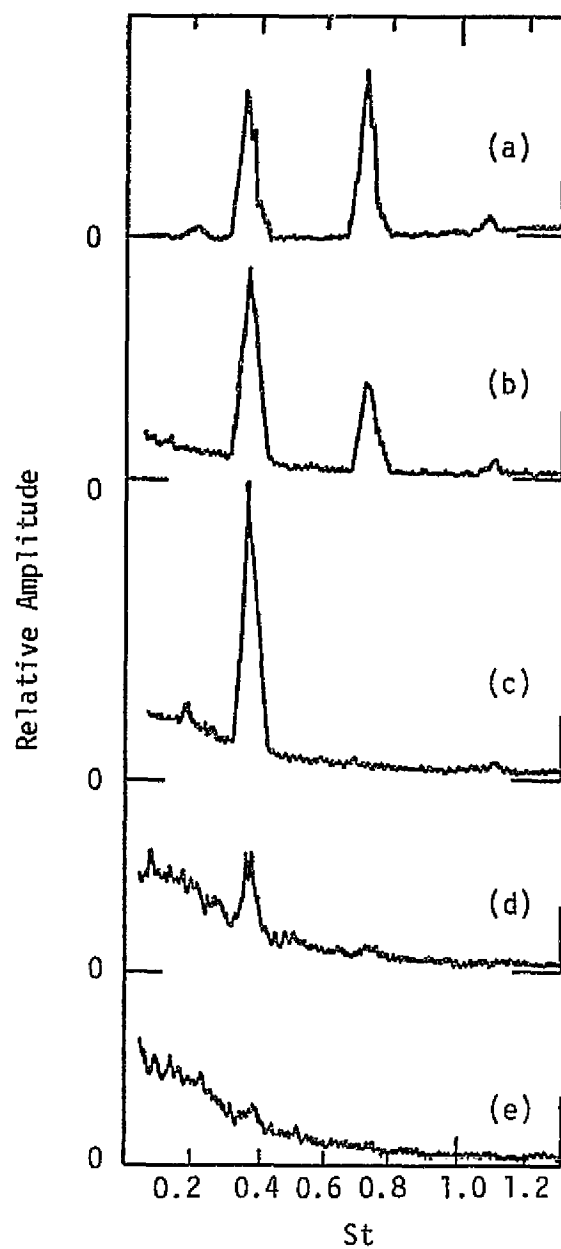


Figure 16. Hot-wire spectra in jet shear layer; jet excited at  $St = 0.38$ .  $x/D$ : (a) 1, (b) 3, (c) 6, (d) 8, (e) 10.

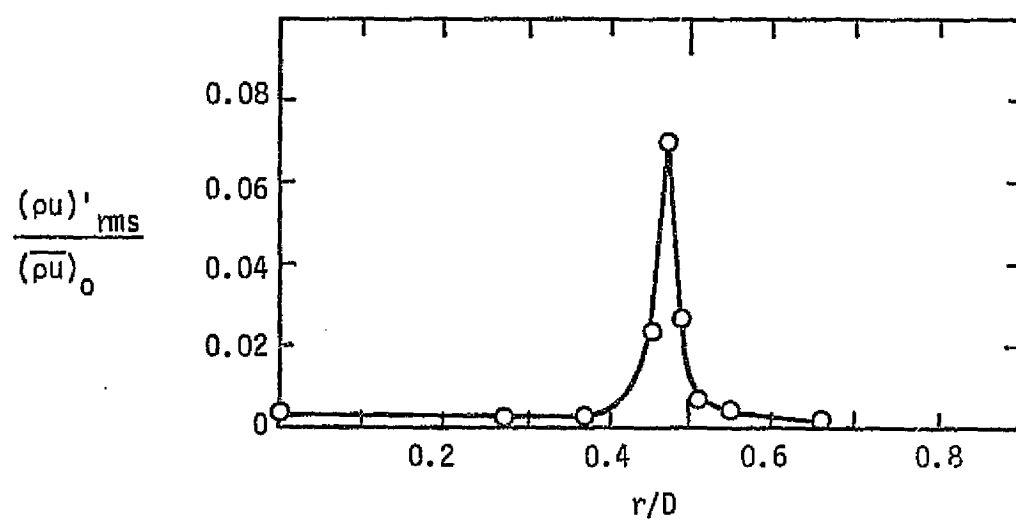


Figure 17. Radial profile of mass velocity fluctuation amplitude,  $x/D = 1$ ; jet excited at  $St = 0.19$ .

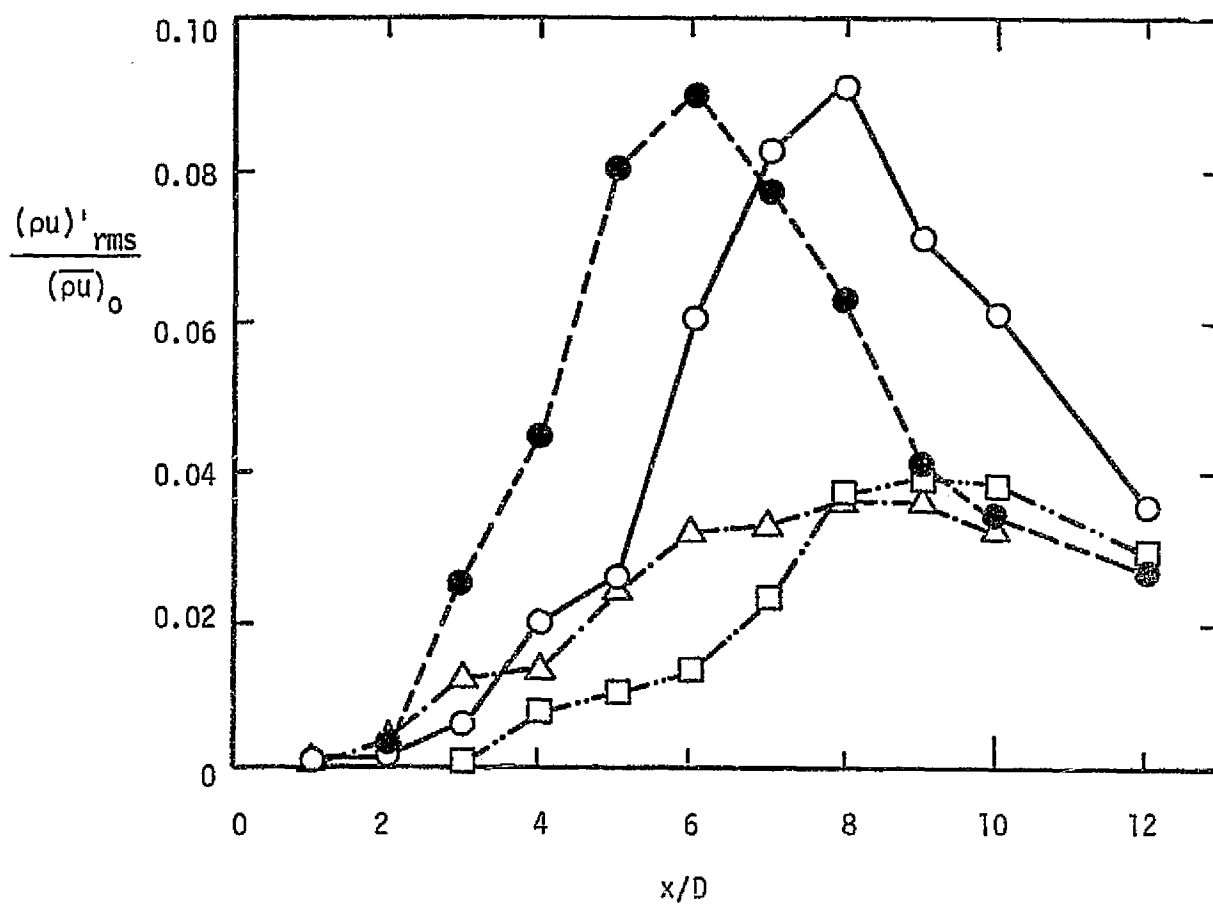


Figure 18. Band-passed mass velocity fluctuation amplitude on the jet centerline. Excitation St: □ 0.09, ○ 0.19, ● 0.38, △ 0.57.

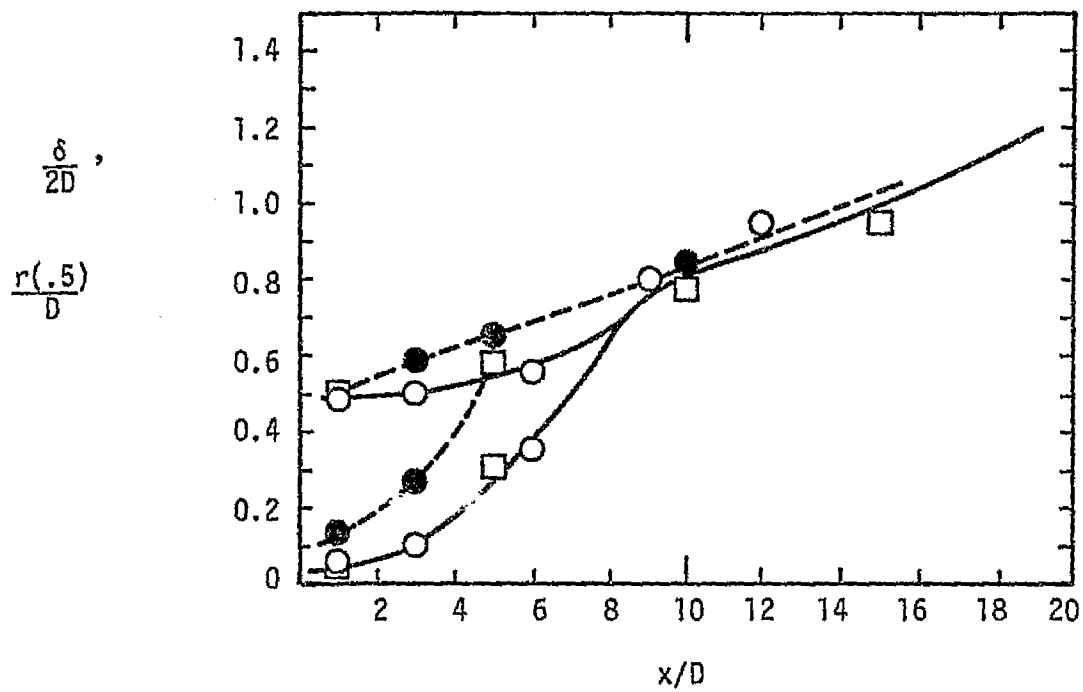


Figure 19. Axial distribution of mean velocity profile parameters.  $\circ$ — $\square$ , natural jet;  $\bullet$ — $\bullet$  excited jet.

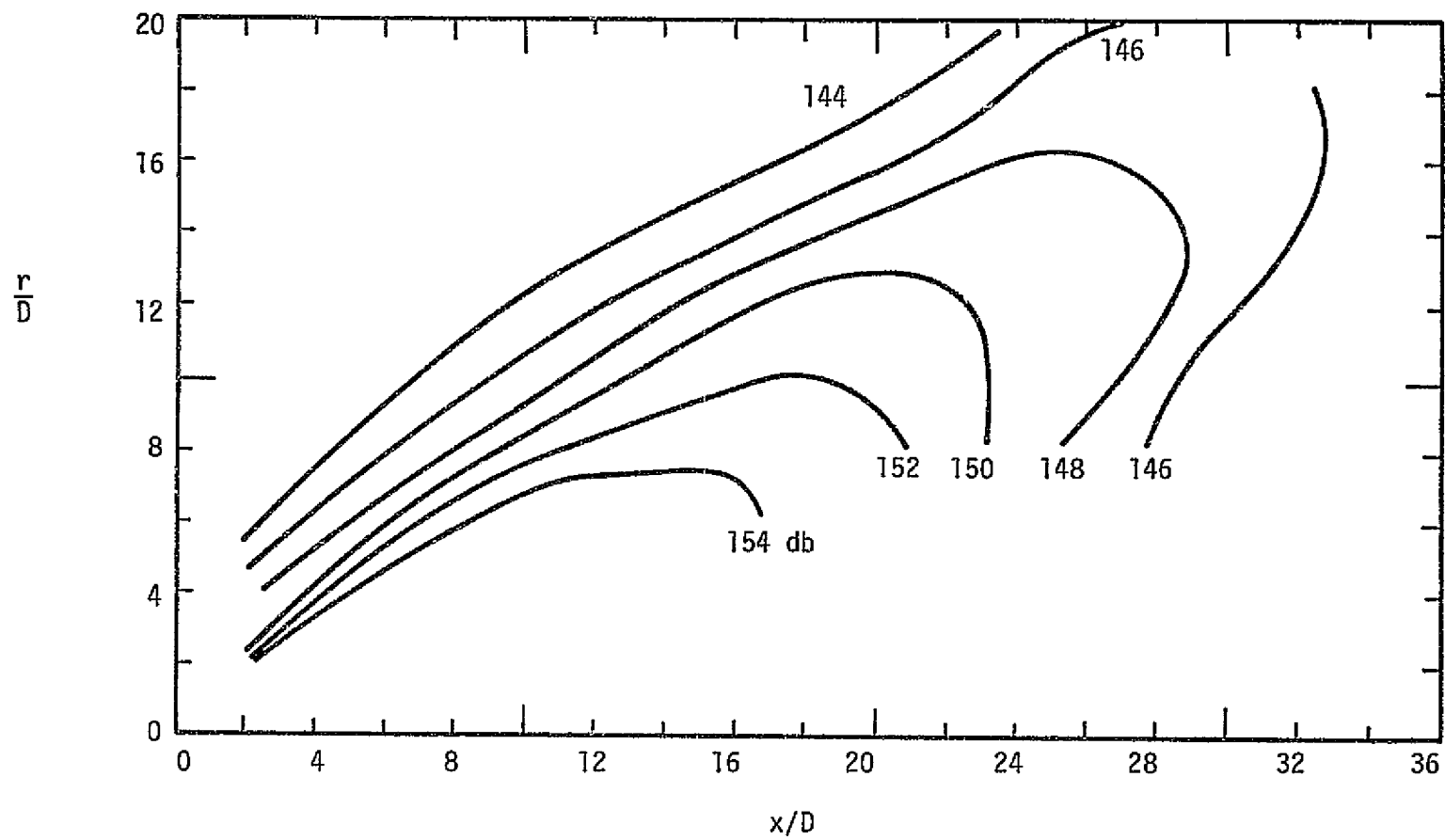


Figure 20. Overall sound pressure level contours; jet excited at  $St = 0.19$ .

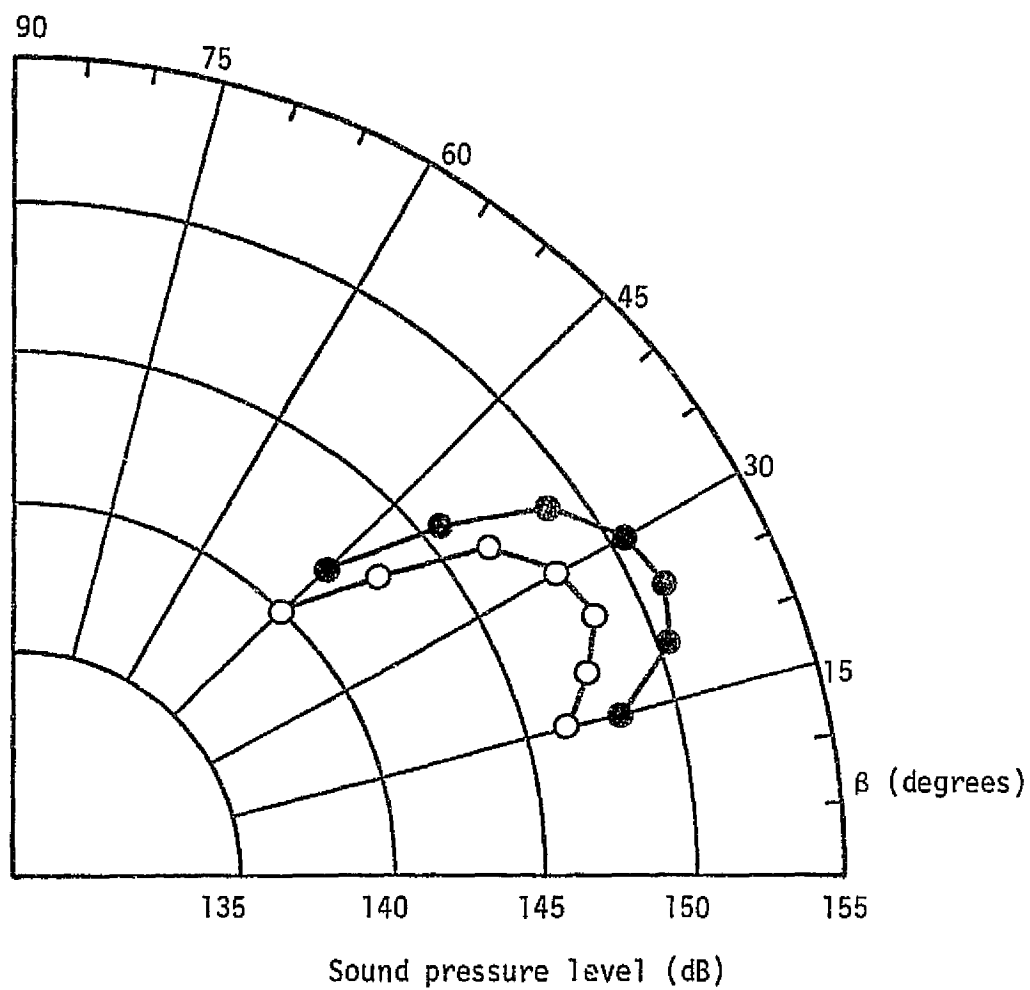


Figure 21. Overall sound pressure level directivity,  $R/D = 24$ .  
 O natural jet; ● excited jet.

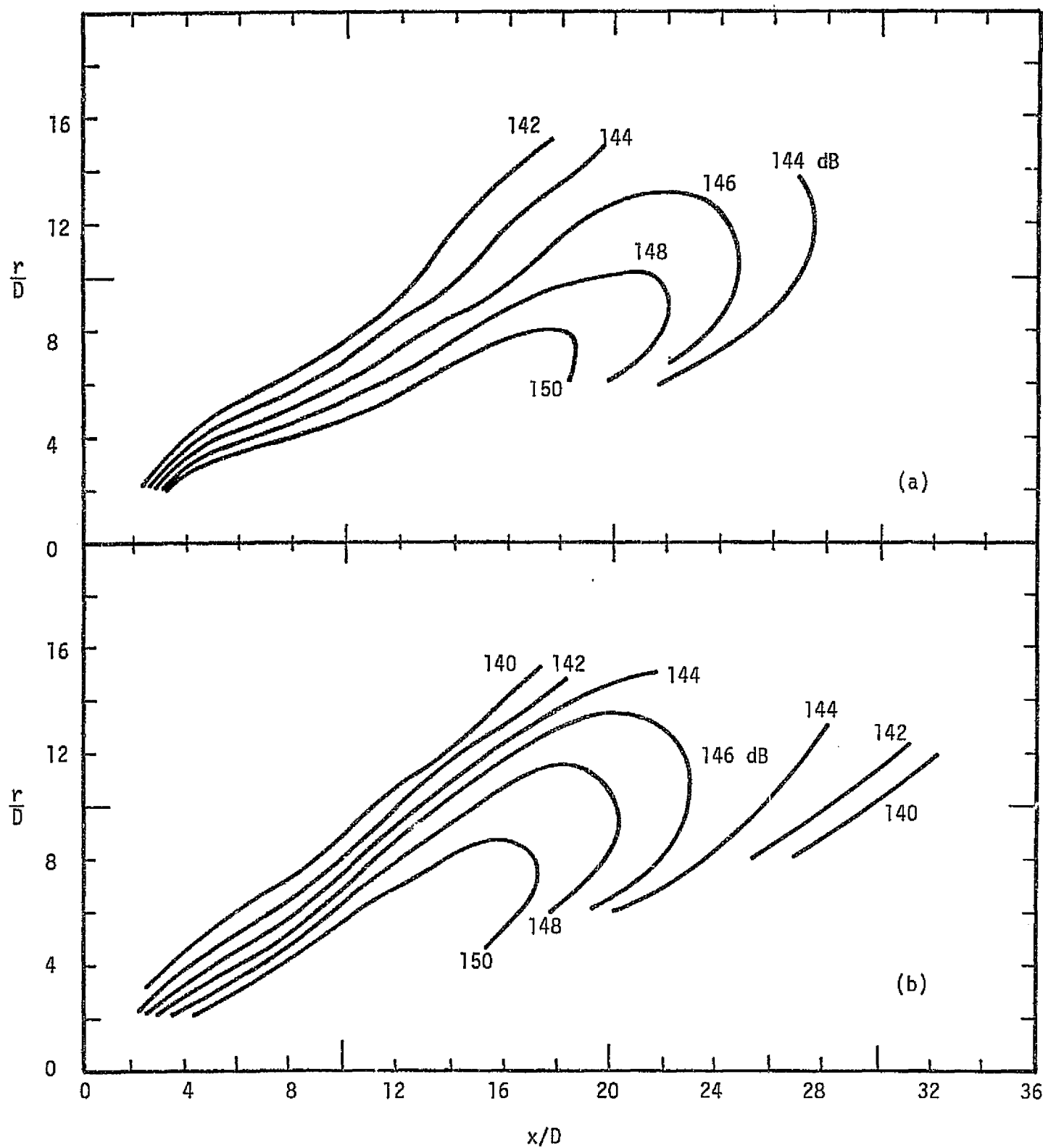


Figure 22. Band-passed sound pressure level contours for excited jet.

(a)  $St = 0.15 - 0.23$ , excited at  $St = 0.19$ ; (b)  $St = 0.30 - 0.45$ ,  
excited at  $St = 0.38$ .

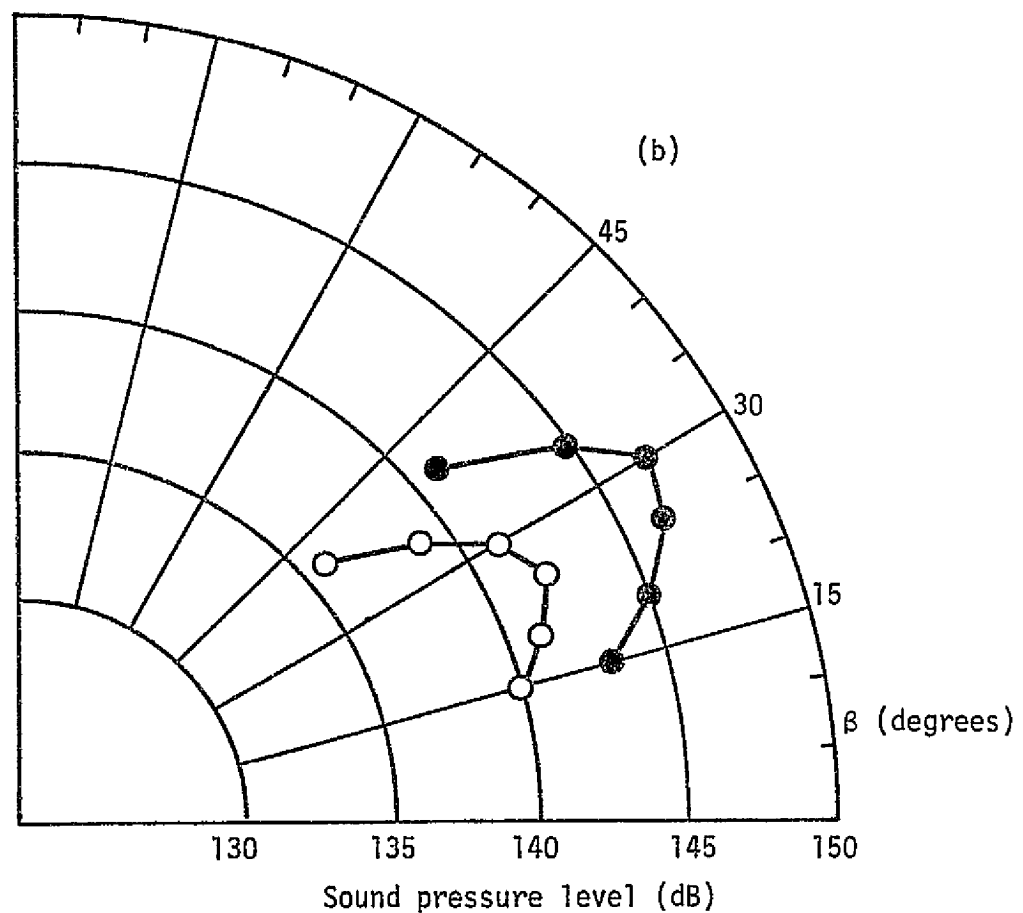
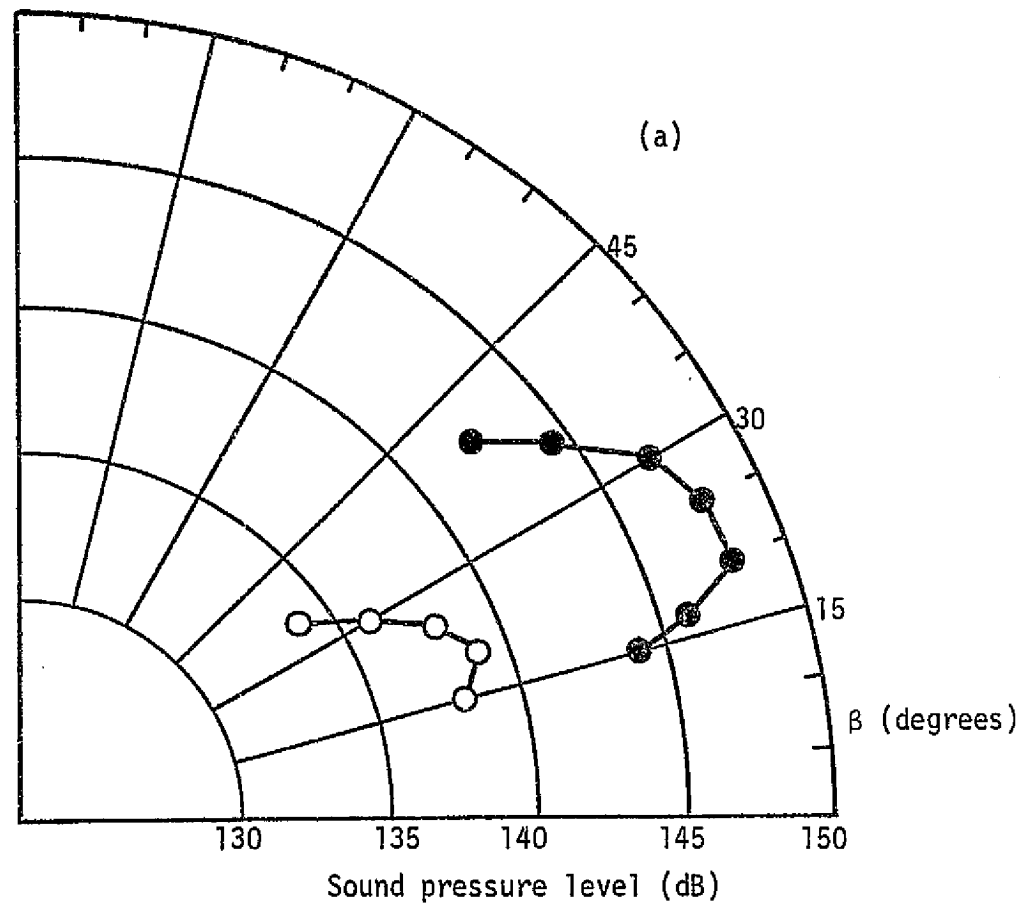


Figure 23. Band-passed sound pressure level directivity plots.

○ Natural jet; ● Excited jet. Excitation St:

(a) 0.19 (b) 0.38.

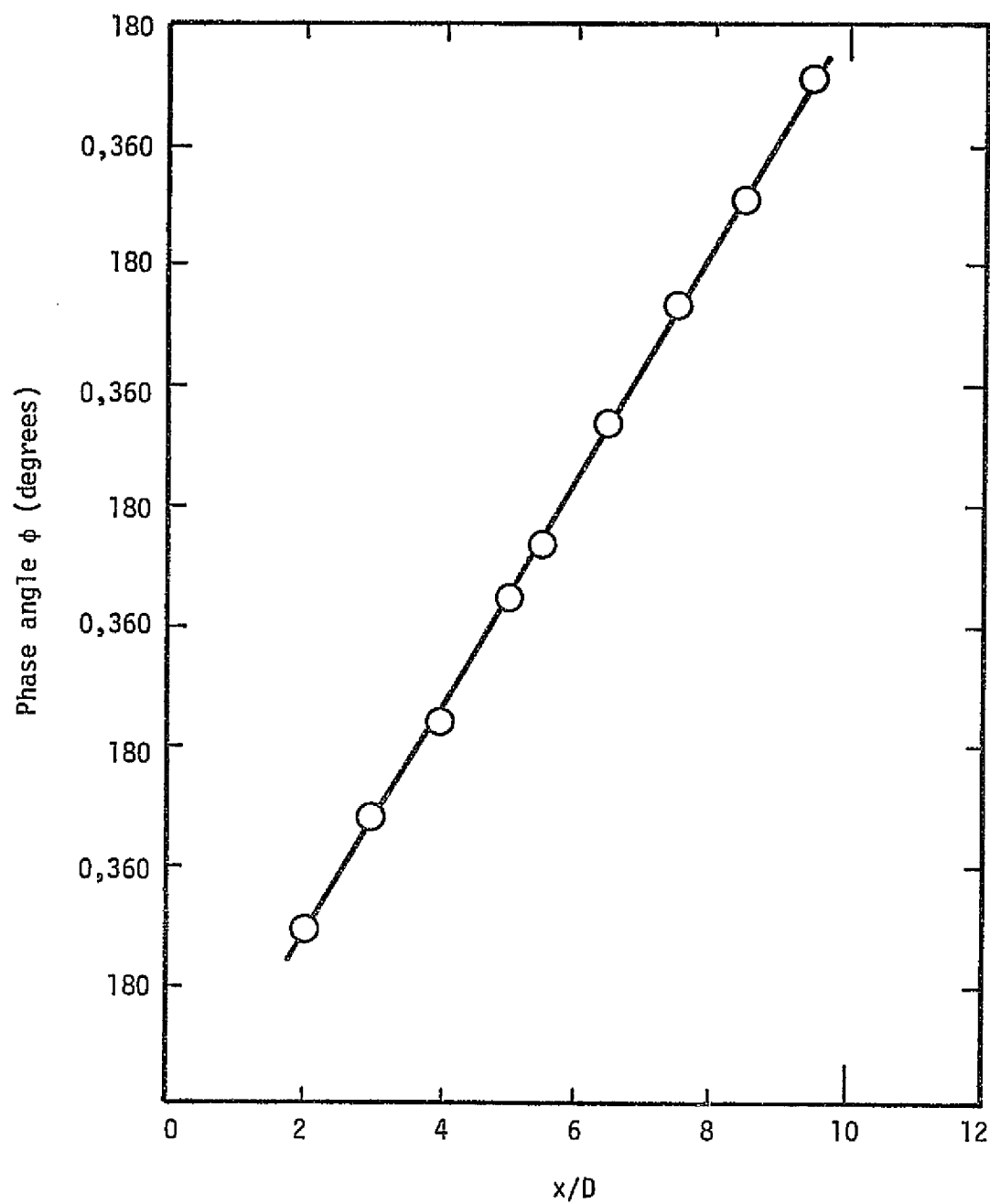


Figure 24. Flow disturbance phase angle; jet excited at  $St = 0.38$ .

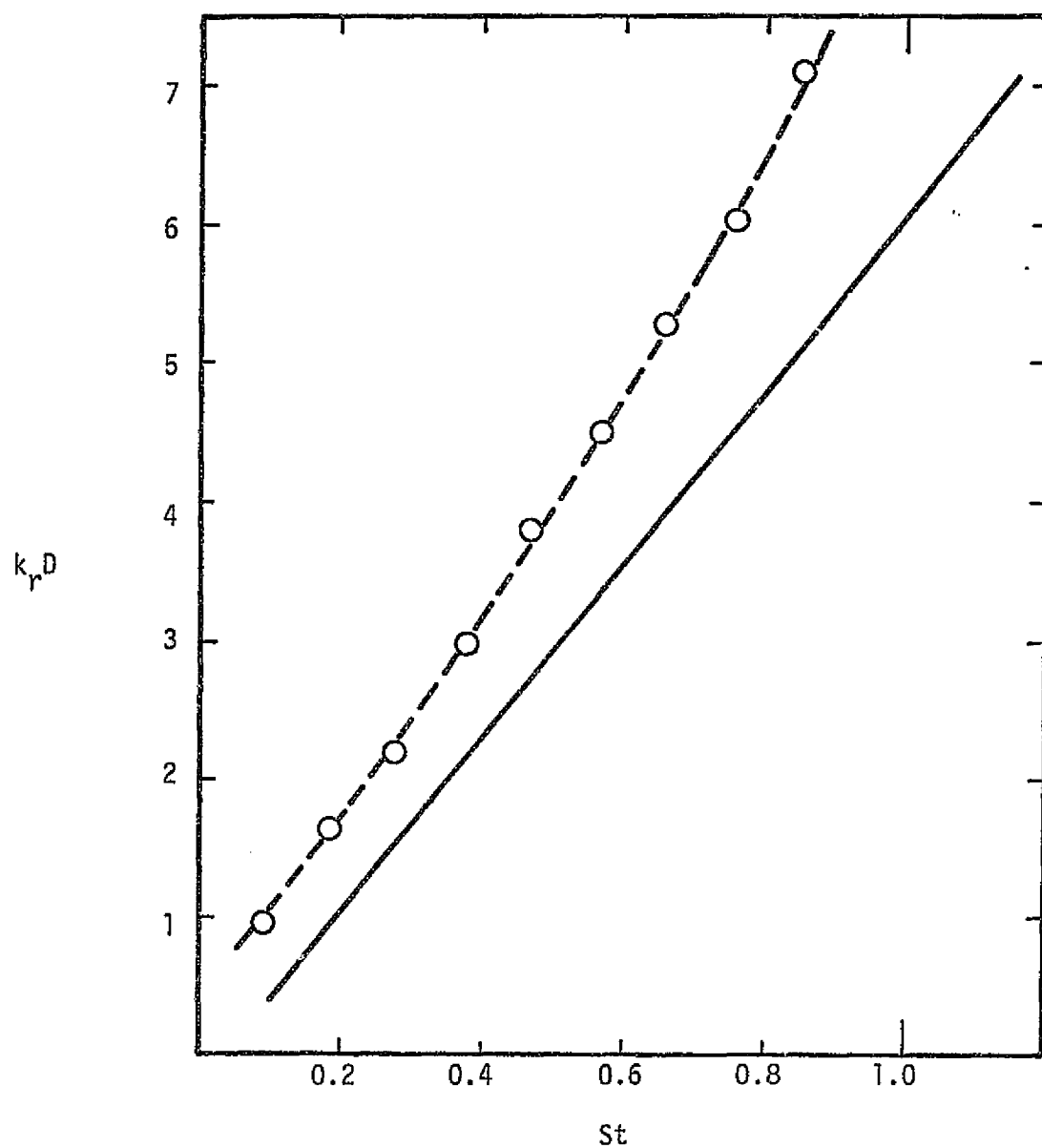


Figure 25. Axial wavenumber of excited disturbance.  
O present experiment; — Tam (1972)  
prediction.

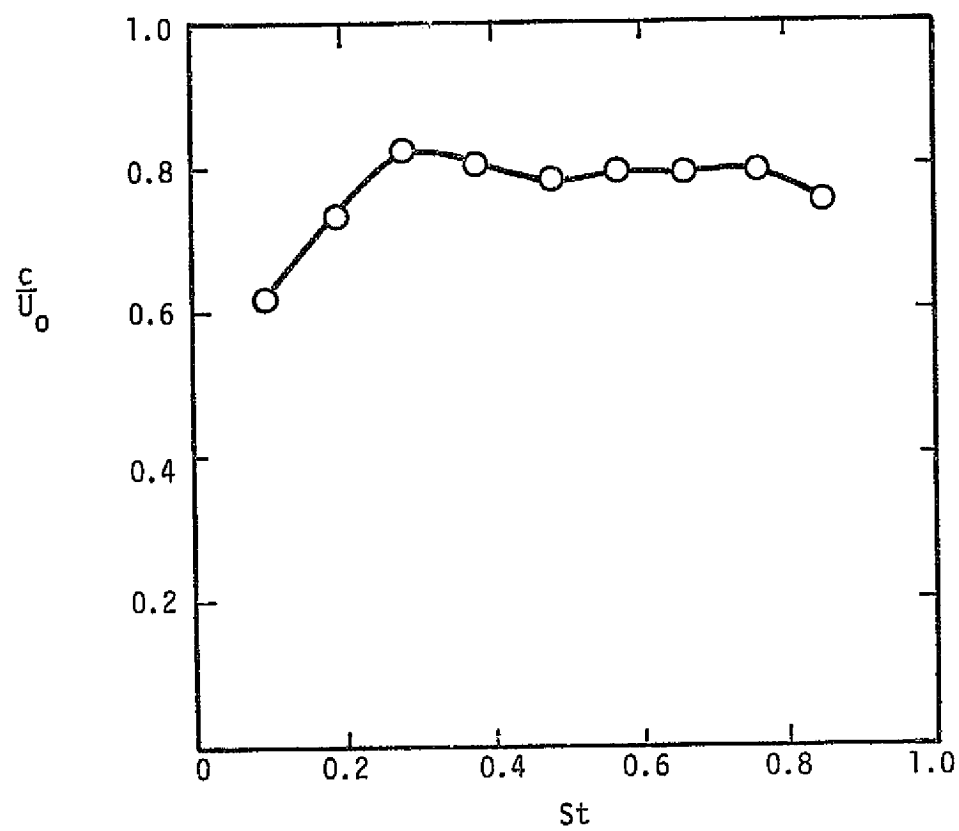


Figure 26. Axial phase velocity of excited disturbance.

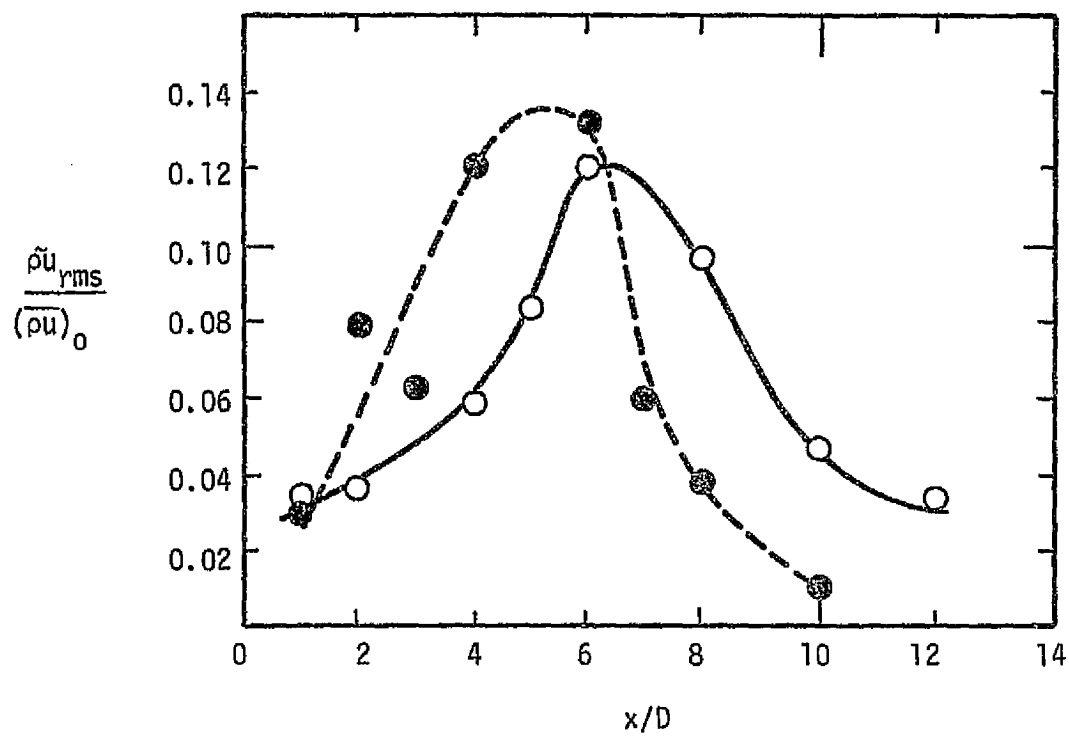


Figure 27. Coherent mass velocity fluctuation amplitude in jet shear layer.  $St$  component:  $\circ$  0.19,  $\bullet$  0.38.

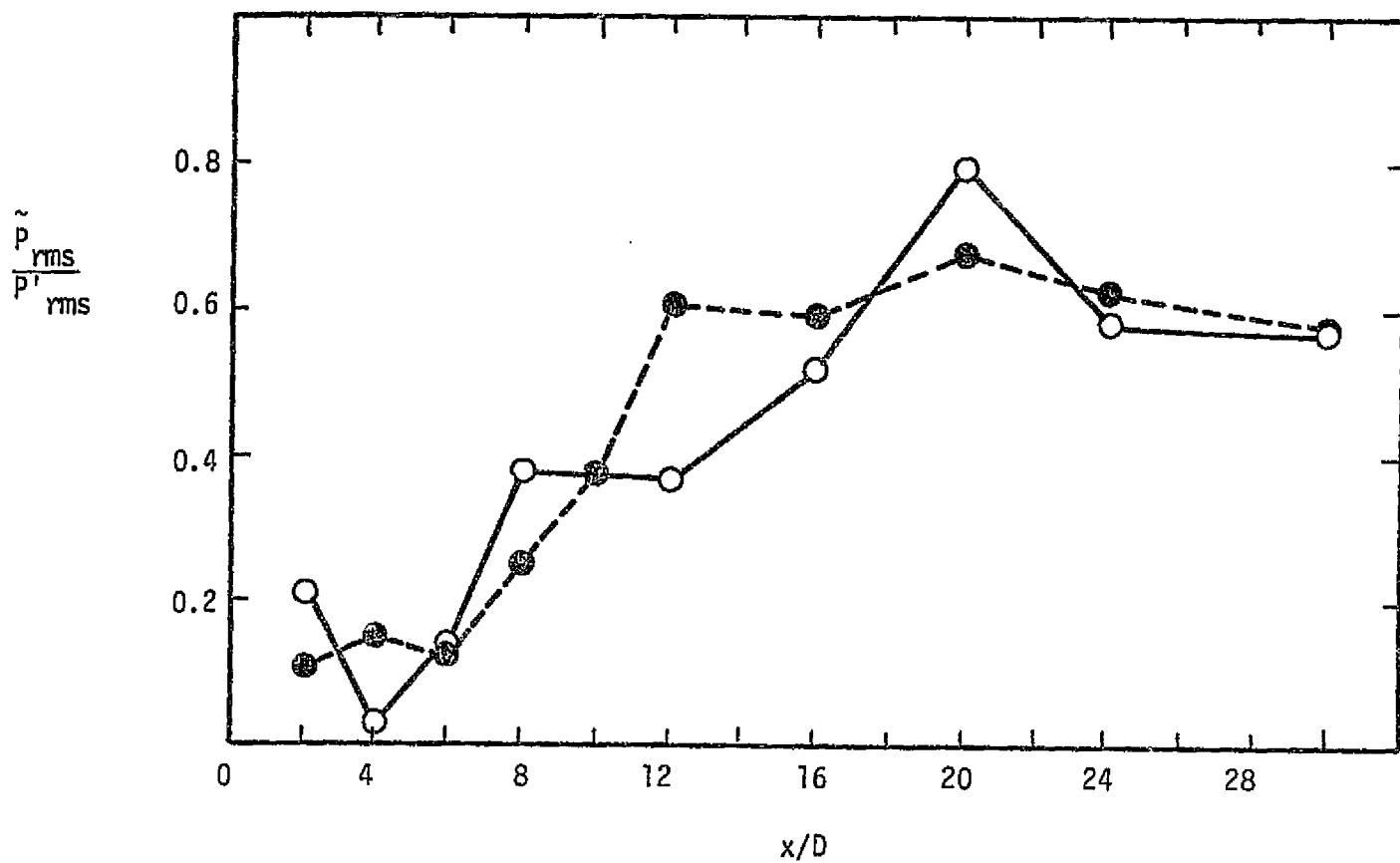


Figure 28. Coherent sound pressure level;  $r/D = 8$ . St. component:  
 0 0.19, ● 0.38.

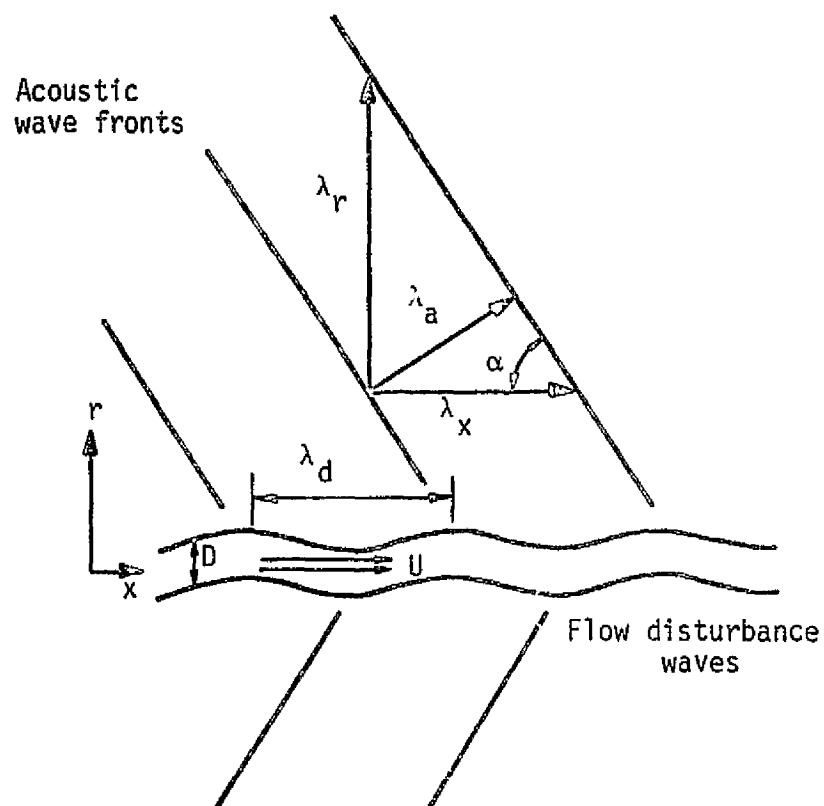


Figure 29. Schematic of the orientation of the flow disturbance and acoustic waves.

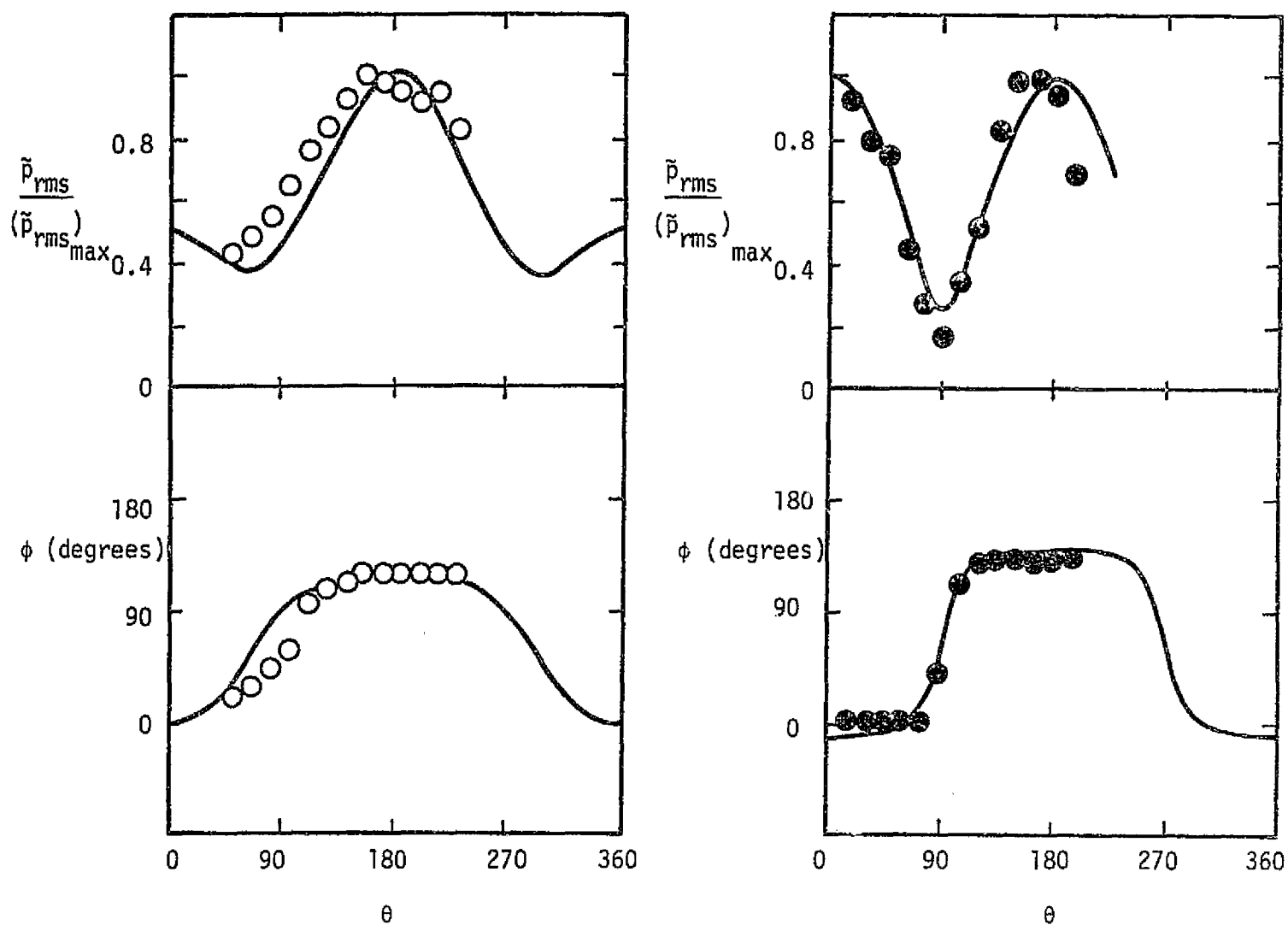
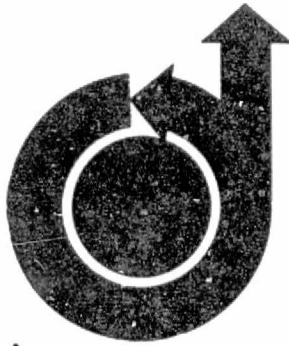


Figure 30. Coherent sound pressure fluctuation amplitude and phase angle as a function of azimuthal angle.  $\circ, \bullet$  Experimental data, — numerical curve fit. St component:  $\circ$  0.19,  $\bullet$  0.38.



**79-0593**

**Flowfield and Acoustic Properties  
of a Mach Number 0.9 Jet at a Low  
Reynolds Number**

J.L. Stromberg, Oklahoma State University,  
Stillwater, Okla. and D.K. McLaughlin,  
Oklahoma State University, Stillwater, Okla.  
and T.R. Troutt, Oklahoma State University,  
Stillwater, Okla.

**AIAA 5th AEROACOUSTICS  
CONFERENCE**

Seattle, Washington—March 12-14, 1979

American Institute of Aeronautics and Astronautics  
1290 Avenue of the Americas New York, N.Y. 10019

FLOWFIELD AND ACOUSTIC PROPERTIES OF A MACH  
NUMBER 0.9 JET AT A LOW REYNOLDS NUMBER

by

J. L. Stromberg\*, D. K. McLaughlin†, and T. R. Troutt‡  
School of Mechanical and Aerospace Engineering  
Oklahoma State University, Stillwater, Oklahoma

Abstract

An experimental study of the flowfield and acoustic properties of a low Reynolds number ( $Re = 3600$ ),  $M = 0.9$  jet has been performed in an anechoic vacuum chamber test facility. The mean flowfield was surveyed with a conventional Pitot pressure probe and flow fluctuations were detected with a normal hot-wire probe. Also, condenser microphone measurements were made in the acoustic field. The major goal of the study was to develop a better understanding of the noise generation mechanisms of subsonic jets.

The flow fluctuations within the jet were found to be dominated initially by a relatively discrete large scale wave-like instability centered around a Strouhal number of 0.44. The axial wavelength of this instability was determined to be 1.45 jet diameters and its azimuthal character includes both  $n = 0$  and  $n = \pm 1$  modes. The growth of this instability coupled with its non-linear breakdown are major contributors to the termination of the potential core region of the jet.

The acoustic field of the jet, in contrast to the flowfield, has a broad frequency spectrum with a peak amplitude near a Strouhal number of  $St = 0.2$ . These results indicate that a non-linear mechanism involving the large scale flow instability is responsible for a dominant portion of the noise generated from this jet.

I. Introduction

This paper presents the results of an experimental study of the flow fluctuations and the noise radiation of a Mach number 0.9 axisymmetric air jet. The jet is operated at a low Reynolds number ( $Re = 3600$ ) for the purpose of specifically examining the behavior of the large scale 'orderly' structure with particular emphasis on its noise generating capabilities.

The 'orderly' structure in the turbulence of free shear flows is receiving the attention of numerous researchers since the relatively recent identification of its existence by Brown and Roshko<sup>1</sup>, Crow and Champagne<sup>2</sup> and others.<sup>3-5</sup> Subsequent experimental studies by Laufer et al<sup>6</sup>, Michalke and Fuchs<sup>7</sup>, and Dahan and Elias<sup>8</sup> have suggested that an orderly, coherent portion of the turbulence in a jet is important in the noise generation process. All of the above experiments dealt with subsonic

free shear flows.

For several years we have been making measurements on the flowfield and acoustic properties of supersonic jets in the Mach number range from  $M = 1.3$  to  $M = 2.5$ .<sup>9-12</sup> These measurements have provided a substantial body of evidence to demonstrate that coherent fluctuations in the form of instability waves are powerful noise generators in the supersonic jets.

The approach used to obtain most of our supersonic jet noise data was unique in that the jets were operated at a low Reynolds number, in the range from  $Re = 3700$  to 15,000. This compares with most laboratory model high speed jets which typically exceed  $Re = 10^6$ . The low Reynolds number flows are achieved by performing the experiments in an anechoic vacuum chamber where the ambient pressure is maintained at a fraction of atmospheric pressure. Lowering the Reynolds number in this fashion tends to stabilize the jet so that it is dominated by fluctuations which are characteristic of a laminar instability in the initial stages of transition to turbulent flow.

Observation of the flow character of these low Reynolds number supersonic jets has produced some surprising results. First, the mean flow properties of the low Reynolds number jets are very similar to reported high Reynolds number measurements in profile shape and potential core length. (See for example Lau, Morris and Fisher.<sup>13</sup>) However, for the region upstream of the end of the potential core, a large scale, discrete frequency instability dominates the flow fluctuation spectra. In fact the growth of the instability is a major contributor to the development of the mean flow profile.

Another, perhaps more important result which we obtained from the supersonic jet noise experiments was that the instability waves radiate noise equivalent in strength to that produced by the noise generators of conventional, turbulent, high Reynolds number jets. We also established this remarkable fact is true in cases where the instability waves travel downstream subsonically with respect to the ambient air thus precluding the possibility of eddy Mach wave radiation in these cases. Such a determination is substantial motivation for the development of a noise generation theory which models some portion of the organized structure of turbulence within the jet as instability waves.

Instability theories for jets in the subsonic to supersonic flow regime are currently under development by several researchers. Early analyses by Lesson and his co-workers<sup>14,15</sup> were followed by many other instability analyses<sup>16-24</sup> some of which have been motivated by the noise generation problem. In addition, turbulence modeling, using an instability like wave formulation as a basis has been undertaken by Liu,<sup>25</sup> Morris<sup>26</sup> and Tam and Chen.<sup>27</sup> Large scale structure analytical modeling of turbulent jets using some form of stability theory appears to hold

\*Research Assistant, presently, Engineer at Mechanical Research and Development, Halliburton Services Co., Duncan, Oklahoma

†Professor, presently Visiting Aerospace Engineer, Acoustics and Noise Reduction Division, NASA Langley Research Center, Hampton, Virginia, Member AIAA

‡Research Associate, presently Post Doctoral Fellow, Department of Aerospace Engineering, University of Southern California, Los Angeles, California

considerable promise particularly for the prediction of the noise radiated by the jets. Results which have been obtained from the earliest formulations of several researchers<sup>19,26,28-30</sup> indicate that more sophisticated analyses may produce accurate predictive capability.

In the Mach number range of the present study (around  $M = 0.9$ ) only the analyses of Lesson *et al.*<sup>14</sup> and Michalke<sup>16</sup> apply. (All other analyses mentioned above are for either the incompressible or the supersonic jet.) Comparisons will be made in this study with the analysis of Michalke since he uses a more realistic family of velocity profiles than do Lesson *et al.*

The overall goal of the present research is to extend the techniques successfully employed in our laboratory in the study of supersonic jets into the subsonic flow regime to investigate the role of large scale instabilities in the noise production process. The specific objectives of the study are to perform experiments on a low Reynolds number  $M = 0.9$  axisymmetric, cold air jet to:

- (1) characterize the nature of the large scale flow fluctuations by making hot-wire measurements to determine the growth rate, wavelength, and wavefront orientation of the dominant spectral components;
- (2) determine the general properties of the acoustic field with single microphone surveys and two-microphone cross correlations; and
- (3) relate the radiated noise to the flow fluctuations to identify and gain understanding of the dominant noise generating mechanisms.

## II. Description of the Experiments

The experiments were performed in the free jet test facility shown schematically in Figure 1. This facility has been described in detail in references 10, 11 and 31 so that only a brief description will be included in this paper. The  $0.7 \times 0.8 \times 1.2$  meter anechoic vacuum chamber and the 5 cm Scott Pyrell acoustic foam liner produce an anechoic environment for frequencies above 1 kHz. All signals are high pass filtered to eliminate the portion caused by the low frequency acoustic resonance of the test chamber. Within the frequency range of interest, the reverberant pressure field has been estimated to be less than 2db.

The facility is equipped with a 3 directional probe drive, Pitot pressure and hot-wire probes, and B & K 1/8 inch (3.2mm) diameter type 4138 condenser microphones. The hot-wire probes are operated in the constant temperature mode with DISA 55 M electronics having a frequency response in excess of 40 kHz.

The simple converging nozzle has a contour shown approximately in Figure 1. The contour coordinates were taken from Smith and Wang<sup>37</sup> who designed a nozzle to provide uniform parallel flow at the exit with an exit diameter  $D$  of 7.9 mm. The stilling section has acoustic foam, perforated plates, a honeycomb section and 6 fine mesh screens. Air is supplied to the stilling chamber from compressed and dehumidified air storage. The stagnation temperature of the jet flow is room temperature (approximately 297K).

For some of the measurements presented the jet

was artificially excited using a glow discharge excitation device developed and reported earlier.<sup>9</sup> The exciter consists of a 1.5 mm tungsten electrode insulated with ceramic tubing and positioned approximately 2 mm from the nozzle exit. The level of excitation is relatively low so that in most cases it has a small effect on the development of the natural instability. However, it does provide the phase reference necessary to make instability wavelength and wave orientation measurements.

Sound pressure level data in this paper is presented using a reference pressure scaled to the ambient pressure in the test facility:

$$p_{\text{ref}} = (2 \times 10^{-5}) \left( \frac{p_c}{p_a} \right) N/m^2, \text{ where}$$

$p_c$  is the pressure of the test chamber and  $p_a$  is standard atmospheric pressure. A total uncertainty of  $\pm 3\text{db}$  was estimated for the sound pressure level data which includes the uncertainty due to chamber reverberation effects.

The relative phase of the hot-wire (or microphone signal) referenced to the excitation signal was measured with a Saicor Model SAI 43A correlation and probability analyzer in the cross correlation mode. The procedure used was to measure the time lag to the peak of the cross correlation (between the exciter and sensor signals) for various probe positions. The Saicor analyzer was also used in the enhance mode, in order to phase average the sensor signal using the exciter signal as a time reference. The phase averaged signal is mathematically expressed as:

$$\langle e(t) \rangle = \lim_{N \rightarrow \infty} \frac{1}{N} \sum_{n=0}^N e(t + n\tau)$$

where  $\tau$  is the period of the fundamental coherent component in the jet (and of the excitation) and  $t$  is time. In this manner the coherent portion can be extracted from the full signal and a measurement of the fraction of coherent structure in the full spectrum can be obtained.

All measurements reported in this study were obtained at a jet Reynolds number of  $Re = 3600$ . This Reynolds number was chosen because the fundamental instability was most clearly apparent at this flow condition. Measurements at higher and lower Reynolds numbers near 3600 indicated that the characteristics of the flow fluctuations were not strongly dependent on Reynolds number in this range. However, if the Reynolds number is increased by an order of magnitude the shear layer close to the nozzle exit becomes unstable and the downstream flow fluctuations become much more complex.

A summary of the jet conditions is presented in Table 1.

Table 1. Jet Test Conditions

Exit Mach number	M	0.90
Nozzle exit diameter	D	7.9 mm
Jet exit velocity	U	284 m/sec
Jet Reynolds number	Re	3600

Table 1 (continued)

Jet Characteristic frequency	U/D	35.9 kHz	
Jet stagnation pressure	$P_o$	17.1 N/m <sup>2</sup>	for nominal
Test chamber pressure	$P_c$	10.1 N/m <sup>2</sup>	Re condition
Jet stagnation temperature	$T_o$	297 K	
Coordinate system	x, r, $\theta$		

### III. Properties of the Flow Fluctuations

#### Mean Flow Measurements

Figure 2 presents mean Mach number profiles in the jet deduced from Pitot pressure data using the assumptions that the Pitot probe measures local stagnation pressure and the local static pressure equals the ambient test chamber pressure. The measurements demonstrate flowfield features which are common with conventional, high Reynolds number, turbulent jets. The jet exits the nozzle with approximately uniform flow surrounded by a thin cylindrical shear layer. The shear layer thickens until it merges at the end of the potential core, which in this jet occurs at about six diameters downstream of the jet exit. The length of the potential core, clearly distinguishable by the centerline Mach number distribution presented in Figure 3, is approximately the same as Lau et al.<sup>13</sup> found in a high Reynolds number,  $M = 0.9$  jet. It appears that for the low Reynolds number jet, the momentum transport of the instability waves in combination with the molecular viscosity is approximately equivalent to the turbulent mixing of the conventional high Reynolds number jet.

#### Spectral Content of Hot-Wire Fluctuations

Figure 4 presents several hot-wire frequency spectra with the probe positioned at various axial locations in the jet shear layer at the radial location of maximum fluctuation level. These spectra show that an instability with a relatively discrete frequency, centered at a Strouhal number of  $St = fD/U = 0.44$ , dominates the initial fluctuations in the jet shear layer. This instability is similar to those typically measured previously in low Reynolds number supersonic jets. (See references 9-11). As in our previous experience,<sup>9-11</sup> the frequency of the instability drifts a little from day to day despite close control on the jet conditions. However, in all cases measured the primary instability varied no further than 10% from the  $St = 0.44$  value.

The initial non-linear processes become apparent in the frequency spectrum at  $x/D = 5$  shown in Figure 4 as well as in the spectrum shown in Figure 5 corresponding to a probe location of  $x/D = 4$ . The spectrum presented in Figure 5 was recorded with the probe located inward from the radial location of maximum fluctuation level. Attention is drawn in these two noted spectra, to the minor spectral peaks at  $St = 0.22$  and  $0.29$ . Note that these frequencies are exactly one-half and two-thirds of the frequency of the primary instability ( $St = 0.44$ ).

Browand and Laufer<sup>13</sup> conducted extensive flow visualization experiments with water jets in the

Reynolds number range from 5000 to 15,000, the results of which are pertinent to this study. They found the initial development of the jet to be controlled by the coalescence or pairing of discrete vortex structures. The vortex structures result from the migration of vorticity, present in the instability waves, toward regions of vorticity concentration. These structures occur in both axisymmetric (donut shaped) and helical azimuthal shapes. The pairing of donut vortices produces a larger vortex with a passage frequency which is one-half of the pre-pairing frequency. The coalescence of a helical vortex produces a structure with a passage frequency which is two-thirds of its original value. The one-half, and two-thirds frequencies of the initial instability noted above in the discussion of our measurements are consistent with this vortex interaction description of the developing region of the jet. Detailed phase measurements discussed later lend further support to this scenario.

Downstream of  $x/D = 5$  a second stage of non-linear development is evidenced. Several discrete peaks are present in the frequency spectrum at  $x/D = 7$ , and by  $x/D = 8$  the flow is almost completely turbulent. The numerous discrete peaks are similar to those measured in a two-dimensional mixing layer by Miksad<sup>34</sup> which he attributed to the non-linear interaction of discrete spectral components in the flow. The broad 'turbulent' spectra are a result of the total disintegration of the organized structure of the jet.

#### Instability Characterization

Conventional hydrodynamic instability analyses such as performed by Michalke<sup>16</sup> cast the disturbance quantities in the following wave form:

$$q(x, r, \theta, t) = \hat{q}(r) \operatorname{Re} \{ \exp [i (k_r x - \omega t + n\theta) - k_i x] \}$$

where  $\operatorname{Re}$  here stands for the real part of  $\{ \}$ . Determination of the eigenvalues ( $k_r$  and  $k_i$ ) corresponding to the combinations of  $n$  and  $\omega$  of the dominant spectral components are required to characterize the instability. These quantities can be measured with the hot-wire probe.

Accurate quantitative measurements with a hot-wire probe in low Reynolds number, transonic Mach number flows is extremely difficult. Perhaps because of this, little published data is available corresponding to this flow regime. The most pertinent information is contained in Horstman and Rose<sup>35</sup>; however, the local Reynolds number range of their measurements is an order of magnitude higher than that of the present study. The technique used to reduce our raw hot-wire data is discussed in detail in Stromberg.<sup>31</sup> In summary, the hot-wire voltage fluctuations were found to be proportional to local density fluctuations ( $\rho'$ ) in the flow. This unusual result is a consequence of the overwhelming proportion of heat transfer from the wire that is end-loss conduction to the wire supports. (See Reference 36 for a discussion of this problem.)

Figure 6 depicts the growth of the dominant spectral component in the flowfield as the  $St = 0.44$  component of  $\rho'_{rms}/\bar{\rho}$  is plotted as a function of the axial coordinate. The data for this figure was gathered at a constant radial location of approximately  $r/D = 0.35$ , a location which maximizes the hot-wire fluctuating voltage  $e'_{rms}$ . The data of Figure 6 shows that the  $St = 0.44$  component grows

approximately exponentially with a growth rate of  $-k_i D = 2.1$  for the first 3 diameters downstream of the nozzle. Beyond  $x/D = 3$  the measurements indicate a slowing of the growth rate (probably due to non-linear effects) leading to an amplitude equilibration region extending from approximately  $x/D = 4$  to  $x/D = 6$ . Beyond  $x/D = 6$ , which is near the end of the potential core, the fluctuation amplitude steadily decreases.

The measured initial growth rate of the  $St = 0.44$  component was compared to predictions of the stability analysis of Michalke<sup>16</sup> using the mean velocity profile at  $x/D = 1$  (deduced from the Mach number data of Figure 2). The input parameters to Michalke's analysis were thus calculated to be  $D/2\theta = 18$  and  $T_0/T_{jet} = 1.16$  where  $\theta$  here refers to the momentum thickness of the shear layer of the jet. For these conditions the analysis of Michalke predicts a growth rate of  $-k_i D = 2.0$  for the  $St = 0.44$  component of the instability which is within the experimental uncertainty of the measured growth rate. (Considerable extrapolation of the data in Michalke's paper was required to obtain this result).

The accuracy of Michalke's theory in predicting the growth of the primary instability is encouraging. However, some of the details of the phenomenon are not predicted by the results contained in his paper. Although the peak frequency of the predicted amplification curve corresponding to the mean flow parameters at  $x/D = 1$ , is within the range of the  $St = 0.44$  measured instability, the theory does not predict the sharp frequency selection that the measurements demonstrate. In addition, the theory does not appear to predict the details of the subharmonic production measured here, and visualized by Browand and Laufer.<sup>3</sup> Nevertheless, the theory does have an automatic frequency downshifting mechanism as the mean profile changes to an approximately Gaussian shape. In our view, further analytical development, along with more detailed experiments, should prove to be both interesting and profitable.

Aside from the growth properties, it is important to the characterization of the instability to determine the wavelength, phase velocity and wave-orientation of the dominant spectral components. To this end the relative phase  $\phi$  of the hot-wire signal referenced to the excitation input signal was measured for several spectral components. In this manner the axial wave number  $k_x$ , and in two cases the azimuthal mode number  $n$  were determined. The results of the measurements are of fundamental importance to our interpretation of the flow and noise generation phenomena.

Figure 7 is a plot of relative phase  $\phi$  versus axial position for the Mach number 0.90 jet excited at  $St = 0.22, 0.44, 0.55$ , and  $0.69$ . A straight line was fit to each set of data using a least squares linear regressor. The wavelength was determined from the slope of each line and the phase velocity was calculated from the frequency and the wavelength. The resulting wave properties, tabulated in Table 2, are in the expected range of values based upon previous experience of Chan<sup>10</sup> and Morrison and McLaughlin<sup>11</sup> (See Stromberg<sup>31</sup> for details of comparison.)

Table 2. Wave Properties of Various Spectral Components of the Flow Fluctuations

Frequency Component St	Wave Number $k_x D$	Wave-length $\lambda/D$	Phase velocity $c/U$	Azimuthal mode n
0.22	2.03	3.10	0.68	0
0.44	4.34	1.45	0.64	0 and $\pm 1$
0.55	4.91	1.28	0.70	-
0.69	6.51	0.97	0.67	-

Azimuthal phase measurements with the hot-wire probe were made of both the  $St = 0.44$  and  $St = 0.22$  spectral components. The phase distribution of the primary instability (the  $St = 0.44$  component) is presented in Figure 8. For these measurements the probe was positioned at  $x/D = 5$  and at the radial location of maximum hot-wire fluctuations at this frequency. The curve that is drawn through the data represents the phase distribution obtained from a modal decomposition of the form:

$$Q(\theta) = A_0 e^{i\alpha_0} + A_1 e^{i\theta} + A_{-1} e^{-i\theta}$$

This represents the  $\theta$  dependence of a disturbance made up of a superposition of right and left hand helicities ( $n = 1$  and  $n = -1$  azimuthal mode numbers) and an axisymmetric ( $n = 0$ ) mode. The curve is the result of a numerical fit to the data resulting in the following choice of parameters:  $A_0 = 0.5$ ,  $A_1 = .65$ ,  $A_{-1} = .85$  and  $\alpha_0 = -60^\circ$ . This data indicates the  $St = 0.44$  instability has slightly different amounts of right and left hand spiral mode and a significant amount of axisymmetric mode.\* Exactly equal right and left hand helicities superpose to produce a flapping, or sinusoidal instability mode of the type found by Morrison and McLaughlin<sup>11</sup> in supersonic jets.

Figure 9 presents the phase distribution for the  $St = 0.22$  component of the flow fluctuations. This data demonstrates a predominantly axisymmetric mode for this spectral component. Several important points should be made regarding the determined azimuthal phase behaviour of the  $St = 0.22$  and  $St = 0.44$  components in the flow. It is perhaps not unexpected to find both the  $n = 0$  and  $n = 1$  modes as such was the case in the subsonic jet measurements of Browand and Laufer,<sup>33</sup> Michalke and Fuchs,<sup>7</sup> Chan,<sup>21</sup> and Dahan and Elias,<sup>8</sup> and the supersonic jet acoustic field measurements of Dutt<sup>36</sup> and Troutt.<sup>37</sup> However, the determination of two azimuthal modes represents a new feature in the experimental experience gained in our laboratory. Extensive measurements of low Reynolds Number supersonic jets, 9-11 have shown that the supersonic jet instability is dominated by the helical ( $n = +1$  or  $n = -1$ ) modes. In the case of the supersonic jets, from  $M = 1.3$  to  $M = 2.5$ <sup>10,12</sup> the  $n = \pm 1$  mode proved to be a powerful noise generator. However, as will be seen in the next section, the helical instability does not directly radiate significant noise.

Finally, it is important to recognize that the axisymmetric mode of the  $St = 0.22$  component was excited by an asymmetric disturbance, the point

\*Stromberg<sup>31</sup> interpreted these and additional phase measurements such that only the  $n = \pm 1$  modes were present in the jet. However, further analysis using only our most reliable data (Figure 8) resulted in the multimodal decomposition discussed herein.

exciter. In private communication, several researchers have doubted the ability of the point exciter to do this.

#### Acoustic Field Measurements

Figure 10 presents the results of near field sound pressure level (SPL) measurements of the Mach number 0.9 jet. (As in all the hot-wire measurements the Reynolds number of this jet was  $Re = 3600$ .) It is evident from comparing the SPL measurement of Mollo-Christensen *et al*<sup>39</sup> in a high Reynolds number  $M = 0.9$  jet, that the noise radiation of the two jets is approximately equivalent. The shape and amplitude of the two jet's SPL contours are very similar. As mentioned earlier, McLaughlin *et al*<sup>10</sup> showed that the noise fields of low Reynolds number supersonic jets are also very similar to their high Reynolds number counterparts. In all cases the low Reynolds number jets produce noise equivalent in strength to the high Reynolds number jets of the same Mach number.

Figure 11 presents a nearfield acoustic spectrum recorded with the microphone located at approximately the angle of maximum noise emission. The figure shows that the noise produced by the jet has a rather broad spectral distribution which maximizes near  $St = 0.2$ . This spectrum is representative of spectra recorded at various positions in the near field in the general vicinity of the maximum noise radiation angle. A comparison of the spectrum depicted in Figure 11 with the hot-wire spectra of Figure 4, which were dominated initially by an  $St = 0.44$  component, indicates that this component does not directly generate the dominant portion of radiated noise. This result is astonishing in that it is in direct contrast with our previous results for low Reynolds number supersonic jets.<sup>10,12</sup> In the low Reynolds number supersonic jets, from Mach number 1.3 to 2.5, the acoustic spectra are dominated by the large scale discrete jet instability frequency. A typical example is shown in the spectra presented in Figure 12 corresponding to the  $M = 1.4$  jet, measured by Morrison<sup>40</sup> in the same facility as the present study. This figure which includes both hot-wire and microphone spectra demonstrates that the large scale jet instability at  $St = 0.33$  is a direct generator of a dominant portion of the radiated noise. It is again emphasized, that phase velocity measurements<sup>11</sup> determined that the instability waves in the  $M = 1.4$  jet travel subsonically with respect to the acoustic velocity of the ambient air. Consequently a simple explanation of the contrasting behavior of the two jets based on a Mach wave radiation mechanism for the supersonic jet is not appropriate.

#### Response of the Jet and its Acoustic Field to Pure Tone Excitation

The response of the acoustic field of the jet to artificial excitation was measured with a microphone located at a position  $x/D = 20$ ,  $r/D = 6$ , corresponding to the maximum noise emission region of the naturally excited jet. The response of the microphone is plotted in two ways in Figure 13. The dotted line joins data obtained after band pass filtering the microphone signal, using a bandpass of 1000Hz around the excitation frequency. The solid line joins data obtained from the unfiltered microphone signal. Also shown is the level the microphone measured in the unexcited jet. The natural jet spectrum is similar to the one shown

in Figure 11. The data clearly demonstrates that the preferred spectral component of the acoustic field of the jet is around  $St = 0.22$ . Excitation of the jet at this frequency slightly enhances the sound pressure level measured by the microphone, while excitation at a frequency slightly above or below  $St = 0.22$  actually attenuates the radiated noise of the jet. Excitation at a high frequency including  $St = 0.44$  appears to have little effect on the acoustic field of the jet. It continues to radiate noise of about the same magnitude around  $St = 0.2$ .

The behavior of the jet with low excitation frequencies (less than  $St = 0.1$ ) or frequencies near  $St = 0.3$  is intriguing. Substantial quieting of the jet was obtained by exciting at these frequencies. The reader is cautioned that more extensive measurements are required before substantial conclusions may be drawn regarding this phenomenon. The picture is rather confusing on this point since apparently conflicting evidence has been gathered by different researchers. Both Moore<sup>41</sup> and Bechert and Pfizenmaier<sup>42</sup> have measured an increase in the broadband component of farfield noise due to small levels of pure tone excitation of the jet near a Strouhal number of 0.5. On the other hand, Kibens<sup>43</sup> has measured a decrease in the broadband component of radiated noise with pure tone excitation of the shear layer of the jet. No doubt the details of the forcing play an important role in the noise radiation properties of these jets.

As shown in Figure 14 the flowfield response to discrete tone excitation is considerably different from that of the acoustic field. This data shows that the jet fluctuations maximize when the jet is excited at a frequency of about  $St = 0.4$ . A secondary peak in the response, at  $St = 0.2$ , is also evident corresponding to the peak observed in the acoustic response data. As in the acoustic data, definite attenuation of the jet fluctuations occurs for excitation frequencies slightly above or below the dominant  $St = 0.4$  component. The two curves in Figure 14 are the full spectrum and band-passed signals, as in the acoustic data of Figure 13. The hot-wire probe was located in the middle of the shear layer, five diameters downstream of the exit for all measurements.

Note the slightly increased response of the full spectrum of jet fluctuations to excitation near  $St = 0.8$ . This appears similar to the response of a low subsonic Mach number jet measured by Hussain and Zaman.<sup>44</sup> In their situation, initial vortices were formed with a passage frequency in the  $St = 0.8$  range which paired to produce a larger structure in the  $St = 0.4$  range of passage frequency. The measurements in Figure 14 indicate a similar initial pairing as well as a subsequent pairing to a passage frequency of  $St = 0.2$ .

The azimuthal character of the radiated noise was investigated by measuring the relative phase in the cross correlation of two microphones placed at the same axial and radial location near the maximum noise emission angle of the jet. The azimuthal angle  $\theta$  between the two microphones was varied and the jet was excited at the acoustic field's peak response frequency ( $St = 0.22$ ) to enhance the cross correlation. As shown by the data in Figure 15, the  $St = 0.22$  component of the acoustic field is predominantly axisymmetric. This contrasts with phase measurements made by Troutt<sup>47</sup> of a moderate Reynolds

number  $M = 2.1$  jet which possesses a considerable portion of asymmetric (helical or flapping mode) as well as axisymmetric acoustic radiation. Even though the  $St = 0.22$  component of the  $M = 0.9$  jet noise is predominantly axisymmetric, the acoustic field also contains a measurable portion of helical mode. Obviously the noise generation process is a multifaceted one resulting from several fluid dynamical actions. This contrasts with the low Reynolds number supersonic jet whose noise is generated primarily by the disintegration of the fundamental helical instability.

#### IV. Conclusions

The mean flow of the low Reynolds number  $M = 0.9$  jet was found to develop in much the same manner as does the conventional high Reynolds number  $M = 0.9$  jet.<sup>13</sup> A large scale discrete frequency instability centered around  $St = 0.44$  was found to dominate the natural flow fluctuations in the jet shear layer prior to the end of the potential core region. Near the end of the potential core non-linear flow interactions shift the spectral content to lower frequencies, most notably the  $1/2$  and  $2/3$  subharmonics of the fundamental. These non-linear interactions may be attributable to the vortex pairing phenomena observed in the low speed axisymmetric jet.<sup>33</sup>

Using the artificial excitation mechanism the axial wavelength of the fundamental instability (the  $St = 0.44$  component) was determined as were the wavelengths of the  $St = 0.22$ ,  $0.55$  and  $0.69$  components. The axial phase velocities of these spectral components calculated from the dispersion relation, were found to be between  $0.6$  and  $0.7$  times the mean jet exit velocity.

The azimuthal phase distribution of the primary instability is consistent with one produced by simultaneous axisymmetric ( $n = 0$ ) and helical ( $n = \pm 1$ ) modes. The azimuthal phase distribution of the subharmonic at  $St = 0.22$  is predominantly axisymmetric ( $n = 0$ ).

The sound pressure level contours measured for the low Reynolds number  $M = 0.9$  jet are approximately the same as those reported for the high Reynolds number jet.<sup>33</sup> Around the angle of maximum noise emission the acoustic spectra were found to have broad frequency content centered around  $St = 0.2$ . This observation is in direct contrast to our previous experience with low Reynolds number supersonic jets whose noise spectra are dominated by the fundamental jet instability frequency.

The  $St = 0.22$  component of the radiated sound was determined to have an axisymmetric phase distribution. However, some portion of the radiated noise has the same asymmetric behavior determined for the fundamental  $St = 0.44$  instability. In summary, the noise generation results from complicated non-linear interactions which follow the development of the fundamental instability. The results are not inconsistent with a vortex pairing model for noise generation first proposed by Laufer et al.<sup>16</sup> and discussed further by Browand and Laufer,<sup>33</sup> Davis and Hardin<sup>45</sup> and Ffowcs Williams and Kempton.<sup>29</sup>

#### Acknowledgment

This research was supported by the National

Science Foundation under Grant No. ENG 75-21405 and the National Aeronautics and Space Administration under Grant No. NSG 1467. The authors take pleasure in acknowledging the assistance of Dr. G.L. Morrison and Mr. J.D. Swearingen.

#### References

1. Brown, G., and Roshko, A. "The Effect of Density Difference on the Turbulent Mixing Layer." AGARD Conference on Turbulent Shear Flows, Conference Proceedings No. 93, 1971, p. 23.
2. Crow, S.C., and Champagne, F.H. "Orderly Structure in Jet Turbulence." Journal of Fluid Mechanics, Vol. 48, 1971, pp. 547-591.
3. Winant, C.D., and Browand, F.K. "Vortex Pairing, the Mechanism of Turbulent Mixing Layer Growth at Moderate Reynolds Number." Journal of Fluid Mechanics, Vol. 63, 1974, pp. 237-256.
4. Mollo-Christensen, E. "Jet Noise and Shear Flow Instability Seen from an Experimenter's Viewpoint." Journal of Applied Mechanics, Vol. 34, 1967, pp. 1-7.
5. Lau, J.C., Fisher, M.J., and Fuchs, H.V. "The Intrinsic Structure of Turbulent Jets." Journal of Sound and Vibration, Vol. 22, 1972, pp. 379-406.
6. Laufer, J., Kaplan, R.E., and Chu, W.T. "On the Generation of Jet Noise." AGARD Conference Proceedings No. 131 on Noise Mechanisms, 1973.
7. Michalke, A., and Fuchs, H.V. "On Turbulence and Noise of an Axisymmetric Shear Flow." Journal of Fluid Mechanics, Vol. 70, 1975, pp. 179-205.
8. Dahan, C., and Elias, G. "Source Structure Pattern in a Hot Jet by Infrared-Microphones Correlations." AIAA Paper No. 76-542, 1976.
9. McLaughlin, D.K., Morrison, G.L., and Troutt, T.R. "Experiments on the Instability Waves in a Supersonic Jet and Their Acoustic Radiation." Journal of Fluid Mechanics, Vol. 69, 1976, pp. 73-95.
10. McLaughlin, D.K., Morrison, G.L., and Troutt, T.R. "Reynolds Number Dependence in Supersonic Jet Noise." AIAA Journal, Vol. 15, 1977, pp. 526-532.
11. Morrison, G.L., and McLaughlin, D.K. "The Instability Process in Low Reynolds Number Supersonic Jets." submitted for publication, Journal of Fluid Mechanics, 1978.
12. Morrison, G.L., and McLaughlin, D.K. "The Noise Generation by Instabilities in Low Reynolds Number Supersonic Jets" Journal of Sound and Vibration, to be published.
13. Lau, J.C., Morris, P.J., and Fisher, M.J. "Turbulence Measurements in Subsonic Jets Using a Laser Velocimeter." AIAA Paper No. 76-348, 1976.

14. Lessen, M., Fox, J.A., and Zien, H.M. "The Instability of Inviscid Jets and Wakes in Compressible Fluid." Journal of Fluid Mechanics, Vol. 21, 1965, pp. 129-143.
15. Lessen, M., and Singh, P.J. "The Stability of Axisymmetric Free Shear Layers." Journal of Fluid Mechanics, Vol. 60, 1973, pp. 433-457.
16. Michalke, A. "Instabilität eines kompressiblen runden Freistrahls unter Berücksichtigung des Einflusses der Strahlgrenzschichtdicke." Z. Flugwiss., Vol. 19, 1971, pp. 319-328.
17. Tam, C.K.W. "On the Noise of a Nearly Ideally Expanded Supersonic Jet." Journal of Fluid Mechanics, Vol. 51, 1972, pp. 69-95.
18. Morris, P.J. "The Spatial Viscous Instability of Axisymmetric Jets." Journal of Fluid Mechanics, Vol. 77, 1976, pp. 511-529.
19. Morris, P.J., and Tam, C.K.W. "Near and Far Field Noise from Large-Scale Instabilities of Axisymmetric Jets." AIAA Paper 77-1351, 1977
20. Chan, Y.Y. "Spatial Waves in Turbulent Jets." The Physics of Fluids, Vol. 17, 1974, pp. 46-53.
21. Chan, Y.Y. "Noise Generated Wavelike Eddies in a Turbulent Jet." ICAS Paper No. 76-42, 1976.
22. Mattingly, G.E., and Chang, C.C. "Unstable Waves on an Axisymmetric Jet Column." Journal of Fluid Mechanics, Vol. 65, 1974, pp. 541-560.
23. Crighton, D.G. "The Excess Noise Field of Subsonic Jets." Journal of Fluid Mechanics, Vol. 56, 1972, pp. 683-694.
24. Crighton, D.G., and Gaster, M. "Stability of Slowly Diverging Jet Flow." Journal of Fluid Mechanics, Vol. 77, 1976, pp. 397-413.
25. Liu, J.T.C. "Developing Large-Scale Wavelike Eddies and the Near Jet Noise Field." Journal of Fluid Mechanics, Vol. 62, 1974, pp. 437-464.
26. Morris, P.J. "Flow Characteristics of the Large-Scale Wavelike Structure of a Supersonic Round Jet." Journal of Sound and Vibration, Vol. 53, 1977.
27. Tam, C.K.W., and Chen, K.C. "A Statistical Model of Turbulence in Two Dimensional Mixing Layers." Submitted for publication to the Journal of Fluid Mechanics.
28. Tam, C.K.W. "Supersonic Jet Noise Generated by Large Scale Disturbances." Journal of Sound and Vibration, Vol. 38, 1975, pp. 51-79.
29. Williams, J.E. Ffowcs, and Kempton, A.J. "The Noise from the Large-Scale Structure of a Jet." Journal of Fluid Mechanics, Vol. 84, 1976, pp. 673-694.
30. Gatski, T.B. "Sound Production Due to a Large-Scale Coherent Structures." AIAA Paper No. 79-0596, 1979.
31. Stromberg, J.L. "Flowfield and Acoustic Measurements of Low Reynolds Number Jets in the Transonic Range." M.S. Thesis, Oklahoma State University, Stillwater, Oklahoma, 1978.
32. Smith, R.H., and Wang, C.T. "Contracting Cones Giving Uniform Throat Speeds." Journal of the Aeronautical Sciences, 1974, pp. 356-360.
33. Browand, F.K., and Laufer, J. "The Role of Large Scale Structures in the Initial Development of Circular Jets." in Proceedings of the Turbulence in Liquids Conference, Vol. 4, 1975, pp. 333-344.
34. Miksad, R.W. "Experiments on the Nonlinear Interactions in the Transition of a Free Shear Layer." Journal of Fluid Mechanics, Vol. 59, 1973, pp. 1-21.
35. Horstman, C.C., and Rose, W.C. "Hot-wire Anemometry in Transonic Flow." AIAA Journal, Vol. 15, 1977, pp. 395-401.
36. Ko, C.L., McLaughlin, D.K., and Troutt, T.R. "Supersonic Hot-wire Fluctuation Data Analysis With a Conduction End Loss Correction," Journal of Physics E. Scientific Instruments, Vol. 11, 1978, pp. 488-494.
37. Troutt, T.R. "Measurements on the Flow and Acoustic Properties of A Moderate Reynolds Number Supersonic Jet." Ph.D. Dissertation, Oklahoma State University, Stillwater, Oklahoma, 1978.
38. Dutt, B. "Role of Large Scale Structures in the Noise Generation of a Turbulent Supersonic Jet." Ph.D. Dissertation, University of Southern California, Los Angeles, California, 1977.
39. Mollo-Christensen, E., Kolpin, M.A., and Martuccelli, J.R. "Experiments on Jet Flows and Jet Noise Far-Field Spectra and Directivity Patterns." Journal of Fluid Mechanics, Vol. 18, 1964, pp. 285-301.
40. Morrison, G.L. "Flow Instability and Acoustic Radiation Measurements of Low Reynolds Number Supersonic Jets." Ph.D. Dissertation, Oklahoma State University, Stillwater, Oklahoma, 1977.
41. Moore, C.J., "The Role of Shear-layer Instability Waves in a Jet Exhaust Noise." Journal of Fluid Mechanics, Vol. 80, 1977, pp. 321-357.
42. Bachert, D., and Pfizenmaier, E. "On the Amplification of Broad Band Jet Noise by a Pure Tone Excitation." Journal of Sound and Vibration, Vol. 43, 1975, pp. 581-587.
43. Kibens, V., "Noise Generated by Large Scale Structures in an Axisymmetric Jet." Paper EEL, American Physical Society, Division of Fluid Dynamics Conference, Los Angeles, California, 1978.
44. Hussain, A.K.M.F., and Zaman, K.B.M.Q. "Controlled Perturbation of Circular Jets." Structure and Mechanisms of Turbulence I, Proceedings of the Symposium on Turbulence held at the Technische Universität Berlin,

1977, pp. 31-42.

45. Davies, P.O.A.L. and Hardin, J.C. "Potential Flow Modelling of Unsteady Flow." in Numerical Methods in Fluid Dynamics, ed. C.A. Brebbia and J.J. Connor, Pentech Press, London, 1973, pp. 42-64.

# Figures

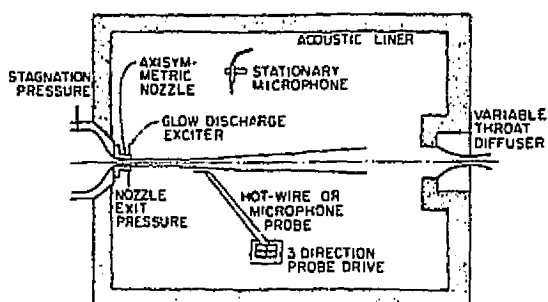


Fig. 1 Schematic diagram of jet test facility.

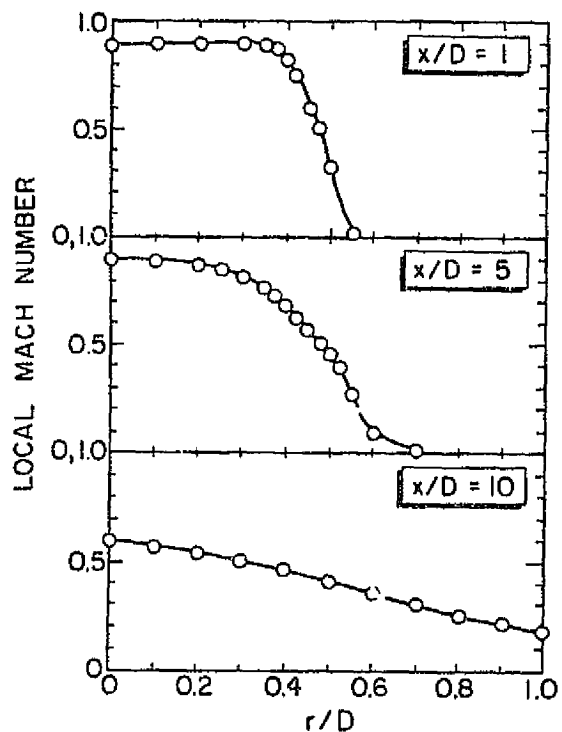


Fig. 2 Jet mean Mach number profiles.

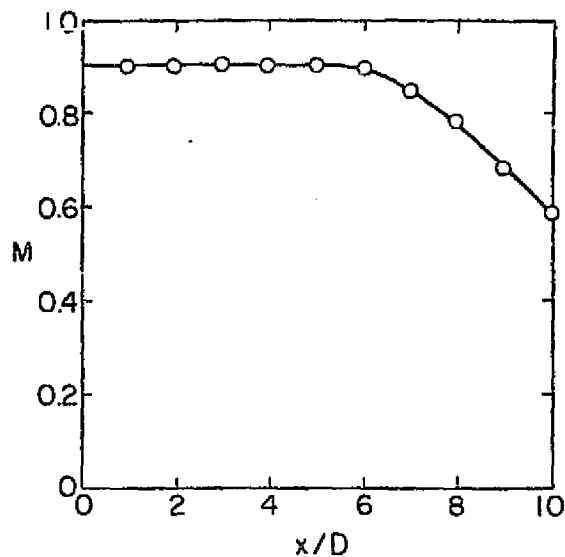


Fig. 3 Axial distribution of centerline Mach number.

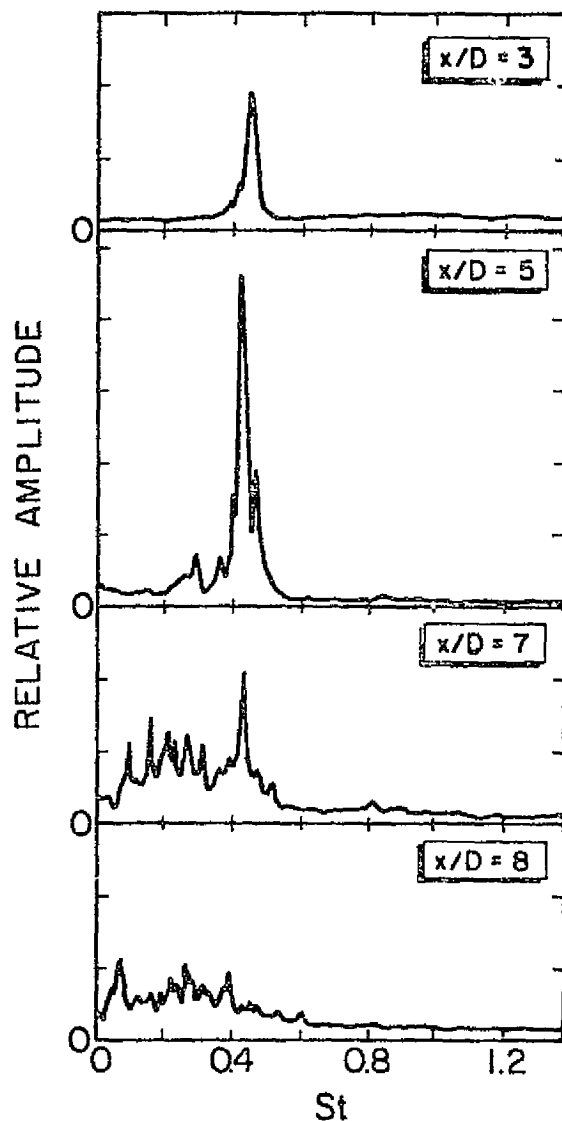


Fig. 4 Hot-wire frequency spectra for various probe locations.

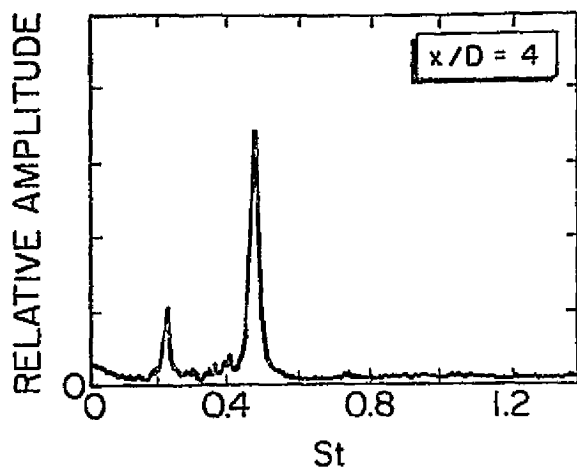


Fig. 5 Hot-wire frequency spectrum for probe located at  $x/D = 4$  on the inside of the shear layer.

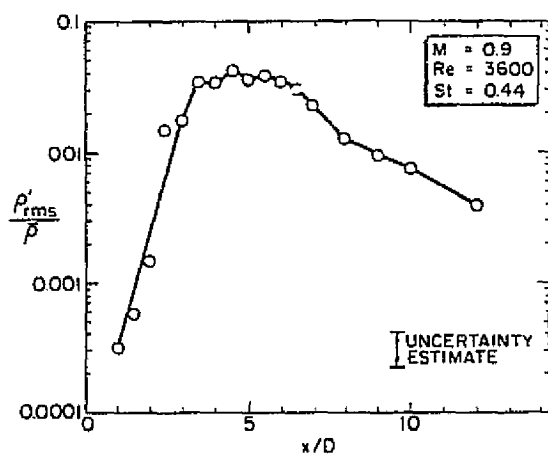


Fig. 6 Axial distribution of peak hot-wire fluctuation level.

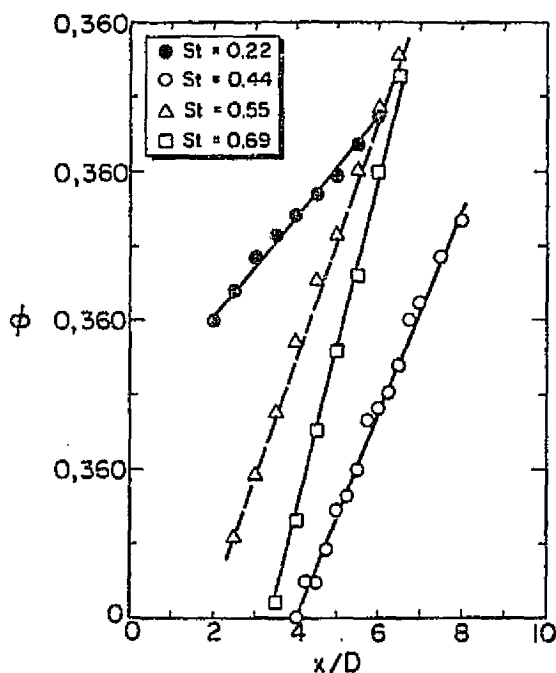


Fig. 7 Axial distribution of relative phase of several spectral components of the flow fluctuations.

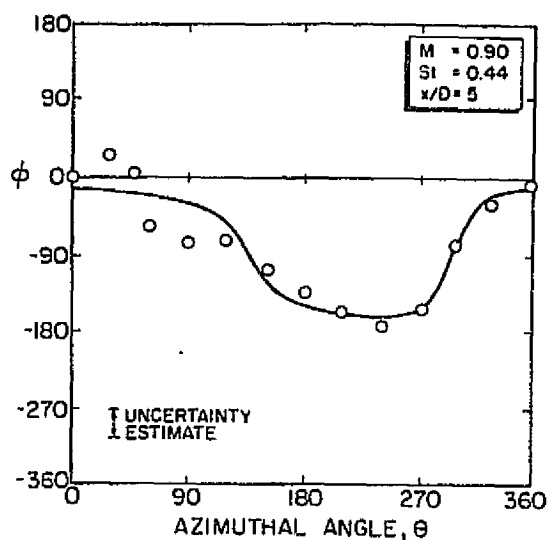


Fig. 8 Azimuthal distribution of relative phase of  $St = 0.44$  spectral component.

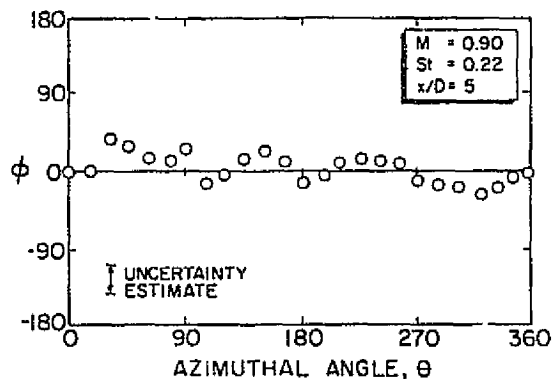


Fig. 9 Azimuthal distribution of relative phase of  $St = 0.22$  spectral component.

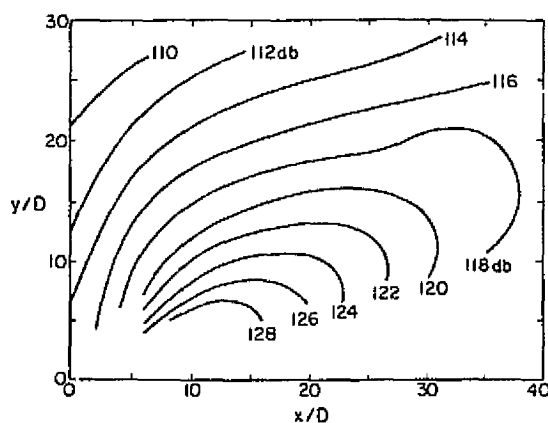


Fig. 10 Sound pressure level contours measured for the low Reynolds number  $M = 0.9$  jet.

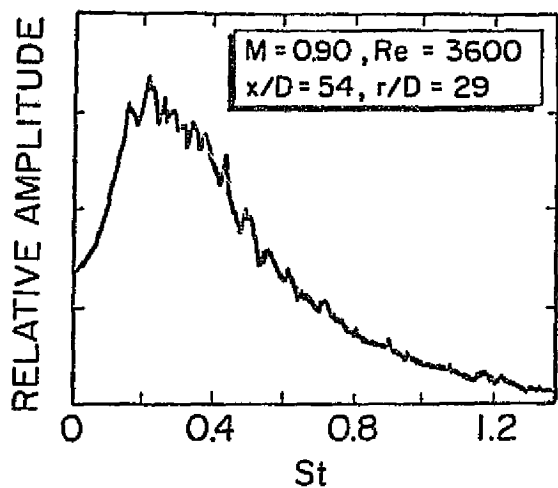


Fig. 11 Acoustic field microphone spectrum.

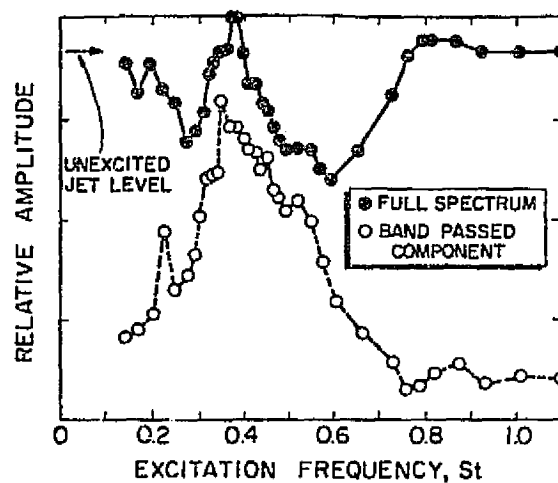


Fig. 14 Response of the jet to pure tone excitation.

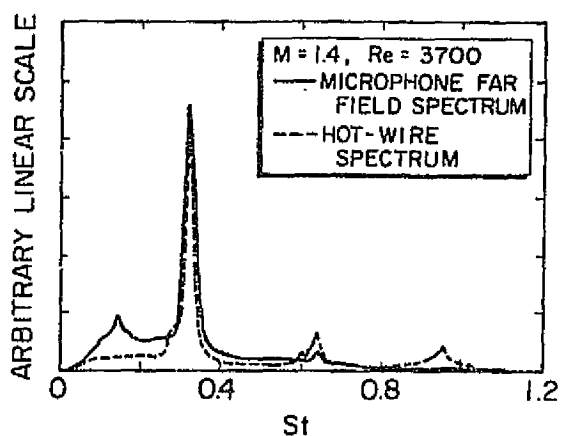


Fig. 12 Comparison of hot-wire and farfield microphone spectra measured in the low Reynolds number  $M=1.4$  jet. (Ref. 41)

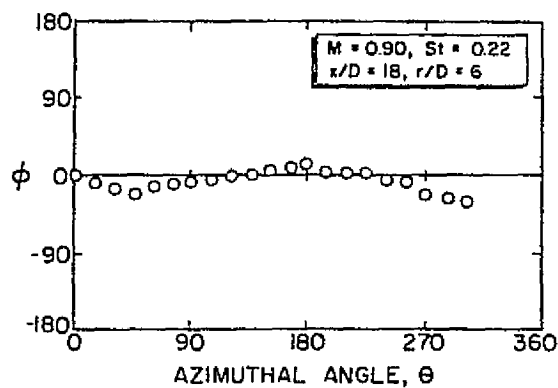


Fig. 15 Azimuthal distribution of relative phase of the  $St = 0.22$  spectral component in the acoustic field.

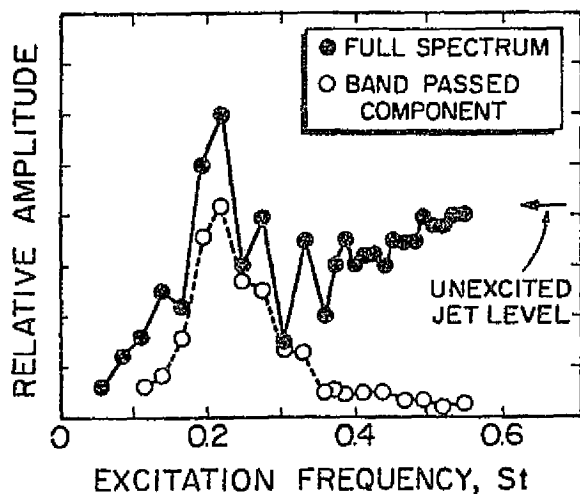


Fig. 13 Acoustic field response to pure tone excitation of the jet.

CROSSED HOT-WIRE MEASUREMENTS IN LOW REYNOLDS  
NUMBER SUPERSONIC JETS

By

JERRY DALE SWEARINGEN

Bachelor of Science in Mechanical Engineering

Oklahoma State University

Stillwater, Oklahoma

1977

Submitted to the Faculty of the Graduate College  
of the Oklahoma State University  
in partial fulfillment of the requirements  
for the Degree of  
MASTER OF SCIENCE  
December, 1979

Name: Jerry Dale Swearingen

Date of Degree: December, 1979

Institution: Oklahoma State University

Location: Stillwater, Oklahoma

Title of Study: **CROSSED HOT-WIRE MEASUREMENTS IN LOW REYNOLDS NUMBER  
SUPERSONIC JETS**

Pages in Study: 62

Candidate for Degree of Master of Science

Major Field: Mechanical Engineering

Scope of Study: Experimental measurements of the flow processes of low Reynolds number ( $Re < 10,000$ ), axisymmetric jets were made. Cold air jets were used with Mach numbers of 2.1 and 2.5. The overall goal of this study was to increase the basic understanding of the flow processes in the major noise producing regions of the jets. Advanced crossed hot-wire anemometry techniques were employed to obtain axial and radial velocity fluctuation measurements as well as a measure of their covariance (a component of the Reynolds stress tensor). Spectra of the fluctuations were made to determine spectral components present in the various fluctuations. Percent coherent structure measurements from the crossed hot-wire signals were also made in the artificially excited  $M = 2.5$  jet.

Findings and Conclusions: Comparisons of preliminary crossed hot-wire measurements in a subsonic jet to similar previous studies demonstrated the validity of the experimental technique and data reduction scheme. Measurements of the flow fluctuations in the supersonic jets were found to be low in amplitude due to a probe resolution problem when compared to previously reported data; but basic trends such as growth rates and jet development remained the same. Spectra of the fluctuations from the crossed hot-wire signals showed similar frequency content as previous work (shear layer fluctuations in the  $M = 2.5$  jet centered around the dominant  $St = 0.16$  spectral component). The initial measurements of the velocity covariance were also low in amplitude, but were successful in showing basic development trends. The measurements show that nonlinear effects become important in the jet development near the end of the jet potential core in the major region of noise production. Percent coherent structure measurements in the noise producing regions of the  $M = 2.5$  jet showed a spatial wave cell structure/flow disturbance interaction to occur. The measurements also show a strong decay in the coherence level past the end of the potential core. Additionally, spectra and fraction of coherent structure measurements showed that a coherent disturbance is present in some of the major nonlinear jet interactions.

ADVISER'S APPROVAL

Dennis K M Laughlin

CROSSED HOT-WIRE MEASUREMENTS IN LOW REYNOLDS  
NUMBER SUPERSONIC JETS

Thesis Approved:

---

Thesis Adviser

---

---

---

Dean of the Graduate College

## ACKNOWLEDGMENTS

The author wishes to express his appreciation to his major adviser, Dr. Dennis K. McLaughlin, and to his other committee members, Dr. David G. Lilley and Dr. Richard L. Lowery, for their advice and guidance concerning this work. Appreciation is also expressed to Dr. Tim R. Troutt for his assistance with the experiments and helpful comments on the work. The author would also like to express his gratitude to Charlene Fries for the final typing of the text.

The author also recognizes the financial support of the National Aeronautics and Space Administration through Grant No. NSG 1467.

## TABLE OF CONTENTS

Chapter	Page
I. INTRODUCTION . . . . .	1
A. Background . . . . .	1
B. Subject of Research . . . . .	2
C. Objectives . . . . .	4
II. EXPERIMENTAL APPARATUS . . . . .	6
A. General Facility . . . . .	6
B. Instrumentation . . . . .	8
III. EXPERIMENTAL PROCEDURES . . . . .	11
A. General . . . . .	11
B. Crossed Hot-Wire Procedure and Data Analysis . . . . .	11
C. Phase-Averaging Procedure . . . . .	16
IV. EXPERIMENTAL RESULTS . . . . .	18
A. Crossed Hot-Wire Measurements . . . . .	18
B. Phase-Average Measurements . . . . .	27
V. CONCLUSIONS . . . . .	30
A. Summary . . . . .	30
B. Recommendations for Further Study . . . . .	31
BIBLIOGRAPHY . . . . .	34
APPENDIX - FIGURES . . . . .	37

## LIST OF FIGURES

Figure	Page
1. Schematic of Overall Facility . . . . .	38
2. Schematic of Test Chamber . . . . .	39
3. Crossed Hot-Wire Probe, Full Scale . . . . .	40
4. Schematic of Electronic Devices . . . . .	41
5. Facility Coordinate System . . . . .	42
6. Schematic of Crossed Hot-Wire Probe Orientation . . . . .	43
7. Crossed Hot-Wire Calibration, $\bar{e}$ as a Function of $\bar{\rho}\bar{u}$ . . . . .	44
8. Crossed Hot-Wire Calibration, $\bar{A}_m$ as a Function of $Re_{wt}$ . . . . .	45
9. Crossed Hot-Wire Calibration, $\bar{e}/\bar{E}$ as a Function of $\alpha$ . . . . .	46
10. Crossed Hot-Wire Calibration, $\bar{A}_v$ as a Function of $Re_{wt}$ . . . . .	47
11. Radial Profiles of Axial Velocity Turbulence Intensity for the Subsonic Jet . . . . .	48
12. Radial Profiles of Radial Velocity Turbulence Intensity for the Subsonic Jet . . . . .	49
13. Axial Distribution of Peak Mass Velocity Fluctuations, M = 2.5 . . . . .	50
14. Axial Distribution of Peak Radial Velocity Fluctuations, M = 2.5 . . . . .	51
15. Crossed Hot-Wire Mass Velocity Spectra in the Jet Shear Layer, M = 2.5 . . . . .	52
16. Crossed Hot-Wire Radial Velocity Spectra in the Jet Shear Layer, M = 2.5 . . . . .	53
17. Variation of Shear Layer Half-Thickness Parameter ( $\delta/2d$ ) With Downstream Distance $\Delta M = 2.1$ , $OM = 2.5$ . . . . .	54
18. Radial Distributions of Velocity Covariance, $\sqrt{u'v'}/\bar{u}$ , M = 2.5 . . . . .	55

Figure	Page
19. Momentum Transport, $(\rho u)'v'$ , Spectra in the Jet Shear Layer, Unexcited $M = 2.5$ . . . . .	56
20. Momentum Transport, $(\rho u)'v'$ , Spectra in the Jet Shear Layer, Excited $M = 2.5$ . . . . .	57
21. Axial Distributions of Peak Mass Velocity and Peak Radial Velocity Fluctuations, $M = 2.1$ . . . . .	58
22. Radial Distributions of Velocity Covariance, $\sqrt{u'v'}/\bar{u}$ , $M = 2.1$ . . . . .	59
23. Axial Distribution of Percent Coherent Structure, $\langle (\rho u)' \rangle_{rms} / (\rho u)'_{rms}$ , in the Mass Velocity Fluctuations, $M = 2.5$ . . . . .	60
24. Wavelength Measurement of Axial Coherent Structure Oscillation, $M = 2.5$ . . . . .	61
25. Axial Distribution of Percent Coherent Structure, $\langle (\rho u)'v' \rangle_{rms} / [(\rho u)'v']_{rms}$ , in the Velocity Covariance, $M = 2.5$ . . . . .	62

## NOMENCLATURE

$A_m$	mass velocity fluctuation sensitivity coefficient
$A_t$	stagnation temperature fluctuation sensitivity coefficient
$A_v$	radial velocity fluctuation sensitivity coefficient
$b$	$(\gamma - 1) M^2_s$
$d$	effective nozzle exit diameter, nozzle exit diameter minus twice the displacement thickness
$D$	nozzle exit diameter
$e$	hot-wire voltage
$E$	$(e_1 + e_2)/2$ , $e_1$ and $e_2$ evaluated at $\alpha = 0$
$f$	frequency (Hz)
$f(\vec{x}, t)$	general fluctuating quantity
$k$	complex wave number
$k_i$	imaginary part of the complex wave number
$k_r$	real part of the complex wave number
$M$	Mach number
$P$	pressure
$P_{ch}$	test chamber pressure
$P_n$	static nozzle exit pressure
$r$	radial distance from jet centerline, cylindrical coordinate system
$R$	radial distance from center of jet at nozzle exit, spherical coordinate system

Re	Reynolds number, $U_0 D/\nu$
$R_w$	hot-wire resistance
s	$[1 + ((\gamma - 1)/2) M^2]^{-1}$
St	Strouhal number, $fd/U_0$
t	time
T	temperature
$T_w$	hot-wire temperature
u	axial velocity
$U_0$	jet centerline exit velocity
v	radial velocity
x	downstream distance from the nozzle
$\vec{x}$	general spatial quantity
y	vertical distance from the nozzle
z	horizontal distance from the nozzle
$\alpha$	yaw angle of the crossed hot-wire probe relative to the jet centerline
$\beta$	angular coordinate in spherical coordinate system
$\gamma$	ratio of specific heats
$\delta$	local shear layer thickness
$\theta$	azimuthal angle
$\nu$	kinematic viscosity
$\lambda$	axial wavelength
$\rho$	density
$\tau$	period of the wave
$( )_t$	quantity evaluated at stagnation conditions
$( )_0$	quantity evaluated at jet exit
$(\overline{\quad})$	time average of quantity

- $\langle \rangle$  phase average of quantity
- $(\ )'$  total fluctuation,  $(\ )' = (\tilde{\ }) + (\ )''$
- $(\ )''$  random portion of fluctuation
- $(\tilde{\ })$  periodic portion of fluctuation

## CHAPTER I

### INTRODUCTION

#### A. Background

In the past 25 years extensive research has been devoted to the study and control of the noise produced by high speed exhaust jets. Many ad hoc attempts have been made to control this noise, but still there is no completely satisfactory jet noise suppressor on commercial aircraft at this time. Clearly, if we are to develop effective jet silencers in the future, a thorough understanding of the jet noise generation processes is needed.

Early theoretical analyses of aerodynamic noise generation were able to approximately predict the radiated acoustic field if the distribution of acoustic sources within the jet flow were known (1) through (7). These theories provided considerable understanding of the noise generation processes. However, since the understanding of the actual flow fluctuations composing the source terms was limited, these efforts typically only resulted in simple scaling laws, particularly in supersonic jet noise analyses.

Originally, the flow fluctuations in turbulent free shear flows were considered to be completely random in nature. In recent years, however, a number of experimental studies have indicated that a coherent structure exists in these flows (8) through (11). It has also been hypothesized

that this organized structure which is large scale in nature, may be of fundamental importance in the noise generation processes (12) (13) (14).

Presently there is extensive debate over the description of the large scale disturbances. The works of Laufer et al. (15) and Lau et al. (11) among others interpret these coherent disturbances as vortex structures that tend to interact (pair) as they convect downstream. The process in which these structures interact has been proposed to be an important mechanism of subsonic jet noise generation (15) (16). Other researchers have attempted to model the organized fluctuations as instability waves (17) through (21). Of these theories, Morris and Tam (21) have developed the most comprehensive noise prediction model for supersonic jets. Their model can be used to calculate the noise generated by the large scale instability waves from a matched asymptotic expansion method. Their predictions are found to be in reasonable agreement with the experimental results of Yu and Dosanjh (22) for an  $M = 1.5$  jet.

#### B. Subject of Research

Over the last few years, extensive experimental measurements have been performed in an ongoing high speed jet noise research program at Oklahoma State University (23) through (28). The major goals of this research were to provide understanding of the noise generation processes and to provide the experimental framework upon which more accurate jet noise theories could build. The measurements were concentrated on the flowfield and acoustic properties of high speed jets in the Mach number range from  $M = 0.9$  to  $M = 2.5$ . A unique approach was taken to obtain most of these data in that the jets were operated at a low Reynolds number, in the range from  $Re = 3700$  to  $15,000$ . Additional measurements

were performed at a moderate Reynolds number ( $Re \approx 70,000$ ) most recently by Troutt (28).

Lowering the Reynolds number from that of conventional laboratory jets exhausting to the atmosphere ( $Re \approx 1 \times 10^6$ ) produces several experimental advantages. The low density of the flows allows standard hot-wire anemometry techniques to be employed for measurement of the fluctuating flow properties. Also the small scale turbulence which tends to mask the coherent flow structure is decreased, making the structure's detection and characterization easier.

These experimental studies have shown that for low Reynolds number (transitional) supersonic jets there are instability waves present which can be characterized by a linear stability theory and that these instability waves produce a major portion of the noise radiated by the jet (23) (24). The noise produced by the instabilities was also found to have comparable amplitudes and directivity patterns to those of high Reynolds number jets. These results suggest that coherent flow disturbances in the form of instability waves are powerful noise generators and that the theoretical approach taken by researchers such as Tam (17), Liu (19), Morris (20), and Chan (18) holds promise.

Results of the low Reynolds number subsonic studies ( $M = 0.9$ ) show comparable acoustic properties to those of a high Reynolds number fully turbulent jet. However, an interesting phenomenon in contrast to previous work with low Reynolds number supersonic jets was observed. The flow and acoustic fields were found to be dominated by quite different peak frequencies. This finding strongly indicates that the noise generation probably results from a mechanism different from that of a supersonic jet. In fact, Stromberg, McLaughlin, and Troutt (27) suggest that

the vortex pairing model proposed by Laufer et al. (15) might be appropriate for this subsonic jet.

The present study was intended primarily to extend the work done previously on the low Reynolds number ( $Re < 10,000$ ) supersonic jets by Morrison and McLaughlin (25) (26). The approach has been to make more detailed flow and acoustic measurements in and around the major noise production region of the jets (i.e., near the end of the potential core). The chosen Mach number of the jets for a majority of the measurements was  $M = 2.5$ . It was considered experimentally advantageous to perform most of the measurements at this Mach number so that most of the transonic hot-wire problems were avoided.

### C. Objectives

The overall goal of the present study was to increase the understanding of the flow processes in the noise producing region of supersonic jets with emphasis on the nonlinear processes and their role in the jet instability and turbulence development. In the future analysis of dominant jet instabilities and the resulting noise production, it will become increasingly desirable to quantify some of the important nonlinear processes.

Nonlinear processes\* have two direct effects on the flow:

1. They broaden the spectral distribution of the fluctuations and produce high amplitude harmonics and subharmonics of the dominant spectral components.

---

\*It should be noted that the primary nonlinear terms in the governing flow equations occur in the Reynolds stress tensor. The term  $\rho \overline{u'v'}$  is the most important component, since it is responsible for the transport of x-momentum in the radial direction.

2. They increase the mixing (or simply the momentum transport) in the shear layer so as to have a direct effect on the mean flow properties.

Thus the specific objectives of this study are as follows:

1. To quantify and characterize some of the important nonlinear processes in the jet flow (i.e., the production of Reynolds stress).
2. To determine what portion of the flow fluctuations is attributable to random turbulence.
3. To obtain information relating the radiated noise to the flow fluctuations in order to gain more understanding of the dominant noise generating mechanisms.

Satisfying the above objectives would give valuable information concerning the significance of nonlinear instability interactions as well as test the appropriateness of a wave model description of the dominant jet fluctuations. Experimental evidence established from these measurements should also be helpful in the development of future instability/turbulence models.

## CHAPTER II

### EXPERIMENTAL APPARATUS

#### A. General Facility

The experiments in this study were performed in the Oklahoma State University free jet test facility shown in the schematic diagram of Figure 1 (see Appendix). This facility is unlike any other in the United States in that it allows experimental measurements of a jet to be made in a low pressure anechoic environment. The facility consists of three sections: a compressed air source and stilling chamber to supply the jet stream, a test chamber section, and a vacuum system to provide the low pressure environment.

Compressed air is supplied to the jet facility from a 1.8 cubic meter storage tank through a pressure regulator, a throttling valve, and a stilling section. The compressed air is dehumidified prior to storage and the compressor is shut down during the actual experimental measurements to eliminate extraneous vibrations to the system. The pressure regulator and throttling valve combination were used to control the stagnation pressure of the jet. The stilling section is 15 cm in diameter by 55 cm in length and consists of a 5 cm length of acoustical foam, three perforated plates, a 7.6 cm honeycomb section, and six fine mesh screens all to perform turbulence reduction and flow management.

A cubic contoured contraction section (area ratio greater than 200:1) connects the stilling section to the jet nozzle in the test

chamber. Several different axisymmetric supersonic nozzles were used in this study: design Mach number  $M = 2.5$  with an exit diameter ( $D$ ) of 9 mm, and Mach numbers  $M = 2.1$  and  $M = 1.4$  with exit diameters of 10 mm. The inviscid nozzle contours were determined using the method of characteristics to obtain a contour which gave uniform parallel flow at the nozzle exit (29). A boundary layer correction was also added corresponding to an average Reynolds number condition ( $10,000 \leq Re \leq 20,000$ ).

The jet exhausts into a 0.7 x 0.8 x 1.2 meter vacuum chamber with a 5 cm thick Scott Tyrell acoustical absorption form liner. This combination produces an anechoic environment for frequencies above one kilohertz. The vacuum chamber is depicted in Figure 2.

This test chamber is equipped with a probe drive system capable of translation in three orthogonal directions ( $x, y, z$ ) and rotation in the horizontal plane ( $x-z$  plane). Precision ten-turn potentiometers incorporated in the system provide D.C. voltage readout proportional to the probe location. This system gives accurate and repeatable positioning of various sensor probes: normal hot-wire probe, crossed hot-wire probe, pitot pressure probe, static pressure probe, or condenser microphone. Another stationary probe may also be mounted above the jet in the vertical plane through the centerline.

Each jet nozzle is equipped with a glow discharge device which was used to artificially excite the jet. The method of excitation was similar to the technique reported earlier by Kendall (30) and was used in previous studies at Oklahoma State University (23) through (28). The excitation device consists of a 1.5 mm diameter tungsten electrode insulated with ceramic tubing and mounted within 2 mm of the nozzle exit. An oscillating glow discharge is established by applying an alternating

voltage biased to a large negative potential (-300 volts D.C.) to the electrode. The frequency of the alternating voltage can be varied using a signal generator, thus allowing a small controlled disturbance to be input to the jet.

The vacuum chamber has an exhaust diffuser with a variable throat which allows constant and accurate control of the pressure in the chamber. The diffuser is connected to a  $0.1 \text{ m}^3/\text{sec}$  Kinney vacuum pump by way of 15 meters of piping and a 30 cubic meter vacuum storage tank. Thus pressure fluctuations and vibrations from the vacuum pump have a negligible effect on the test chamber environment.

#### B. Instrumentation

Pressure measurements were made with a silicone oil (specific gravity of 0.93) manometer and a mercury manometer, both referenced to a vacuum of 30 microns of mercury, absolute pressure. Pressure taps were located at various positions in the facility to measure stilling chamber stagnation pressure, nozzle static pressure, and test chamber pressure. By controlling both the stilling chamber stagnation pressure and the test chamber pressure, it was possible to obtain a perfectly expanded jet at a given Reynolds number over a wide range.

Acoustic measurements were made using a 3.175 mm diameter Brüel and Kjaer condenser microphone type 4138 and associated B & K type 2618 pre-amplifier and type 2804 power supply. The microphone has omnidirectional response within  $\pm 3$  dB for frequencies up to 60 kHz. Calibration of the microphone was performed in a low pressure environment using a B & K type 4220 piston phone. Previous studies have shown that the calibration is essentially independent of the ambient pressure (24).

Flow fluctuation measurements were made using DISA constant temperature anemometry electronics that consisted of a DISA 55M01 main frame with a 55M10 standard bridge (two anemometers were needed in crossed hot-wire measurements). The normal hot-wire probes were DISA 55A53 subminiature probes mounted on slender brass wedges. Crossed hot-wire probes were constructed from round jewelers broaches, perforated thermocouple ceramic insulators, and 5 micron diameter platinum-plated tungsten wire. These were also mounted on brass wedges. Normally the frequency response of the hot-wire probe (normal or crossed) and electronics was found to be near 60 kHz based on square wave response tests. For total level measurements both the hot-wire and microphone signals were band-pass filtered from 3 kHz to 60 kHz to remove chamber and electronic resonances. Construction details of the hot-wire probes are shown in the schematic diagram of Figure 3.

Using a technique similar to that given by Rose (31) (32) it was possible to simultaneously measure the instantaneous axial mass velocity fluctuations and radial velocity fluctuations from the crossed hot-wire probe (refer to the Experimental Procedures chapter). This required special electronics to instantaneously add and subtract the two crossed wire outputs. Using multiplication electronics it was also possible to obtain a component of the Reynolds stress tensor. These electronic configurations were constructed from commercially available analog devices and are detailed in the schematic diagram of Figure 4.

Frequency spectra of both the hot-wire and microphone signals were made using a Tektronix 7L5 spectrum analyzer. A constant bandwidth of one kilohertz was used to generate all spectra in this study. Correlation and phase-averaging of sensor signals were performed using a Saicor

model SAI 43A correlation and probability analyzer. Both instruments have frequency response in excess of 100 kHz and were considered adequate for this study.

## CHAPTER III

### EXPERIMENTAL PROCEDURES

#### A. General

The majority of the experimental measurements contained in this study were performed on a perfectly expanded (nozzle exit pressure  $P_n$  is maintained within 2% of jet back pressure  $P_{ch}$ ) jet of nominal Mach number  $M = 2.5$  and Reynolds number of approximately 8700. These conditions were chosen to correspond to those used in work done previously by Morrison and McLaughlin (25) (26). Additionally, jets of Mach number  $M = 2.1$  and 1.4 were used in the calibration of the cross hot-wire probes. The stagnation temperature of the jets was room temperature (approximately 294 K).

A facility coordinate system (origin at the jet exit) used in all measurements is shown in Figure 5. Positioning within this coordinate system was done based on the effective jet diameter  $d$  and most of the data presented in this study is nondimensionalized using this diameter. The effective diameter is defined to be the physical jet exit diameter  $D$ , minus twice the displacement thickness of the boundary layer (the ratio  $D/d$  was 1.12 for the  $M = 2.5$ ,  $Re = 8700$  jet).

#### B. Crossed Hot-Wire Procedure and Data Analysis

The fluctuating properties (axial mass velocity and radial velocity) of the jet flow were obtained using a crossed hot-wire anemometry

technique similar to that given by Rose (31) (32). The validity of this data reduction procedure in supersonic flow requires that the Mach number of the flow normal to the hot-wire be above 1.2. A crossed hot-wire probe consists of wires inclined approximately 45 degrees to the mean flow direction; thus, detailed measurements were made primarily in the Mach number  $M = 2.5$  jet and in regions of its flow where the Mach number normal to the wire satisfied this criterion.

All measurements using the crossed hot-wire were made with the probe located in the horizontal x-z plane of the jet. Figure 6 shows a schematic diagram detailing the proper orientation of the crossed hot-wire probe in a jet shear layer to measure the mean flow, the flow fluctuations in the axial direction, and the fluctuations in the radial direction. For comparison, the schematic also shows the orientation of a normal hot-wire probe for measuring the mean flow and flow fluctuations in the axial direction in the same shear layer.

Following the ideas of Morkovin and Phinney (33), the instantaneous voltage fluctuation measured from an inclined hot-wire in supersonic flow can be represented by the following expression:

$$\frac{e'}{\bar{e}} = A_m \frac{(\rho u)'}{\bar{\rho u}} + A_t \frac{T_t'}{\bar{T}_t} \pm A_v \frac{v'}{\bar{u}}$$

where  $A_m$ ,  $A_t$ , and  $A_v$  are the sensitivity coefficients for mass velocity fluctuations, total temperature fluctuations, and radial velocity fluctuations, respectively. These coefficients can be evaluated as follows (32).

$$A_m = \left. \frac{\partial \ln \bar{e}}{\partial \ln \bar{\rho u}} \right|_{T_t, R_w, \alpha \text{ constant}}$$

$$A_t = \left. \frac{\partial \ln \bar{e}}{\partial \ln \bar{T}_t} \right|_{\rho u, R_w, \alpha \text{ constant}}$$

$$A_v = \left. \frac{\partial \ln \bar{e}}{\partial \alpha} \right|_{\rho u, R_w, T_t \text{ constant}}$$

Two oppositely inclined wires of a crossed hot-wire probe give outputs that can be instantaneously added and subtracted to result in

$$\begin{aligned} (e'_1 + e'_2) &= (\bar{e}_1 A_{m_1} + \bar{e}_2 A_{m_2}) \frac{(\rho u)'}{\rho u} + (\bar{e}_1 A_{t_1} + \bar{e}_2 A_{t_2}) \frac{T'_t}{\bar{T}_t} \\ &\quad + (\bar{e}_1 A_{v_1} - \bar{e}_2 A_{v_2}) \frac{v'}{u} \\ (e'_1 - e'_2) &= (\bar{e}_1 A_{m_1} - \bar{e}_2 A_{m_2}) \frac{(\rho u)'}{\rho u} + (\bar{e}_1 A_{t_1} - \bar{e}_2 A_{t_2}) \frac{T'_t}{\bar{T}_t} \\ &\quad + (\bar{e}_1 A_{v_1} + \bar{e}_2 A_{v_2}) \frac{v'}{u} . \end{aligned}$$

For the crossed hot-wire measurements reported in this study, it was normally assumed that the total temperature fluctuations were negligible. Both Troutt (28) and Morrison (25) have determined that in supersonic jets at Reynolds numbers from 3700 to 70,000 total temperature fluctuations were typically responsible for less than 2 percent of the hot-wire rms voltage fluctuations, thus justifying the assumption. Also, the crossed hot-wires were matched so that the sensitivity coefficients  $A_m$  and  $A_v$  were approximately the same for each wire. These simplifications resulted in two voltages proportional to  $(\rho u)' / \rho u$  and  $v' / u$ , respectively:

$$(e'_1 + e'_2) = (\bar{e}_1 A_{m_1} + \bar{e}_2 A_{m_2}) \frac{(\rho u)'}{\rho u}$$

$$(e_1' - e_2') = (\overline{e_1 A_{v_1}} + \overline{e_2 A_{v_2}}) \frac{v'}{\bar{u}}.$$

Additionally, the major shear component of the Reynolds stress tensor was determined by multiplication of these voltages proportional to  $(\rho u)' / \bar{\rho} \bar{u}$  and  $v' / \bar{u}$ , and use of the following relationship derived by Rose (31) (32):

$$\frac{\overline{u' v'}}{\bar{u}^2} = \frac{s}{s + b} \frac{\overline{(\rho u)' v'}}{\bar{\rho} \bar{u}^2}$$

where

$$s = \frac{1}{1 + \frac{(\gamma - 1)}{2} M^2}$$

$$b = (\gamma - 1) M^2 s.$$

The required sensitivities in the above relations were evaluated by direct calibration over the range of Mach and Reynolds numbers encountered in this study. The calibration was performed by locating the crossed hot-wire probe on the centerline of the jet near the nozzle exit. The Reynolds number (and thus  $\bar{\rho} \bar{u}$ ) was varied by changing the upstream stagnation pressure. Different Mach numbers were obtained using three nozzles operating at respective design pressure ratios ( $M = 1.4, 2.1$ , and  $2.5$ ).

The calibration of the crossed hot-wire was performed as follows. The probe was positioned in one of the nozzles to give the desired nominal calibration Mach number. With the probe at zero angle of incidence to the free stream flow direction, the mean bridge voltage  $\bar{e}$  was read from the anemometer for each wire for various values of stagnation pressure with  $T_t$  and  $T_w$  held constant. The results of these readings were

then plotted as shown for the three Mach numbers in Figure 7. (The data are plotted in dimensional terms here to show the actual results obtained from the calibration procedure.) The derivative  $\partial \ln \bar{e} / \partial \ln \bar{\rho} \bar{u}$  was needed to obtain the  $A_m$  sensitivity coefficient and the data of the figure were fitted with a second order curve to more readily accomplish this. There was an immeasurable effect of Mach number on the values of  $\partial \ln \bar{e} / \partial \ln \bar{\rho} \bar{u}$ . Figure 8 shows the results of determining these sensitivity coefficients for each wire over the Reynolds number range of interest. (The data are presented as the average value of the two individual wire sensitivities.) Shown also for comparison are calibration data obtained by Morrison (25) in the same facility using a normal hot-wire and data obtained by Rose (32) with a normal hot-wire in a supersonic boundary layer. The data of Rose are substantially different, probably due to greater conduction end loss effects resulting from a low probe aspect ratio. (The length to diameter ratios for the various data are Morrison,  $\ell/d = 200$ , Rose  $\ell/d = 100$ , and present study  $\ell/d = 250$ .)

To obtain the sensitivity to angulation,  $A_v$ , the probe was rotated between  $+5^\circ$  and  $-5^\circ$  incidence angle to the free stream flow direction in increments of  $1^\circ$  using the facility probe drive system. Again at a desired calibration Mach number, the mean bridge voltage of the two wires  $\bar{e}$  was read for each position with the values of  $\bar{\rho} \bar{u}$ ,  $T_t$ , and  $T_w$  held constant. This procedure was repeated for various values of  $\bar{\rho} \bar{u}$ . The results of these readings were plotted as shown in the example of Figure 9 and a linear regression scheme was used to determine the derivatives  $\partial \ln \bar{e} / \partial \alpha$  needed for the  $A_v$  coefficients. (Note that the curves of Figure 9 do not intersect at the zero degree point as one might expect, due to inexact matching of the wires--slight differences in individual

wire output for identical flow conditions.) The sensitivity coefficients (again an average of the individual wire sensitivities) determined from these data are given in Figure 10 along with similar data obtained by Rose (32) using a single inclined hot-wire. The figure demonstrates a significant Mach number effect in this low Reynolds number flow regime and the results of differing conduction end loss effects can again be seen in the comparison with the data of Rose.

To decompose the crossed hot-wire voltages into the appropriate fluctuations, the local  $\overline{pu}$  was determined from the  $\overline{e}$  outputs at the given probe location and the local Mach number was determined from the mean flow data of Morrison (25) for the same jet flow. These quantities were then used with the previously discussed calibration curves to calculate the appropriate sensitivity terms.

### C. Phase-Averaging Procedure

Turbulent flows with an inherent coherent structure lend themselves to a triple decomposition of the type:

$$f(\vec{x}, t) = \overline{f}(\vec{x}) + \tilde{f}(\vec{x}, t) + f''(\vec{x}, t).$$

In this representation (first used by Kendall (34) and Hussain and Reynolds (35)), any flow quantity consists of a sum of the mean flow  $\overline{f}(\vec{x})$ , the organized wave  $\tilde{f}(\vec{x}, t)$ , and the random turbulence  $f''(\vec{x}, t)$ .

The mean flow portion is given by the conventional time average of  $f(\vec{x}, t)$ :

$$\overline{f}(\vec{x}) = \lim_{T \rightarrow \infty} \frac{1}{T} \int_0^T f(\vec{x}, t) dt$$

In order to extract the periodic wave component from the total flow fluctuation, the phase-average of  $f(\vec{x}, t)$  can be defined as

$$\langle f(\vec{x}, t) \rangle = \lim_{N \rightarrow \infty} \frac{1}{N} \sum_{n=0}^N f(\vec{x}, t + n\tau)$$

where  $\tau$  is the period of the organized wave and  $N$  is the number of wave cycles over which the phase-average is taken. The phase-average of a single turbulent quantity is zero. Thus, the periodic wave component can be obtained from the phase-average of the total flow quantity by subtracting the mean flow contribution:

$$\tilde{f}(\vec{x}, t) = \langle f(\vec{x}, t) \rangle - \bar{f}(\vec{x}).$$

To effectively phase-average a fluctuating signal representing a flow quantity, a reference signal oscillating at the wave frequency must be supplied as a triggering source to initiate the measurement. For the measurements presented in this study, the signal supplied to the oscillating glow discharge device was used as the phase-averaging trigger. This is essentially the same procedure used by Hussain and Reynolds (35) to obtain  $\tilde{f}(\vec{x}, t)$ .

## CHAPTER IV

### EXPERIMENTAL RESULTS

#### A. Crossed Hot-Wire Measurements

##### A.1 Preliminary Subsonic Flowfield Measurements

In view of the absence of pertinent published fluctuating flow data for a supersonic jet obtained from an inclined hot-wire, preliminary crossed hot-wire measurements were made in a low-speed jet--for which considerably more published data exist--to assess the validity of the experimental technique and data reduction schemes discussed in the Experimental Procedures section. Comparisons of radial profiles of turbulence intensity for two axial locations obtained by this method in a one-inch diameter  $Re = 30,000$ ,  $M = 0.05$  jet are made in Figures 11 and 12 with those obtained by Bradshaw et al. (36) for a  $Re = 300,000$ ,  $M = 0.3$  jet. (Additionally, Seiner (37) has obtained results in favorable agreement with Bradshaw for a similar jet flow.) The fluctuating velocities are normalized based on the jet exit velocity,  $u_0$ , and the radial and axial distances by the nozzle radius,  $r_0$ . The results of Bradshaw exhibit turbulence levels that are generally lower than those of the present study; however, the curves follow closely the same trends. The results indicate the jet of the present study develops somewhat faster than the jet flow studied by Bradshaw. This would be expected for the more abrupt contraction section and lack of turbulence reduction material in the

stilling section of the facility used here. (The area contraction ratio here is approximately 9:1 whereas the facility used by Bradshaw had a contraction ratio greater than 36:1.) Bushnell (38) has found that at low Reynolds number there is a pronounced increase in turbulent fluctuations near the end of transition and beginning of turbulent flow in a boundary layer. This low Reynolds number effect is suspected to occur in free shear flows also and may give a partial explanation of the discrepancies seen in these data. Additionally, differences may be due in part to the fact that the present measurements did not use a linearizer preceding the rms voltmeter, as is normally standard practice in subsonic flow measurements.

These findings in the low-speed jet provide sufficient evidence that the previously detailed experimental procedure is capable of producing measurements of fluctuating flow quantities with reasonable accuracy. With this impetus, it was considered justifiable to pursue the desired measurements in the supersonic jets using the same techniques.

#### A.2 Flowfield Measurements, Mach Number 2.5 Jet

Crossed wire measurements have been attempted once before in our laboratory by Morrison (25). Unfortunately, older hot-wire electronics were used and their frequency response, in conjunction with the crossed hot-wire in the low Reynolds number supersonic jet flow, was not adequate. Consequently, his results were only of a preliminary nature.

The crossed hot-wire probe was used to measure the axial mass velocity and radial velocity fluctuation amplitudes in the various supersonic jets. Figure 13 shows the peak axial mass velocity fluctuation amplitude (normalized based on the local mean mass velocity) for an unexcited

$M = 2.5$ ,  $Re = 8700$  jet as a function of axial location,  $x/d$ . The radial locations of the peak fluctuation amplitude corresponded to the center of the shear layer until the end of the potential core where the peak was found to be near the jet centerline. The figure contains data from two different experimental runs on separate days, as well as similar data obtained by Morrison (25) using a normal hot-wire probe in the same  $M = 2.5$  jet. Uncertainty estimates based on instrumentation and calibration inaccuracies are shown as brackets on the data of the figure (and other figures that follow as well). These uncertainty estimates do not include consideration of inaccuracies due to probe resolution discussed later. Comparison shows that the data of the present study is some two to three times lower in fluctuation amplitude than the results of Morrison. The initial level of fluctuations measured using the crossed hot-wire probe is less than 0.2 percent ( $2\frac{1}{2}$  times lower than that measured by Morrison). The amplitude of the fluctuations grows exponentially for the first 15 diameters downstream and peaks at a fluctuation level of approximately 16 percent near the axial location of the potential core end. Morrison has found that this exponential growth can be characterized by a linear stability type representation\* with a growth rate,  $-k_i d$ , of  $0.29 \pm 0.04$  (95% confidence interval). Although they are substantially low in amplitude, the measurements of the present study follow this calculated growth rate and other general trends closely.

---

\*A linear stability analysis assumes a representation of the flow disturbance  $Q(x, r, \theta, t)$  in the form:  $Q(x, r, \theta, t) = \hat{Q}(r) \text{Re}\{\exp[i(k_r x - \omega t + n\theta) - k_i x]\}$  where  $\text{Re}$  here stands for the real part of  $\{ \}$ ,  $x$ ,  $r$ , and  $\theta$  are the axial, radial, and azimuthal coordinates, respectively.

Figure 14 shows the corresponding growth of the radial velocity fluctuations measured from the crossed hot-wire probe. The radial velocity fluctuations (normalized based on the local mean velocity) grow approximately exponentially from  $x/d = 5$  to 20. The rate of growth,  $-k_r d$ , in this region is  $0.19 \pm 0.04$  with a peak fluctuation level of 11 percent at  $x/d = 25$ . Measurements made by Lau et al. (39) in several different Mach number jets (including a  $M = 1.4$  jet) using a laser velocimeter indicate that the radial velocity fluctuations are generally somewhat lower in amplitude than the corresponding axial velocity fluctuations. The measurements made using the crossed hot-wire also indicate this trend. However, because of the relative infancy of the use of laser velocimetry in supersonic flow measurements, in particular in the measurement of turbulence quantities, the associated uncertainties in these measurements are also substantial and absolute comparisons with these data are difficult to make. As previously pointed out, the axial mass velocity fluctuation measurements are substantially low in amplitude and the deterministic cause probably also affects measurements of the radially velocity somewhat.

Frequency spectra of the crossed hot-wire signal proportional to the mass velocity fluctuations obtained from the radial position of maximum voltage fluctuation (approximately at the center of the jet shear layer) are shown in Figure 15 for several  $x/d$  locations. Frequencies are presented in terms of the nondimensional Strouhal number,  $St = fd/U_0$ , where  $U_0$  is the exit velocity of the jet and  $d$  is the effective diameter. The figure indicates that there is a band of unstable frequencies present with a majority of the fluctuations centered around the prevalent Strouhal number 0.16 spectral component. These spectra are very similar

in shape and development to those obtained by Morrison (25) in the same jet flow using a normal hot-wire. Figure 16 shows the corresponding crossed hot-wire spectra of the signal proportional to the radial velocity fluctuations for several  $x/d$  locations. These spectra contain a band of frequency components between  $St = 0.04$  and  $St = 0.35$ , as in the mass velocity spectra of Figure 14. At  $x/d = 5$ , although the  $St = 0.16$ , spectral component is present as in the mass velocity spectra, a dominant peak at  $St = 0.10$  is apparent. However, by  $x/d = 10$ , the  $St = 0.16$  spectral component again dominates the spectrum. For the most part, these spectra show the same overall characteristics as the mass velocity spectra do.

In summary, mass velocity fluctuation amplitude measurements made using the crossed hot-wire probe are substantially low in comparison to previous data obtained in the same facility and flowfield using a normal hot-wire. The underlying cause of this discrepancy appears also to affect subsequent measurements of the radial velocity fluctuations. Figure 13, however, seems to demonstrate that the crossed wire measures an approximately correct axial distribution of the mass velocity fluctuations (with an attenuation of about 2). Additionally, spectra of the flow fluctuations are in reasonable agreement with previous results and thus indications are that the problem lies in the amplitude measurement technique and/or data reduction scheme and not in the frequency response of the instrument.

The suspected failing in these measurements is poor probe resolution. Measurements in the subsonic jet (where the ratio of jet diameter to probe size was approximately 17:1) using the described techniques proved to give quite reasonable results. In the measurements in the

$M = 2.5$  jet, however, the probe resolution was lower by a factor of almost three (ratio of jet diameter to probe size was approximately 6:1). Experience shows that this ratio should normally be much greater than this to obtain good resolution in the measurements. Also, in comparison to similar measurements made using a normal hot-wire, there is a difference in probe size on the order of 300:1 between it and the crossed hot-wire probe used here. (This can be seen clearly in the schematic diagram detailing both probes in Figure 6.) Originally the measurements of this study were to be performed in jets two times larger in diameter, thus giving the needed probe resolution; but lack of pumping capability in the jet facility limited the measurements to the smaller jets for the present time. Additional evidence of the probe resolution problem is given in the mass velocity measurements of Figure 13. The discrepancy between the crossed hot-wire measurements and the results of Morrison (25) decreases with increasing axial location. The results are lower by a factor of almost three near the nozzle exit, yet are only low by a factor of 1.7 past the end of the jet potential core where jet spreading gives a much larger flowfield. These results indicate that improved probe resolution should yield substantially better flow fluctuation amplitude measurements.

The emphasis in performing the measurements in this study centers on the development of the nonlinear processes in the jet, in particular on the production of Reynolds stresses. One of the dramatic results of the onset of nonlinear effects can be seen in the mean flow data of Morrison (25). Figure 17 shows how the local shear layer half thickness  $\delta/2$  varies with axial location for two jet Mach numbers of interest. The location where the jet begins to widen at a faster rate coincides

approximately with the end of the potential core and is the point at which significant nonlinear interactions become important in the jet development. Additionally, spectral broadening of the flow fluctuations in this region is also evidence of strong nonlinear interactions.

Typical distributions of the axial and radial velocity covariance, expressed in terms of  $\sqrt{u'v'}/\bar{u}$  are shown in Figure 18. The curves show reasonable trends, but as before, the data appear to be low in amplitude. The laser velocimeter measurements of Lau et al. (39) in a  $M = 1.4$  jet show a peak value for  $\sqrt{u'v'}/\bar{u}$  of approximately 0.10. This would indicate that the discrepancy in amplitude is of the same order as that found in the results of the mass velocity fluctuation measurements. Arguments have been put forward that the major cause of the amplitude discrepancy is the inadequate probe resolution. Despite this problem, the crossed wire measurements do provide some valuable insights into the flow processes in the developing jet. Figure 18 shows that the velocity fluctuation covariance  $\overline{u'v'}$  undergoes a substantial change from  $x/d = 15$  to  $x/d = 20$  in the  $M = 2.5$  jet. Not only has the peak value more than doubled, but the distribution has a substantially increased radial spread. This clearly demonstrates that this important nonlinear transport quantity has considerably more influence at  $x/d = 20$  in comparison with  $x/d = 15$ . The change in the contribution of the Reynolds stress component  $\overline{u'v'}$  from  $x/d = 15$  to  $x/d = 20$  coincides with the saturation and initial decay of the mass velocity fluctuations as depicted in Figure 12. It is also in this region where the mean flow begins to change substantially (refer to Figure 17). The combined evidence indicates that at  $x/d = 15$  nonlinear effects (as measured in terms of  $\overline{u'v'}$ ) become important and by  $x/d = 20$  they are a major effect. This region of the  $M = 2.5$  jet flow

has been shown by Morrison and McLaughlin (25) (26) to be one of dominant noise production in this jet.

Figure 19 contains spectra of the momentum transport  $[(\rho u)'v']$  fluctuations for an unexcited (natural)  $M = 2.5$  jet. These spectra were obtained in the approximate center of the jet shear layer where the velocity fluctuations maximize. As might be expected, the spectra contain a broad band of fluctuations centered at the approximate double frequency of the fundamental  $St = 0.16$  instability. Beyond  $x/d = 16$  the amplitude of the fluctuations increase noticeably and the spectra shift towards lower frequency content with downstream location as indicated by the spectrum at  $x/d = 18$ . Again these changes occur in the region of the end of the potential core where a major portion of the noise is being produced by the jet. Spectra of the momentum transport fluctuations for the same  $M = 2.5$  jet flow excited at the  $St = 0.16$  instability are shown in Figure 20. The spectra show that the excitation frequency plus integer multiples of that frequency. (It is difficult to ascertain the fundamental frequency in these spectra. The expected fundamental would be at  $St = 0.32$  due to doubling of the  $St = 0.16$  instability present in the mass velocity and radial velocity fluctuation when they are multiplied in the momentum transport quantity  $[(\rho u)'v']$ , but this is not clearly the case here.) The excited disturbances begin to grow noticeably past  $x/d = 12$  and between  $x/d = 14$  and  $x/d = 16$  there is a substantial increase in the broad band fluctuations. By  $x/d = 18$  the excited disturbances are virtually indistinguishable from the broad band components. These spectra give an indication that the coherent instability is present, at least to some degree, in some of the major nonlinear processes in the jet, namely in the momentum transport  $[(\rho u)'v']$ .

### A.3 Flowfield Measurements, Mach Number 2.1 Jet

The growth of the mass velocity and radial velocity fluctuations determined using a crossed hot-wire are shown in Figure 21 for an unexcited  $M = 2.1$ ,  $Re = 7900$  jet. Also shown are similar mass velocity data obtained by Morrison (25) using a normal hot-wire in the same jet flow. Again, as in the case of the previous measurements performed on the  $M = 2.5$  jet, the measurements for this jet are considerably low in amplitude. The mass velocity fluctuations increase approximately exponentially for the first six to seven diameters of flow, as do the measurements of Morrison, yet the peak fluctuation amplitude of 12.5 percent at  $x/d = 10$  is only half of the value determined by Morrison. Correspondingly, the radial velocity fluctuations grow exponentially with a peak level attained at  $x/d = 10$  of 8.6 percent. The explanation of the discrepancy in these data is as before in the  $M = 2.5$  jet; poor resolution (ratio of nozzle diameter to probe size here is 7:1) results in fluctuation amplitude data low by a factor of at least two.

Figure 22 presents distributions of the axial and radial velocity covariance for several  $x/d$  locations. Again, the general trends appear to be reasonable, but the absolute amplitude values are suspect due to the probe resolution problem. The data show a peak value for the covariance,  $\sqrt{u'v'}/\bar{u}$ , of 0.04 at  $x/d = 10$  (this is the approximate peak value obtained for the  $M = 2.5$  jet also). Again, as in the  $M = 2.5$  jet data, the velocity fluctuation covariance undergoes a major change in the region of the potential core end where the mean flow changes (refer to Figure 17) and the mass velocity fluctuations saturate and begin to decay. This corresponds also to the major noise production region of this  $M = 2.1$  jet.

#### A.4. Summary of Crossed Hot-Wire Results

The original intent of the crossed hot-wire measurements in this study was to investigate some of the significant nonlinear interactions in the jet (i.e., investigate the development of the axial and radial velocity covariance component of the Reynolds stress tensor in the major noise producing regions of the jet flow near the end of the potential core). This study showed major difficulties in accurately determining flow fluctuation amplitude measurements from the crossed hot-wire in the present jet facility. However, the measurements did show qualitatively that the major nonlinear processes (as measured by the velocity covariance  $\overline{u'v'}$ ) become important in the developing jet flow in the region of the end of the potential core where a majority of the noise is being produced.

#### B. Phase-Average Measurements

The fraction of organized structure present in the mass velocity fluctuations was measured by phase-averaging the signal from a normal hot-wire using the technique described in the Experimental Procedures section. Figure 23 shows the axial variation in the coherent fraction of the mass velocity fluctuations in the noise producing region of the excited  $M = 2.5$ ,  $Re = 8700$  jet. Each point represents a numerical average of all data taken at various radial locations for that particular axial position. The figures shows a distinct oscillation with axial location in the fraction of coherent structure. Morrison (25) performed this measurement for several axial locations, but his measurements were not in sufficient detail to establish this behavior. (The Morrison data are shown also in Figure 23 and are somewhat higher than the data of the

present study. This can be attributed to the fact that the peak values of the coherence are not shown for each axial position; instead average values across the jet for that location are shown.) The major point of note in these measurements is the strong decay in the coherence level (i.e., the disintegration of the coherent instability) past the end of the potential core. Additional detailed measurements were made between  $x/d = 12$  and  $x/d = 16$  on the jet centerline to determine the wavelength of this oscillation and are presented in Figure 24. The data show the axial wavelength to be approximately  $\lambda/d = 2.25$ . Comparison with the axial distribution of centerline Mach number shows this wavelength to correspond closely to the jet spatial wave cell structure (a system of weak expansion and compression waves caused by nonparallel flow at the nozzle exit) wavelength. Measurements of the variation in mean hot-wire voltage along the jet centerline verified the cell structure wavelength to be approximately  $\lambda/d = 2.25$  also. Similar detailed measurements by Stromberg (27) in a subsonic jet showed no behavior of this sort.

Figure 25 shows the fraction of organized structure present in the signal proportional to the axial and radial velocity covariance as a function of downstream position. The level of coherence is much smaller than in the mass velocity fluctuations, as might be expected due to the interaction of spectral components in the velocity fluctuations to produce harmonics and subharmonics. However, it is of sufficient level to indicate the presence of some kind of coherent flow disturbance. An interesting feature of these data is the marked increase and then rapid decline of the coherence level in the vicinity of the potential core end.

In summary, the phase-average measurements of mass velocity fluctuations show some kind of spatial wave cell structure/flow disturbance

interaction to occur in the excited jet development. The measurements also indicate the fraction of coherent structure decreases as the flow progresses downstream and that there is a significant drop in the level after the potential core end. Phase-average measurements of the covariance along with previous spectra of the excited jet fluctuations show the presence of a coherent disturbance in some of the important nonlinear jet interactions.

## CHAPTER V

### CONCLUSIONS

#### A. Summary

Crossed hot-wire measurements were performed in several supersonic jets of Mach number  $M = 2.5$  and  $M = 2.1$  at a low Reynolds number ( $Re < 10,000$ ). The overall goal of the study was to increase the basic understanding of the flow processes in the noise producing regions of the jets by making detailed flow measurements there. The emphasis in the study centered on the nonlinear processes of the flow and their role in the jet instability and turbulence development. The major results derived from the study are listed as follows:

1. Preliminary measurements in a subsonic jet using the discussed crossed hot-wire technique gave results very close to previously published data, thus demonstrating the validity of the technique.
2. Measurements of the mass velocity and radial velocity fluctuations in the low Reynolds number supersonic jets were low in amplitude by a factor of two to three from previously reported data in the same flows, but basic trends such as growth rates and jet development remained the same.
3. Spectra of the flow fluctuations from the crossed hot-wire signals showed similar frequency content as previous work (shear layer fluctuations centered around the dominant  $St = 0.16$  spectral component for the  $M = 2.5$  jet).

4. Initial attempts at determining a component of the Reynolds stress tensor,  $\overline{u'v'}/u$ , from the crossed hot-wire measurements proved somewhat successful in that basic trends in the data were reasonable, but again the absolute amplitudes were low and suffered from a problem attributed to poor probe resolution. The measurements did however provide information demonstrating that there is a major change in the contribution of the Reynolds stress to the jet development in the region of the end of the potential core. It has been shown that this is the region where the mean flow changes dramatically, the flow fluctuations saturate and decay, and a major portion of the noise is being produced.

5. Detailed measurements of the fraction of coherent structure in the noise producing region of an excited  $M = 2.5$  jet ( $x/d = 12$  to  $x/d = 20$ ) showed that some kind of spatial wave cell structure/flow disturbance interaction was present. The measurements also indicated that there is a substantial decrease in the coherence level past the end of the potential core.

6. Spectra and measurements of the fraction of coherent structure in the signal proportional to the Reynolds stress component showed that a coherent disturbance is indeed present in some of the nonlinear jet interactions.

7. Experience useful in future experimental efforts using crossed hot-wire techniques in supersonic jets was gained.

#### B. Recommendations for Further Study

The overshadowing difficulty with the measurements of this study was the lack of good probe resolution that prevented the desired detailed investigation of the flow processes. Originally the measurements were to

be made in an improved jet facility to overcome part of this problem, but a lack of pumping capability dictated the use of smaller jets thus creating the difficulty. Future efforts in this research will be conducted in a facility with greatly increased pumping capability, thus substantially better measurements can be made using the same techniques detailed here.

A viable program to continue this particular research should include a number of improvements:

1. The present pumping facility should be overhauled and evaluated as to its suitability for operating larger-size jets to obtain better probe resolution.
2. An evaluation should be made of the current crossed hot-wire probes. Smaller probes could possibly be constructed to improve probe resolution. An alternative might be to evaluate the suitability (and associated difficulties) of using the smaller-sized split-film sensor probes commercially available in place of the crossed hot-wire.
3. The present electronics associated with the determination of the flow quantities from the crossed wire should be rebuilt to give better accuracy and reliability.
4. Future efforts in this research should probably also include a program to utilize advanced digital data acquisition and processing techniques. Complicated experimental measurements of this nature are difficult to perform using on-line analog electronic equipment. The School of Mechanical and Aerospace Engineering at Oklahoma State University has an existing mini-computer facility (INTERDATA 7/16) suitable for this purpose. A program of this type would utilize the School's Honeywell 7600 FM tape deck for recording hot-wire signals during an experimental

run. (The data could later be digitized and analyzed using the mini-computer.) This plan will require more analog to digital conversion equipment to obtain the desired accuracy in the data reduction.

Additional advantages are also gained in utilizing a program of this type. Use of the computer greatly aids in the ease, speed, and accuracy of basic data reduction. This also enhances the possibility of using conditional sampling procedures in future work that should provide more insight into the physics of the jet flow.

## BIBLIOGRAPHY

- (1) Lighthill, M. J. "On Sound Generated Aerodynamically, I General Theory." Proc. Roy. Soc., A211 (1952), pp. 546-587.
- (2) Lighthill, M. J. "On Sound Generated Aerodynamically, II Turbulence as a Source of Sound." Proc. Roy. Soc., A222 (1954), pp. 1-32.
- (3) Ffowcs Williams, J. E. "The Noise From Turbulence Convected at High Speed." Phil. Trans. Roy. Soc., A255 (1963), p. 459.
- (4) Phillips, O. M. "On the Generation of Sound by Supersonic Turbulent Shear Layer." J. Fluid Mech., Vol. 9 (1960), pp. 1-28.
- (5) Ribner, H. S. "The Generation of Sound by Turbulent Jets." Advances in Applied Mechanics, Vol. 8 (1964), pp. 103-182.
- (6) Pao, S. P., and M. V. Lowson. "Some Applications of Jet Noise Theory." AIAA Paper No. 70-233, 1970.
- (7) Lilley, G. M., P. Morris, and B. J. Tester. "On the Theory of Jet Noise and Its Applications." AIAA Paper No. 73-987, 1973.
- (8) Brown, G., and A. Roshko. "The Effect of Density Difference on the Turbulent Mixing Layer." AGARD Conference on Turbulent Shear Flows. Conf. Proc. No. 93 (1971), p. 23.
- (9) Winant, C. D., and F. K. Browand. "Vortex Pairing, the Mechanism of Turbulent Mixing Layer Growth at Moderate Reynolds Number." J. Fluid Mech., Vol. 63 (1974), pp. 237-256.
- (10) Crow, S. C., and F. H. Champagne. "Orderly Structure in Jet Turbulence." J. Fluid Mech., Vol. 48 (1971), pp. 547-591.
- (11) Lau, J. C., M. J. Fisher, and H. V. Fuchs. "The Intrinsic Structure of Turbulent Jets." J. Sound and Vibration, Vol. 22, No. 4 (1972), pp. 379-405.
- (12) Mollo-Christensen, E. "Jet Noise and Shear Flow Instability Seen From an Experimenter's Viewpoint." J. Appl. Mech., Vol. 34 (1967), pp. 1-7.
- (13) Bishop, K. A., J. E. Ffowcs Williams, and W. Smith. "On the Noise Sources of the Unsuppressed High-Speed Jet." J. Fluid Mech., Vol. 50 (1971), pp. 21-31.

- (14) Tam, C. K. W. "On the Noise of a Nearly Ideally Expanded Supersonic Jet." J. Fluid Mech., Vol. 51 (1972), pp. 69-95.
- (15) Laufer, J., R. E. Kaplan, and W. T. Chu. "On the Generation of Jet Noise." AGARD Conference Proceedings No. 131 on Noise Mechanisms, 1973.
- (16) Ffowcs Williams, J. E., and A. J. Kempton. "The Noise From the Large-Scale Structure of a Jet." J. Fluid Mech., Vol. 84 (1976), pp. 673-694.
- (17) Tam, C. K. W. "Supersonic Jet Noise Generated by Large-Scale Disturbances." J. Sound and Vibration, Vol. 38 (1974), pp. 51-79.
- (18) Chan, Y. Y. "Discrete Acoustic Radiation From a High-Speed Jet as a Singular Perturbation Problem." Canadian Aeronautics and Space Journal, Vol. 38 (1974), pp. 51-79.
- (19) Liu, J. T. C. "Developing Large-Scale Wavelike Eddies and the Near Jet Noise Field." J. Fluid Mech., Vol. 62 (1974), pp. 437-464.
- (20) Morris, P. J. "Flow Characteristics of the Large-Scale Wavelike Structure of a Supersonic Round Jet." J. Sound and Vibration, Vol. 53 (1977), pp. 223-244.
- (21) Morris, P. J., and C. K. W. Tam. "Near and Far Field Noise From Large-Scale Instabilities of Axisymmetric Jets." AIAA Paper No. 77-1351, 1977.
- (22) Yu, J. C., and D. S. Dosanjh. "Noise Field of Supersonic Mach 1.5 Cold Jet." J. Acoust. Soc. Am., Vol. 51 (1973), pp. 1400-1410.
- (23) McLaughlin, D. K., G. L. Morrison, and T. R. Troutt. "Experiments on the Instability Waves in a Supersonic Jet and Their Acoustic Radiation." J. Fluid Mech., Vol. 69 (1976), pp. 73-95.
- (24) McLaughlin, D. K., G. L. Morrison, and T. R. Troutt. "Reynolds Number Dependence in Supersonic Jet Noise." AIAA J., Vol. 15 (1977), pp. 526-532.
- (25) Morrison, G. L. "Flow Instability and Acoustic Radiation Measurements of Low Reynolds Number Supersonic Jets." (Unpublished Ph.D. thesis, Oklahoma State University, Stillwater, Oklahoma, 1977.)
- (26) Morrison, G. L., and D. K. McLaughlin. "The Noise Generation by Instabilities in Low Reynolds Number Supersonic Jets." J. Sound and Vibration (to be published).
- (27) Stromberg, J. L., D. K. McLaughlin, and T. R. Troutt. "Flowfield and Acoustic Properties of a Mach Number 0.9 Jet at a Low Reynolds Number." AIAA Paper No. 79-0593, 1979.

- (28) Troutt, T. R. "Measurements on the Flow and Acoustic Properties of a Moderate Reynolds Number Supersonic Jet." (Unpublished Ph.D. thesis, Oklahoma State University, Stillwater, Oklahoma, 1978.)
- (29) Johnson, C. B., and L. R. Boney. "A Method for Calculating a Real-Gas Two-Dimensional Nozzle Contour Including the Effects of Gamma." NASA TM X-3243, Langley Research Center, Hampton, Virginia, 1975.
- (30) Kendall, J. M. "Supersonic Boundary Layer Stability Experiments." Proceedings of the Boundary Layer Transition Study Group Meeting, Vol. II, Aerospace Report No. TR-0158 (S3816-63)-1, 1967.
- (31) Johnson, D. A., and W. C. Rose. "Laser Velocimeter and Hot-Wire Anemometer Comparison in a Supersonic Boundary Layer." AIAA J., Vol. 13, No. 4 (1975), pp. 512-515.
- (32) Rose, W. C. "The Behavior of a Compressible Turbulent Boundary Layer in a Shock-Wave-Induced Adverse Pressure Gradient." NASA TN D-7092, 1973.
- (33) Morkovin, M. V., and R. E. Phinney. "Extended Applications of Hot-Wire Anemometry to High-Speed Turbulent Boundary Layers." AFOSR TN-58-469, Johns Hopkins Univ., Dept. of Aeronautics, June, 1958.
- (34) Kendall, J. M. "The Turbulent Boundary Layer Over a Wall With Progressive Surface Waves." J. Fluid Mech., Vol. 41 (1970), pp. 259-281.
- (35) Hussain, A. K. M. F., and W. C. Reynolds. "The Mechanics of an Organized Wave in Turbulent Shear Flow." J. Fluid Mech., Vol. 41 (1970), pp. 241-258.
- (36) Bradshaw, P., D. H. Ferriss, and R. H. Johnson. "Turbulence in the Noise Producing Region of a Circular Jet." J. Fluid Mech., Vol. 19 (1964), pp. 591-624.
- (37) Seiner, J. M. "The Distribution of Jet Source Strength Intensity by Means of a Direct Correlation Technique." (Unpublished Ph.D. thesis, Pennsylvania State University, University Park, Pennsylvania, 1974.)
- (38) Bushnell, D. M. "Calculation of Turbulent Free Mixing--Status and Problems." Free Turbulent Shear Flows Vol. I Conference Proceedings, NASA SP-321, 1972.
- (39) Lau, J. C., P. J. Morris, and M. J. Fisher. "Turbulence Measurements in Subsonic and Supersonic Jets Using a Laser Velocimeter." AIAA Paper No. 76-348, 1976.

## APPENDIX

## FIGURES

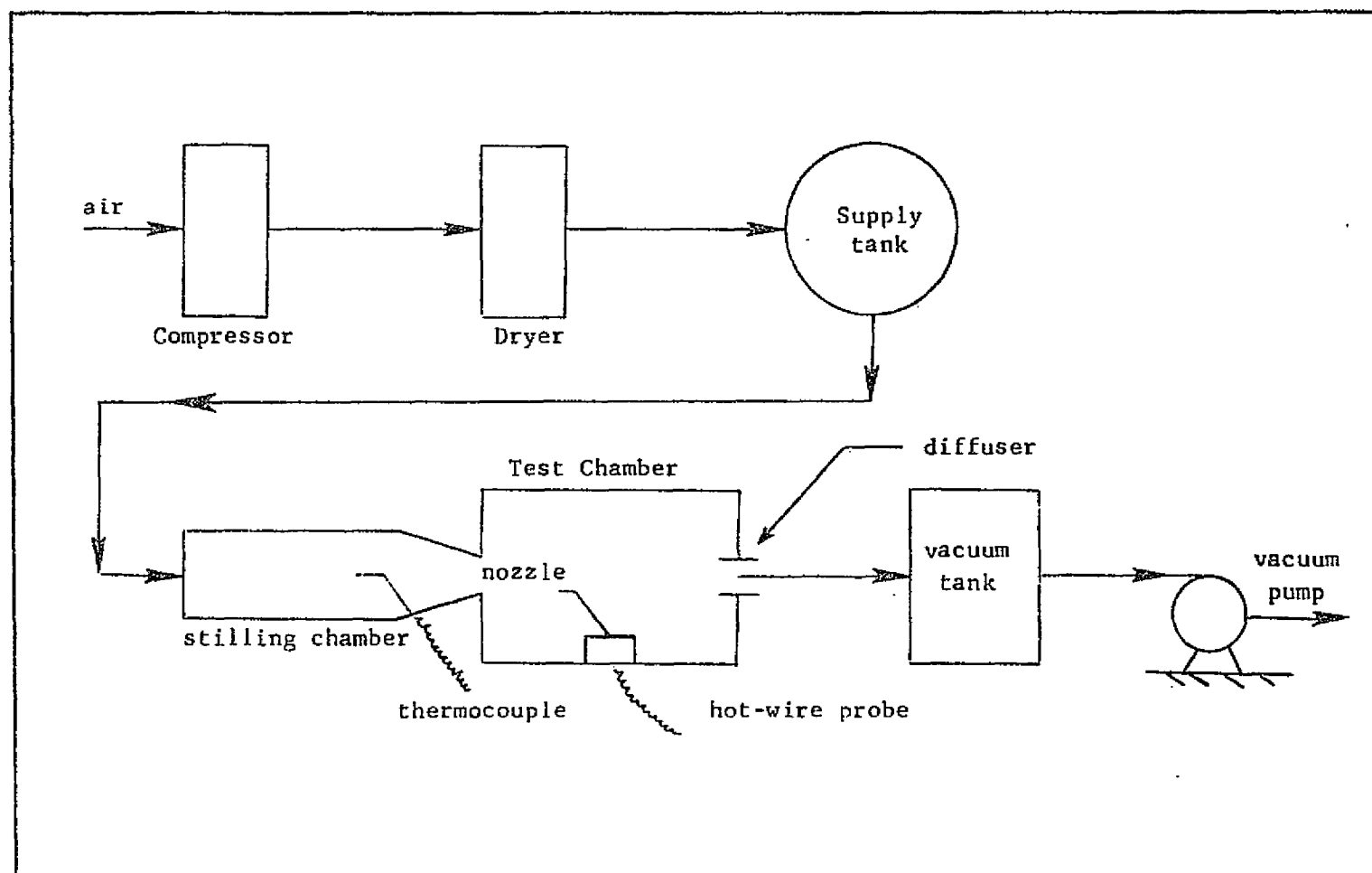


Figure 1. Schematic of Overall Facility

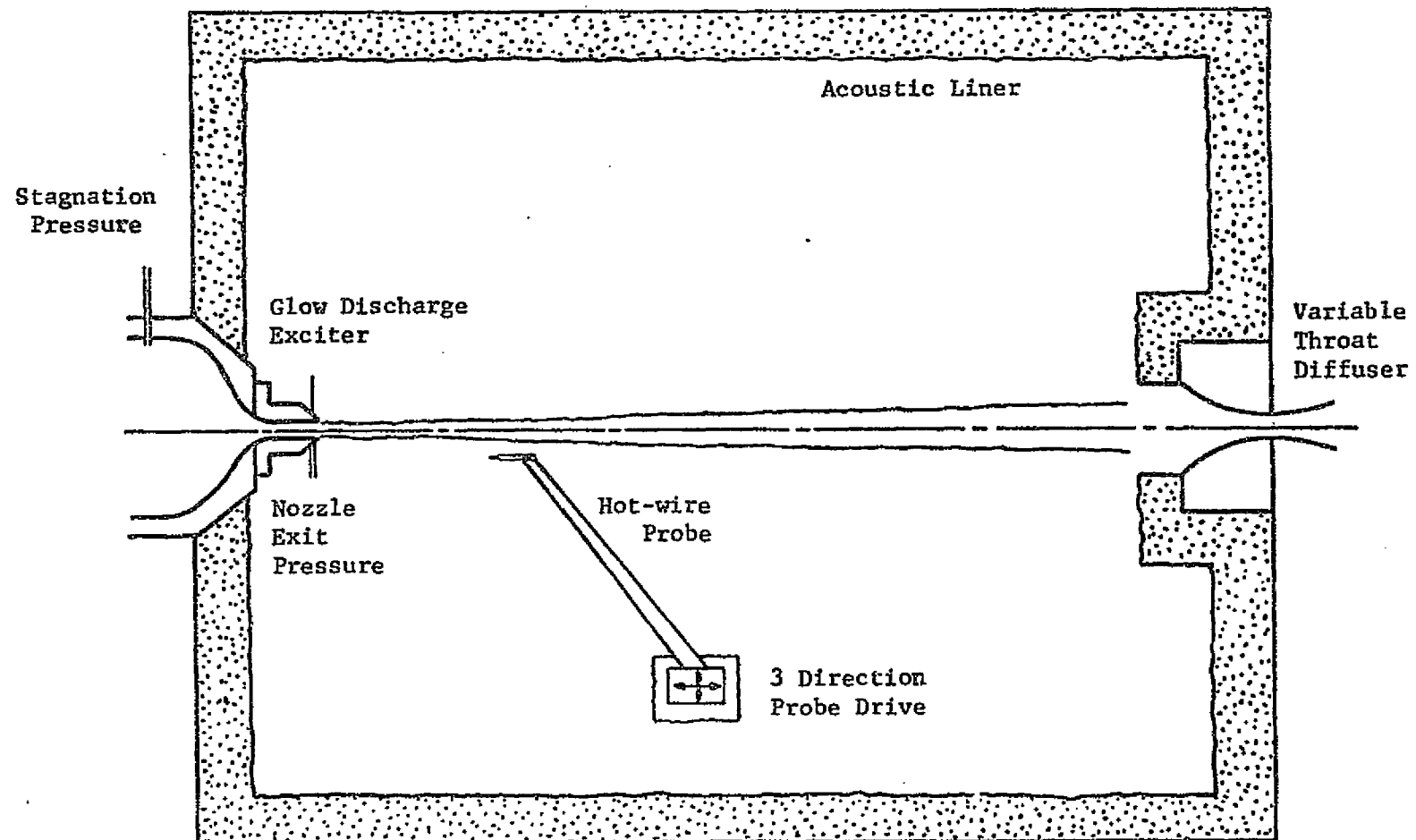


Figure 2. Schematic of Test Chamber

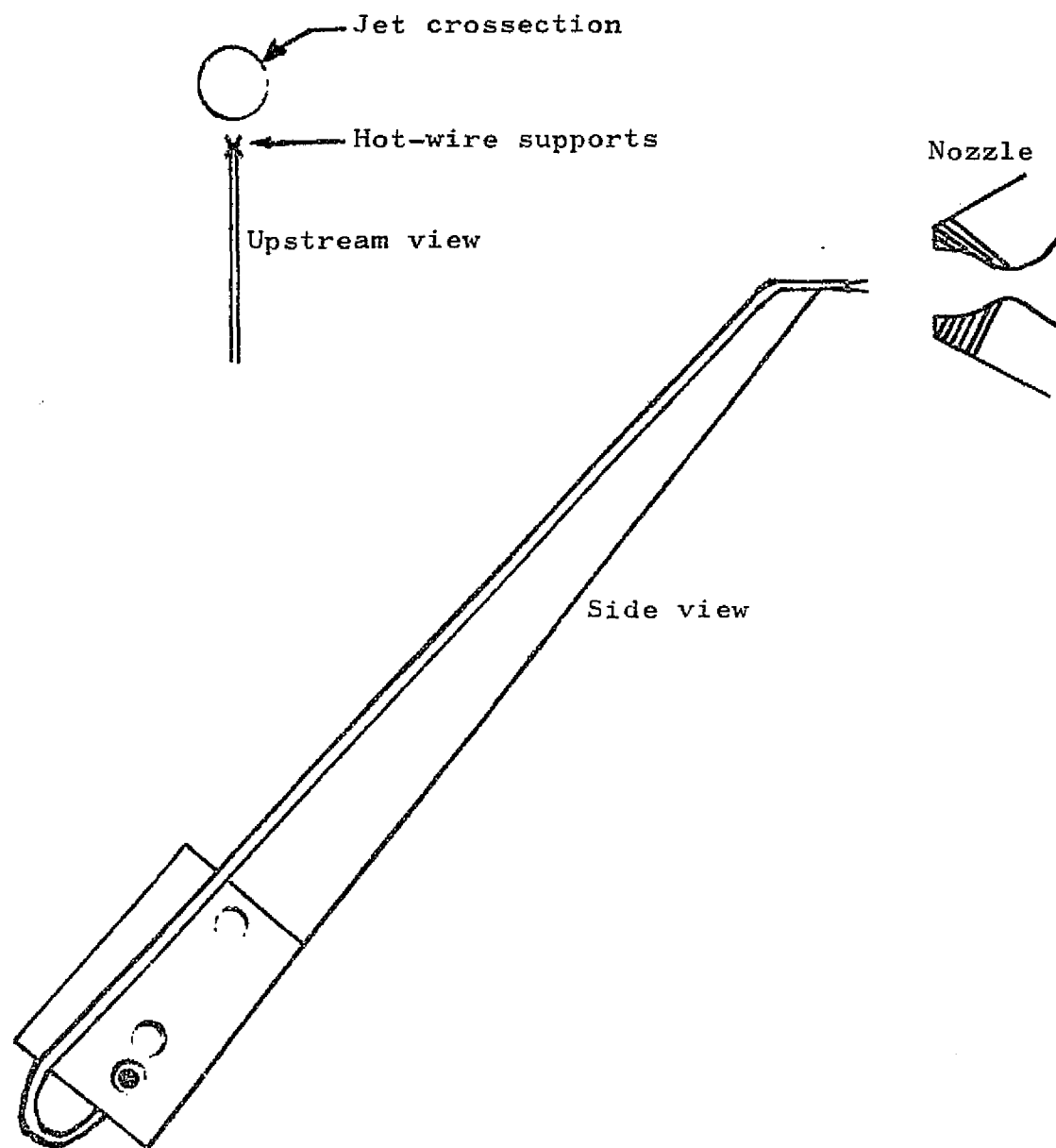
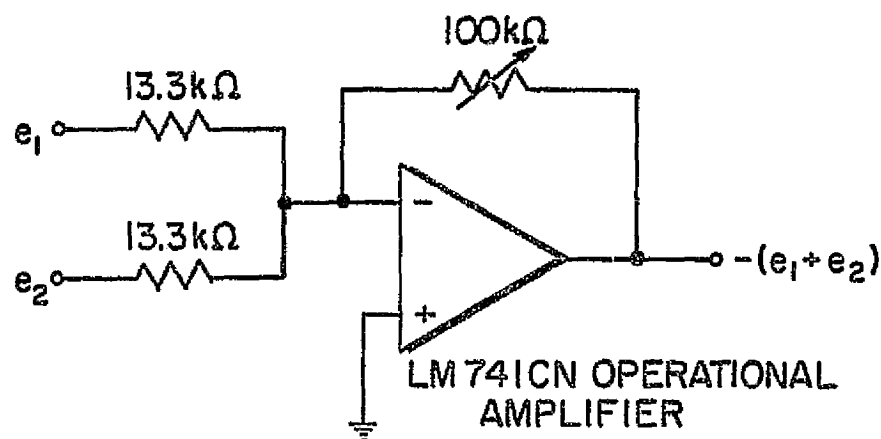
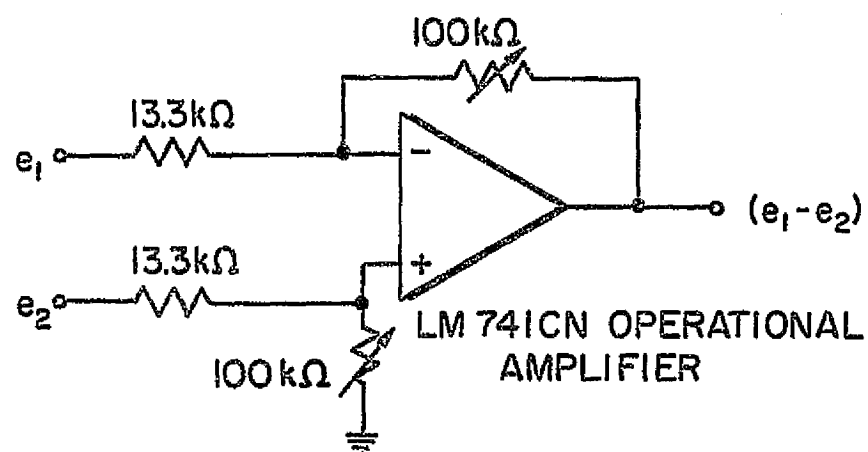


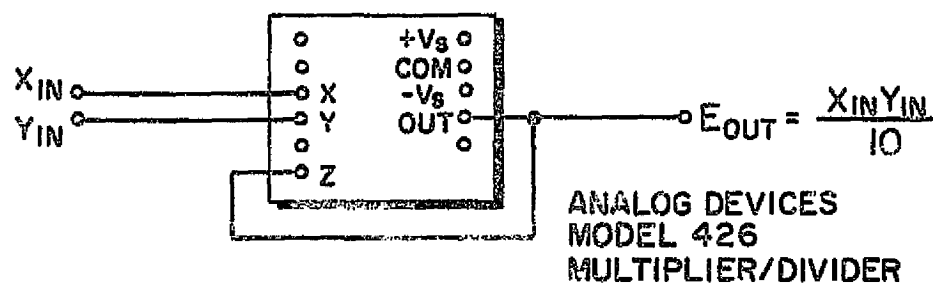
Figure 3. Crossed Hot-Wire Probe, Full Scale



ADDER CIRCUIT



SUBTRACTOR CIRCUIT



MULTIPLIER CIRCUIT

Figure 4. Schematic of Electronic Devices

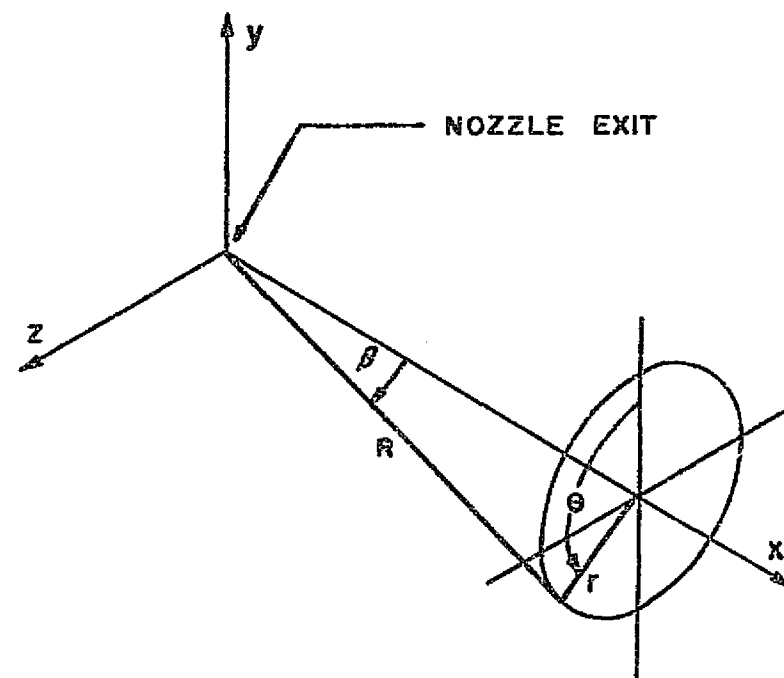
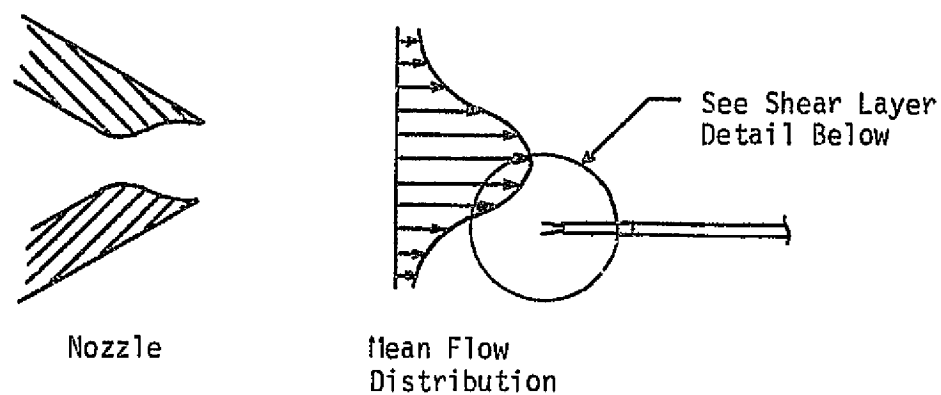


Figure 5. Facility Coordinate System



## Detail

(Probes are shown in relative size to one another)

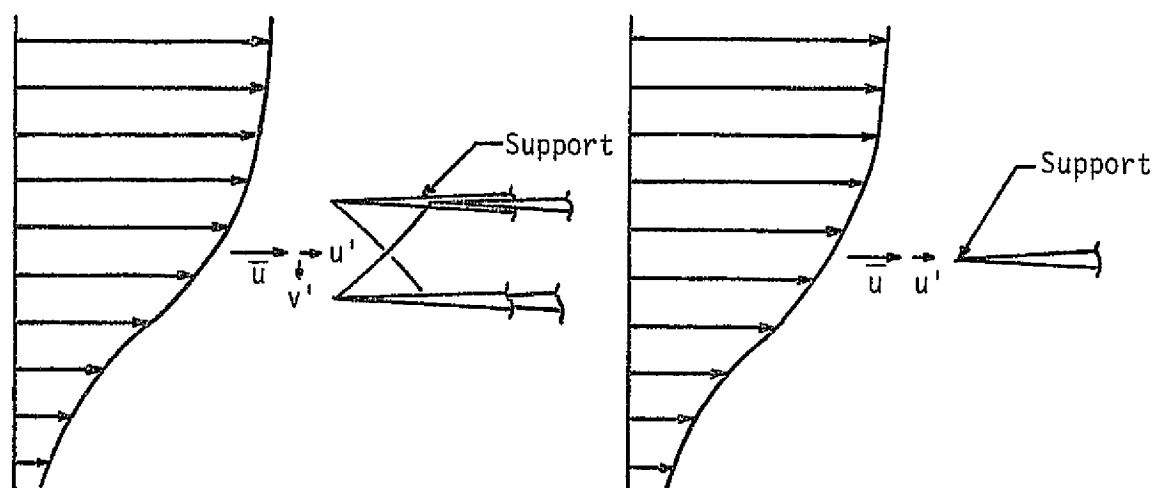


Figure 6. Schematic of Crossed Hot-Wire Probe Orientation

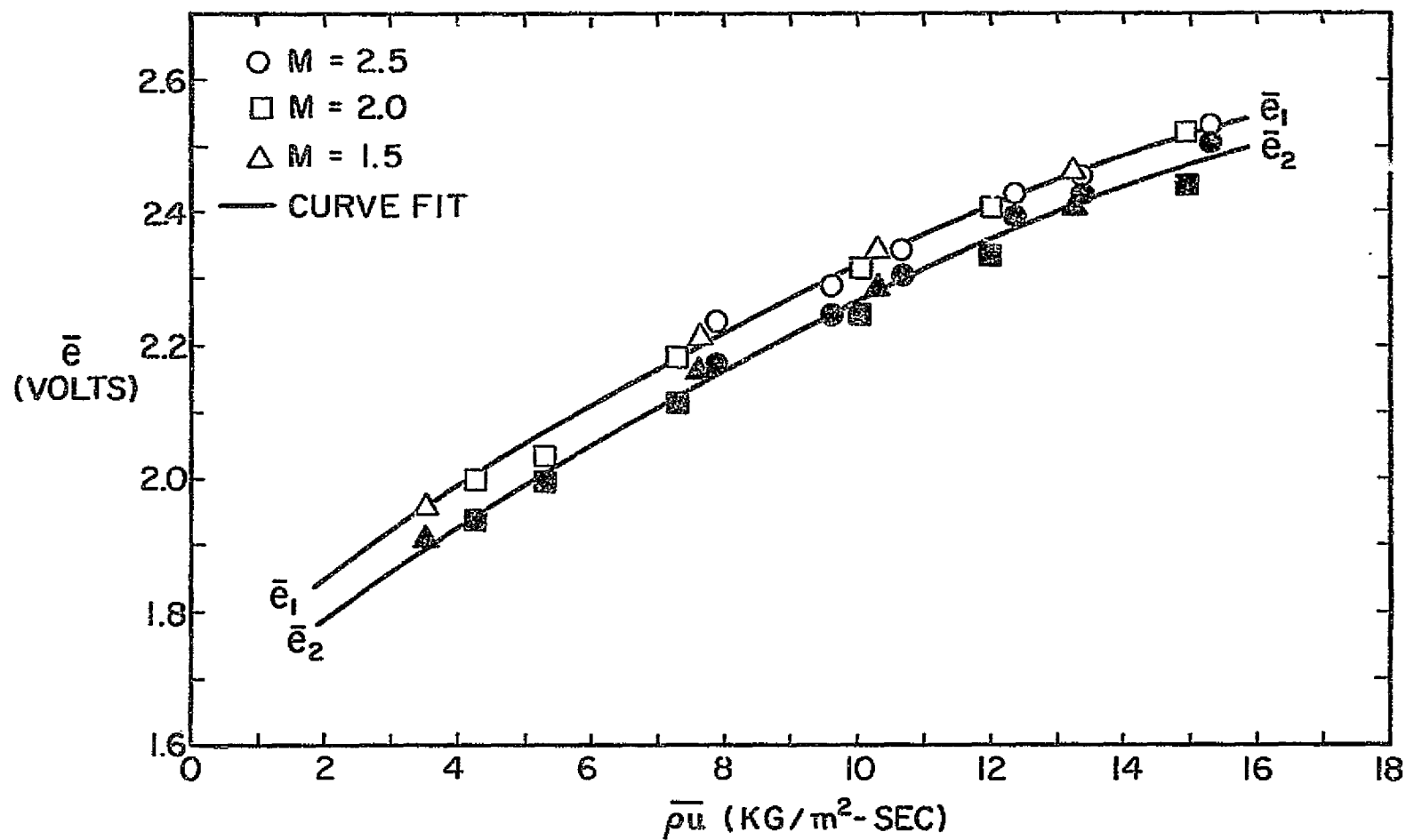


Figure 7. Crossed Hot-Wire Calibration,  $\bar{e}$  as a Function of  $\bar{\rho}u$

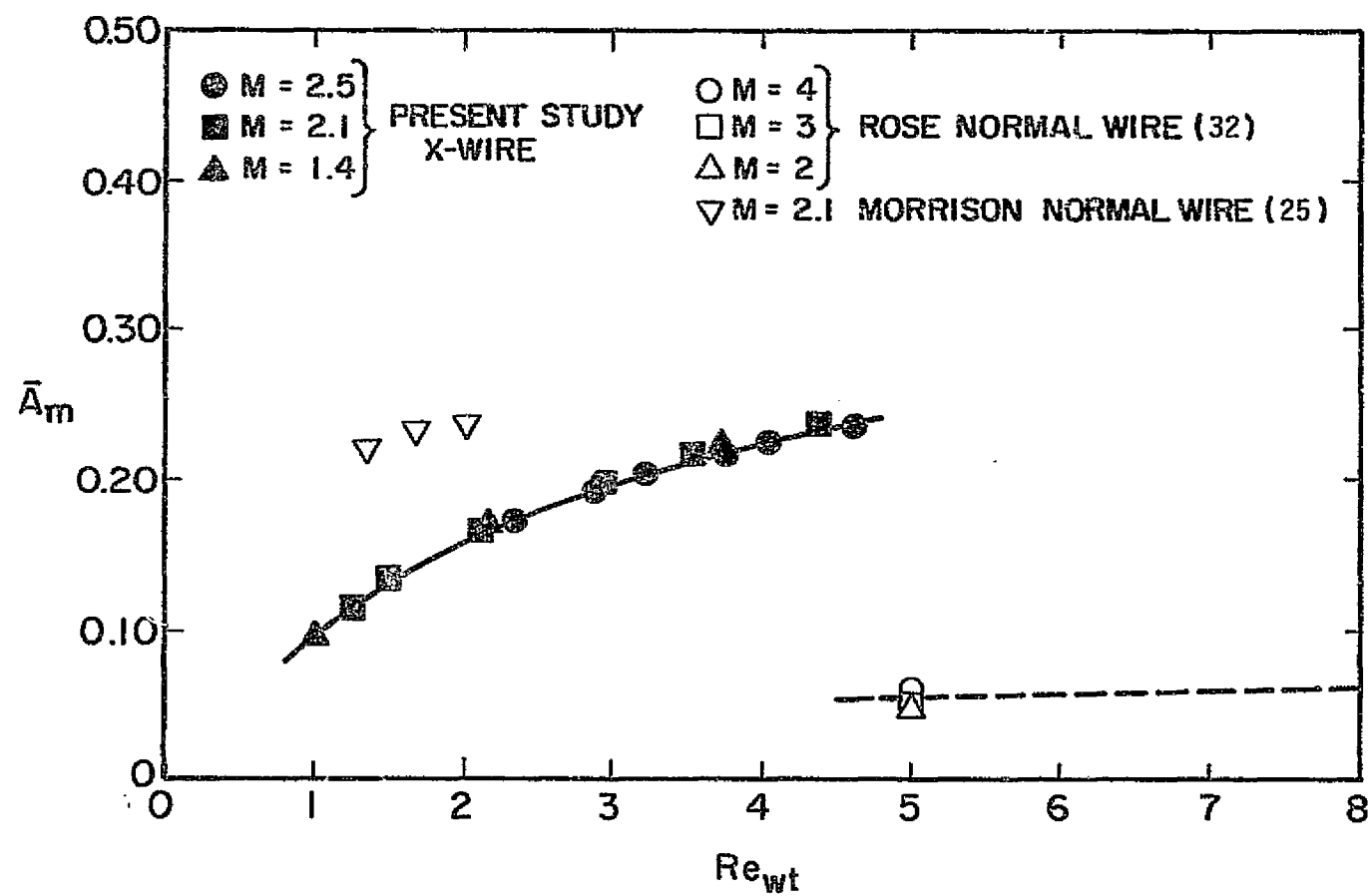


Figure 8. Crossed Hot-Wire Calibration,  $\bar{A}_m$  as a Function of  $Re_{wt}$

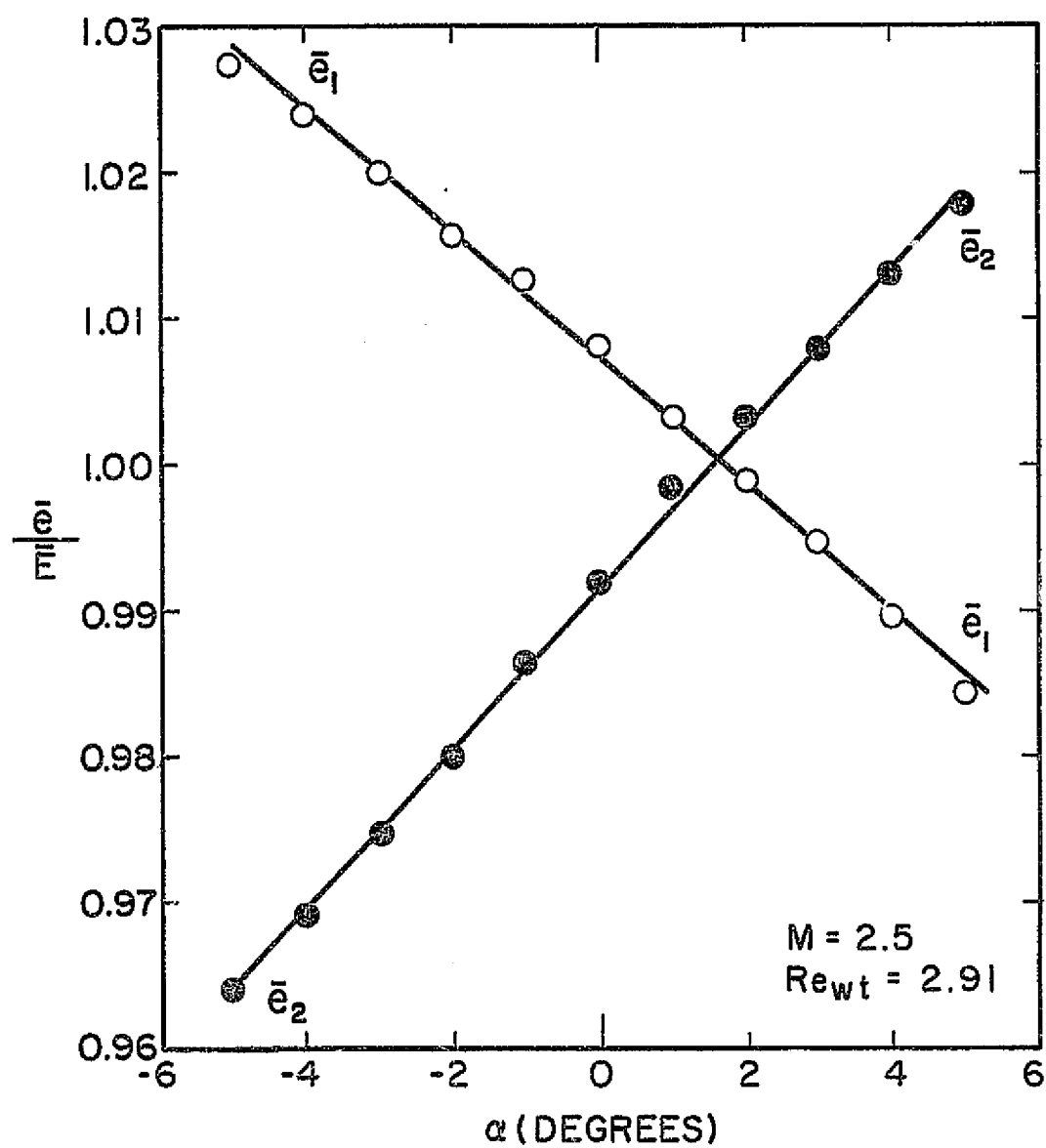


Figure 9. Crossed Hot-Wire Calibration,  $\bar{e}/\bar{E}$  as a Function of  $\alpha$

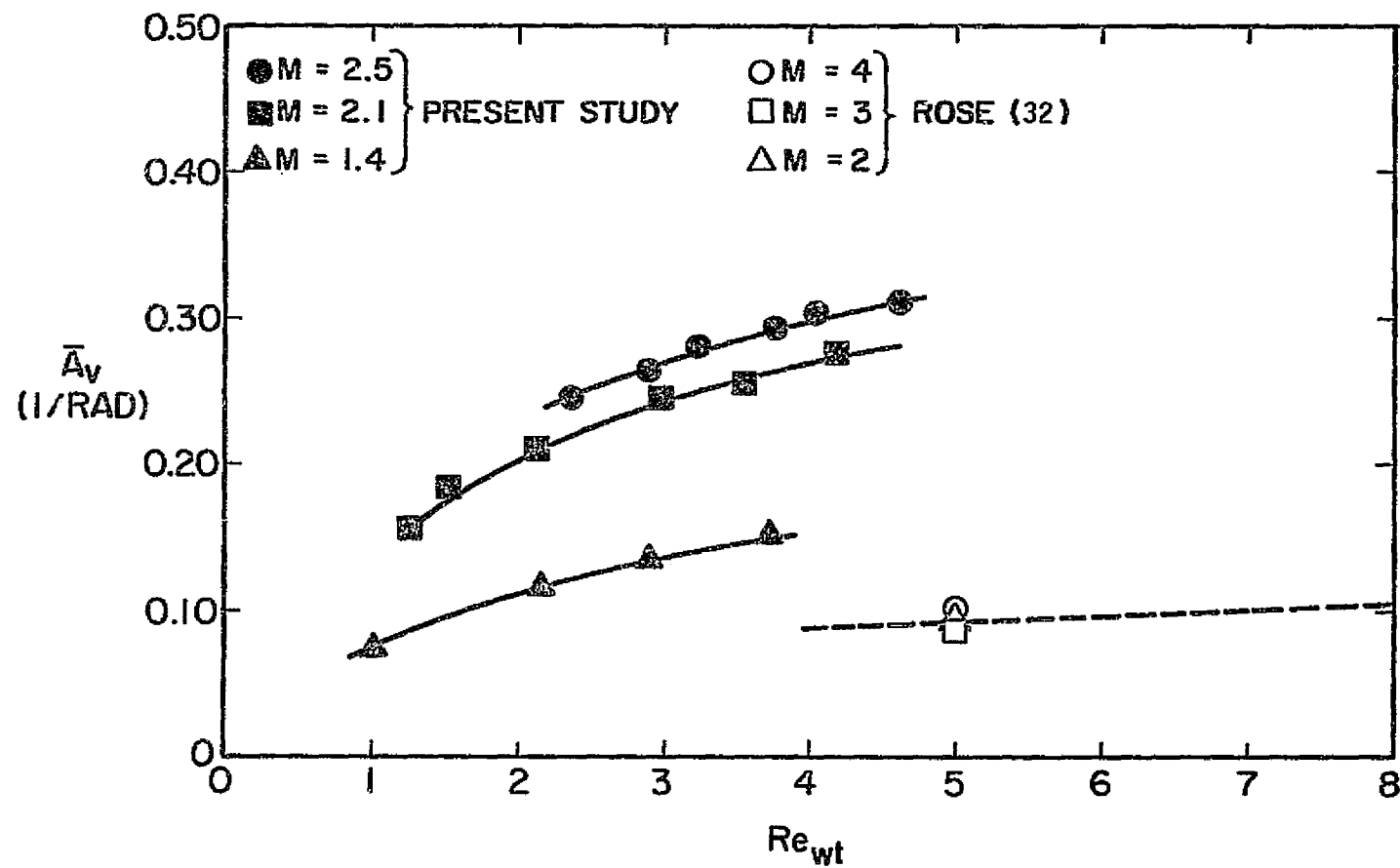


Figure 10. Crossed Hot-Wire Calibration,  $\bar{A}_v$  as a Function of  $Re_{wt}$

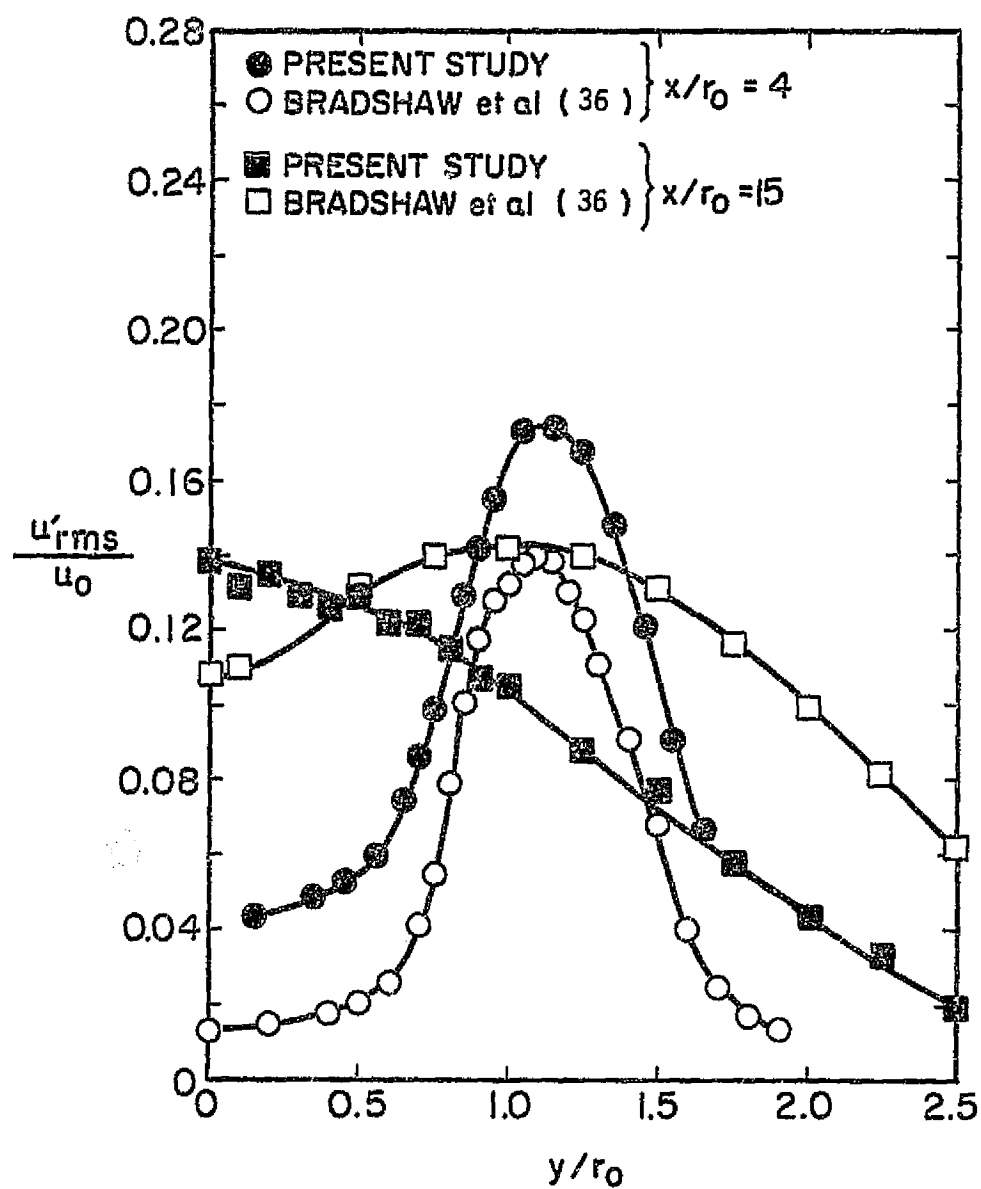


Figure 11. Radial Profiles of Axial Velocity Turbulence Intensity for the Subsonic Jet

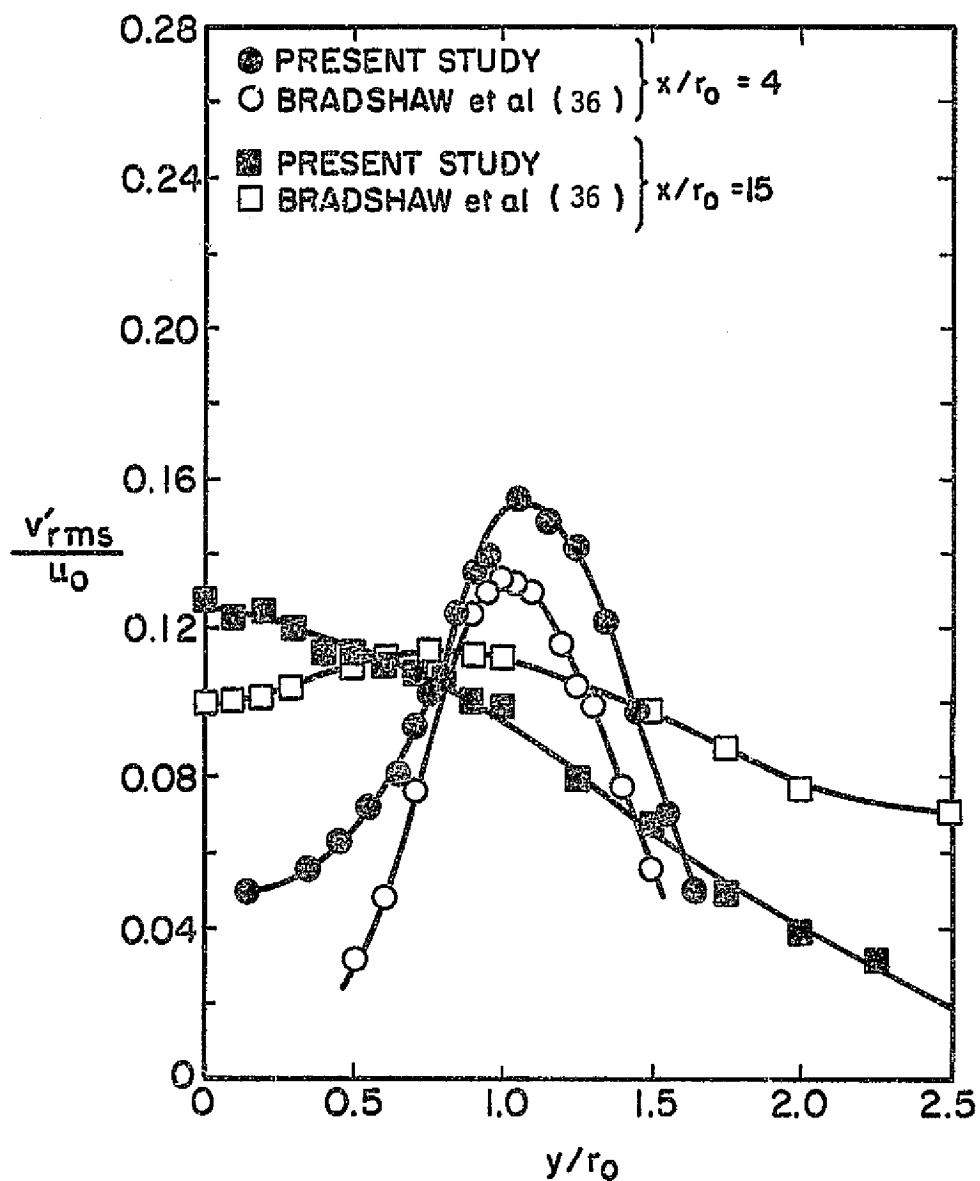


Figure 12. Radial Profiles of Radial Velocity Turbulence Intensity for the Subsonic Jet

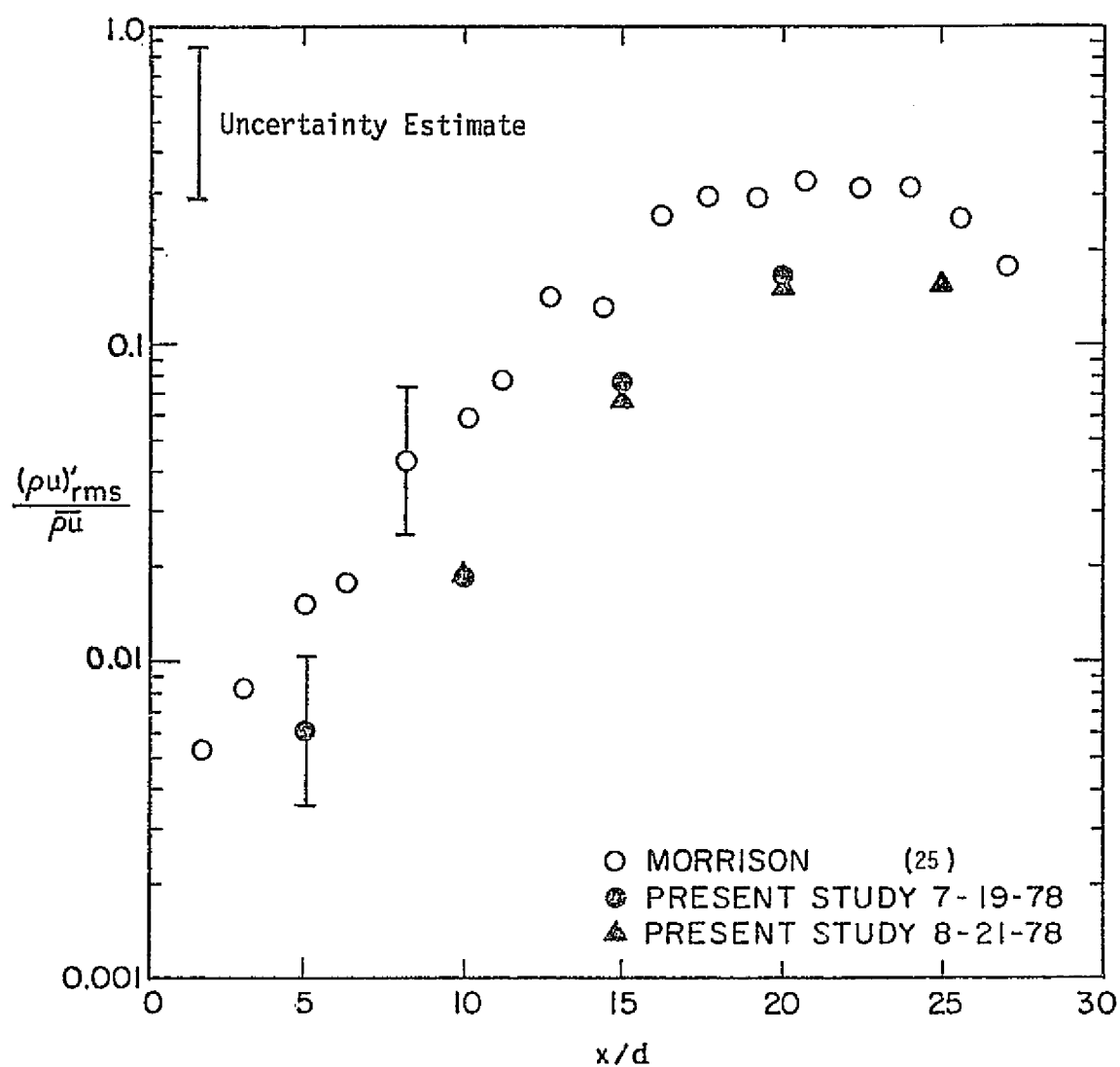


Figure 13. Axial Distribution of Peak Mass Velocity Fluctuations,  $M = 2.5$

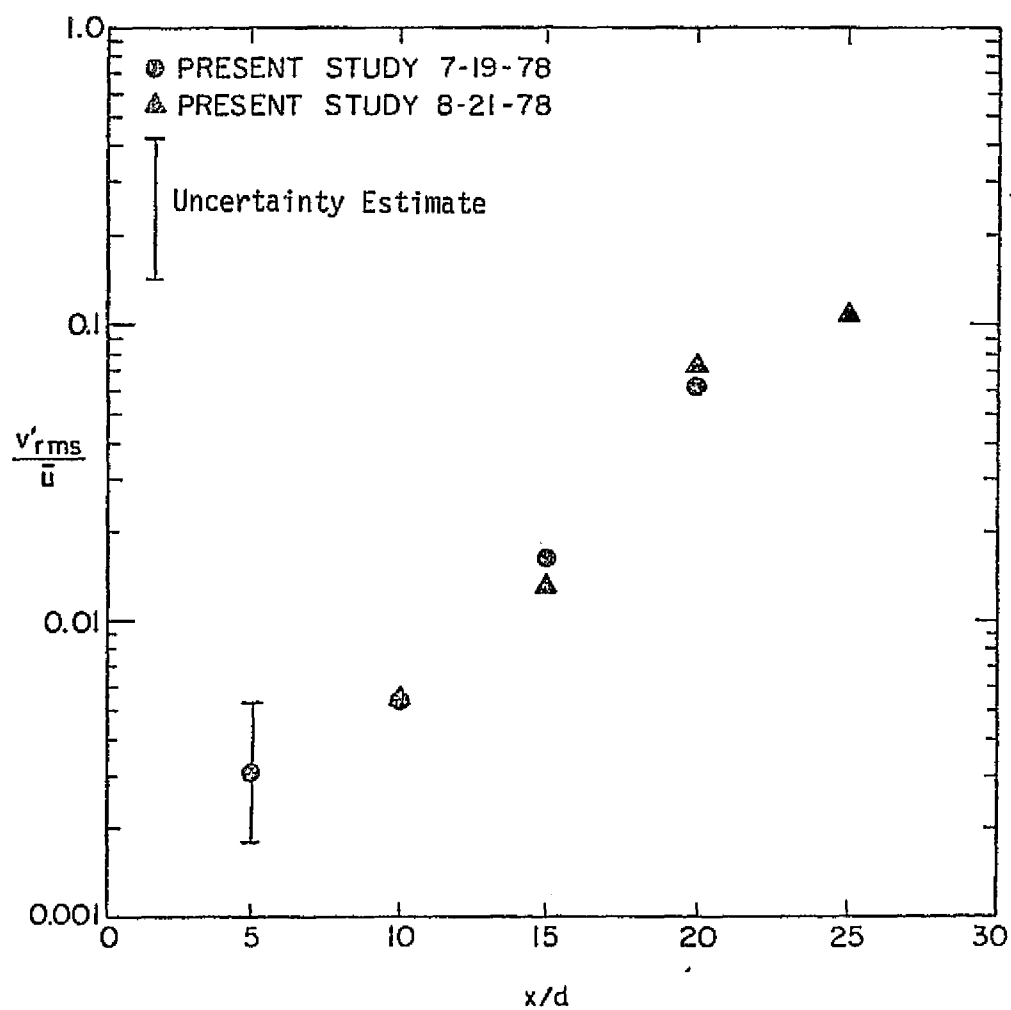


Figure 14. Axial Distribution of Peak Radial Velocity Fluctuations,  $M=2.5$

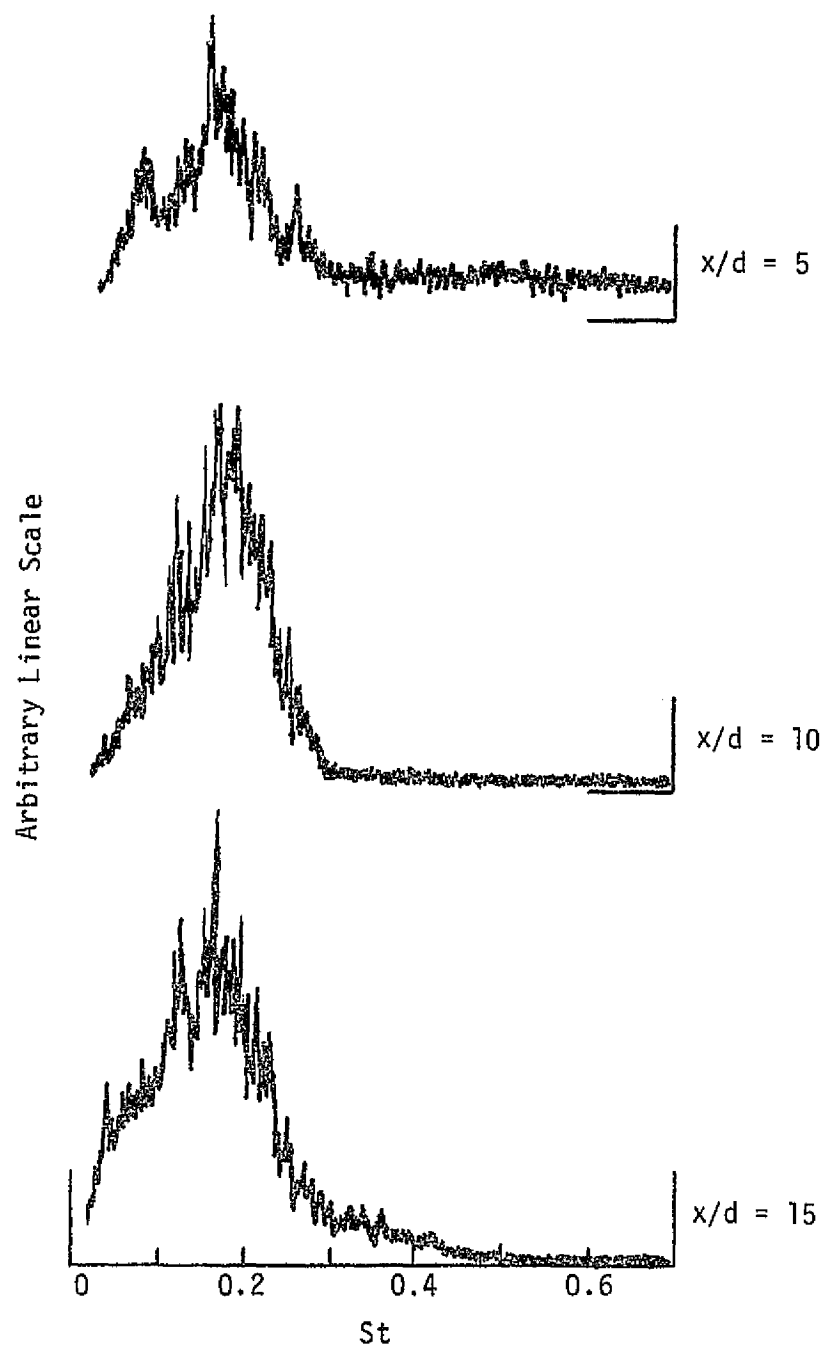


Figure 15. Crossed Hot-Wire Mass Velocity Spectra in the Jet Shear Layer,  $M = 2.5$

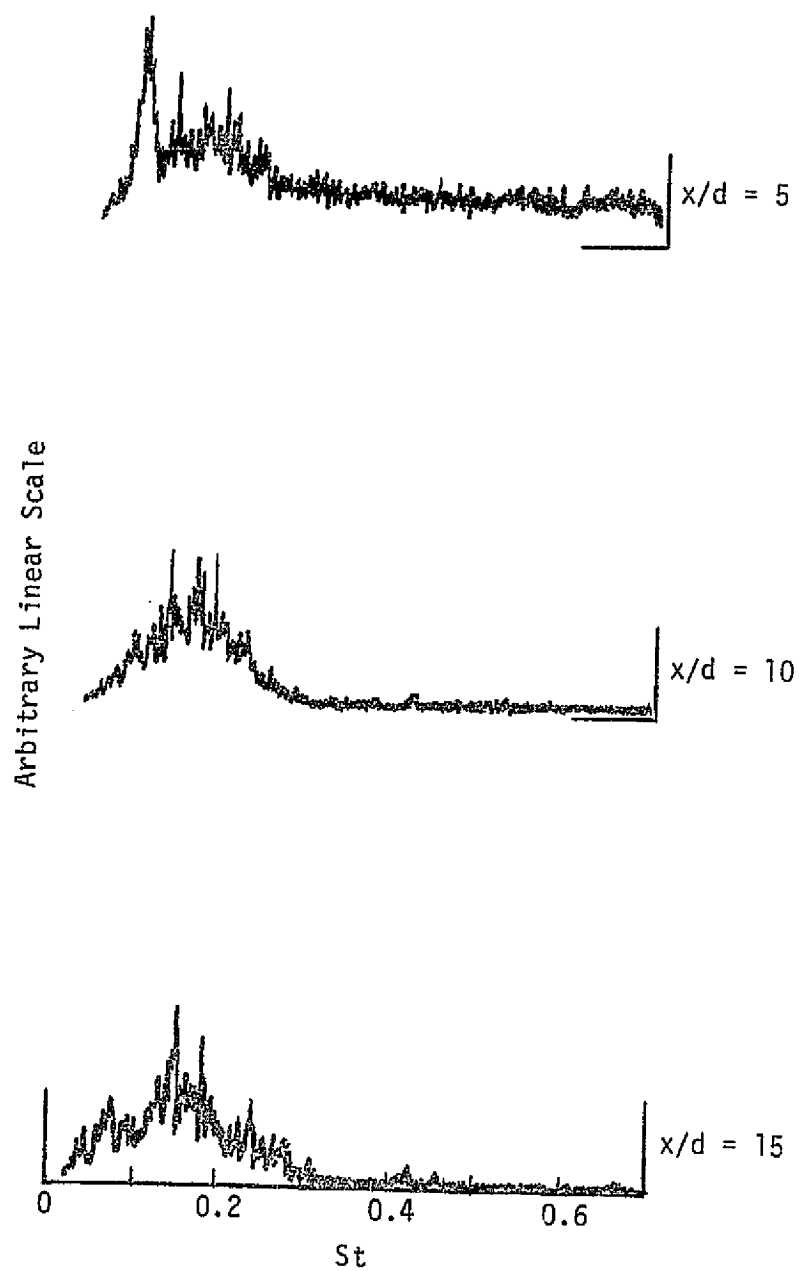


Figure 16. Crossed Hot-Wire Radial Velocity Spectra in the Jet Shear Layer,  $M = 2.5$

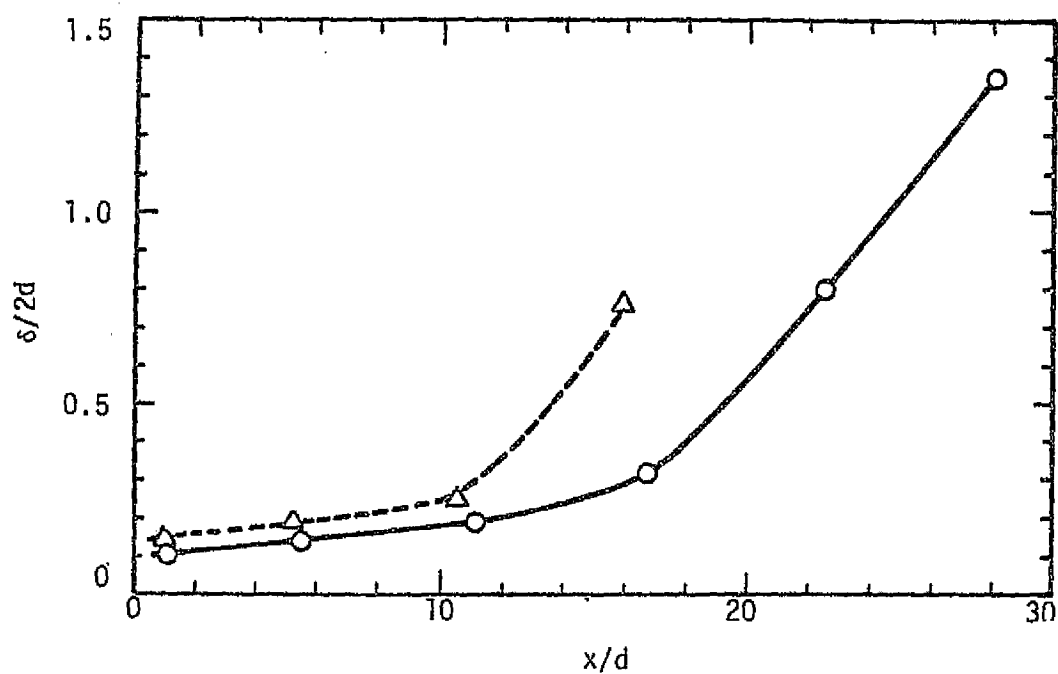
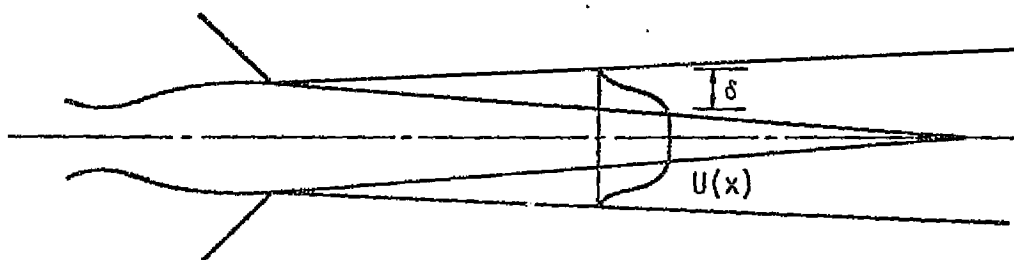


Figure 17. Variation of Shear Layer Half-Thickness Parameter ( $\delta/2d$ ) With Downstream Distance  
 $\Delta M = 2.1$ ,  $OM = 2.5$

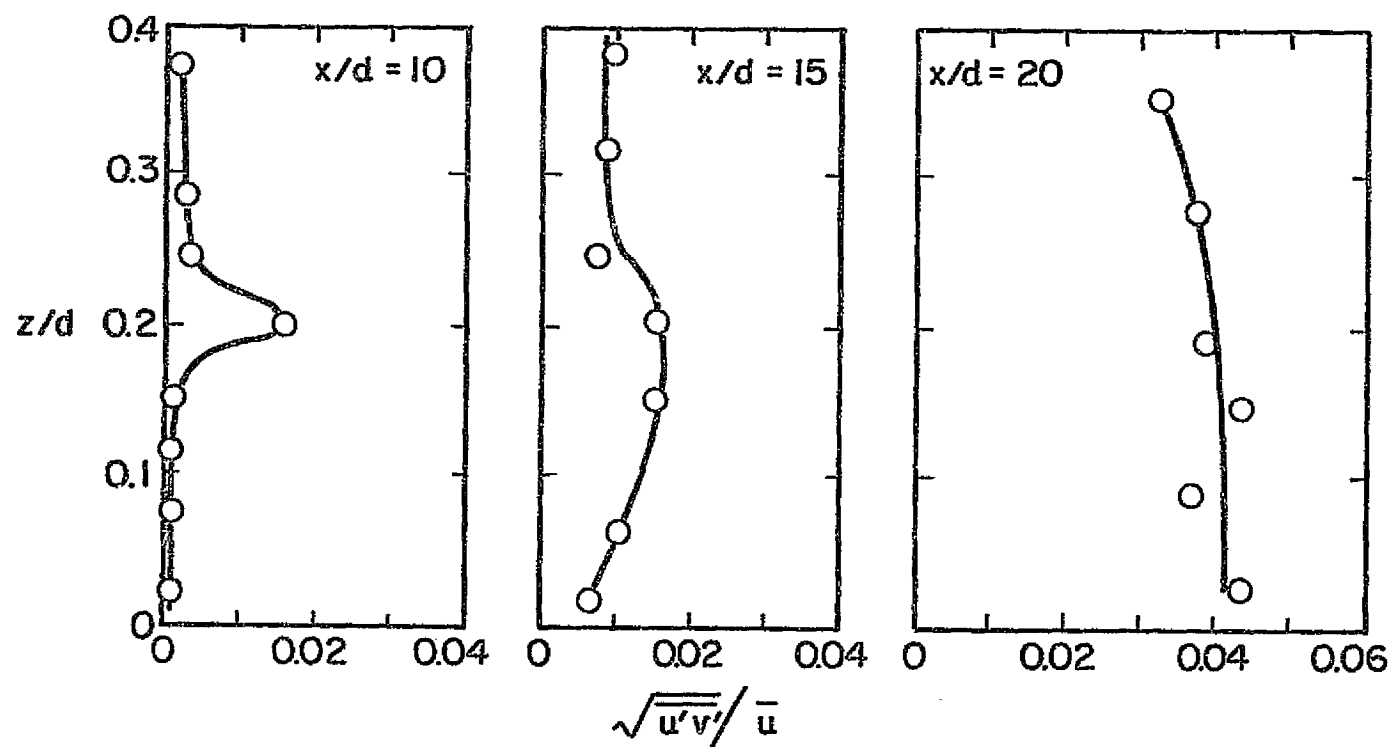


Figure 18. Radial Distributions of Velocity Covariance,  $\sqrt{\overline{u'v'}}/\bar{u}$ ,  $M = 2.5$

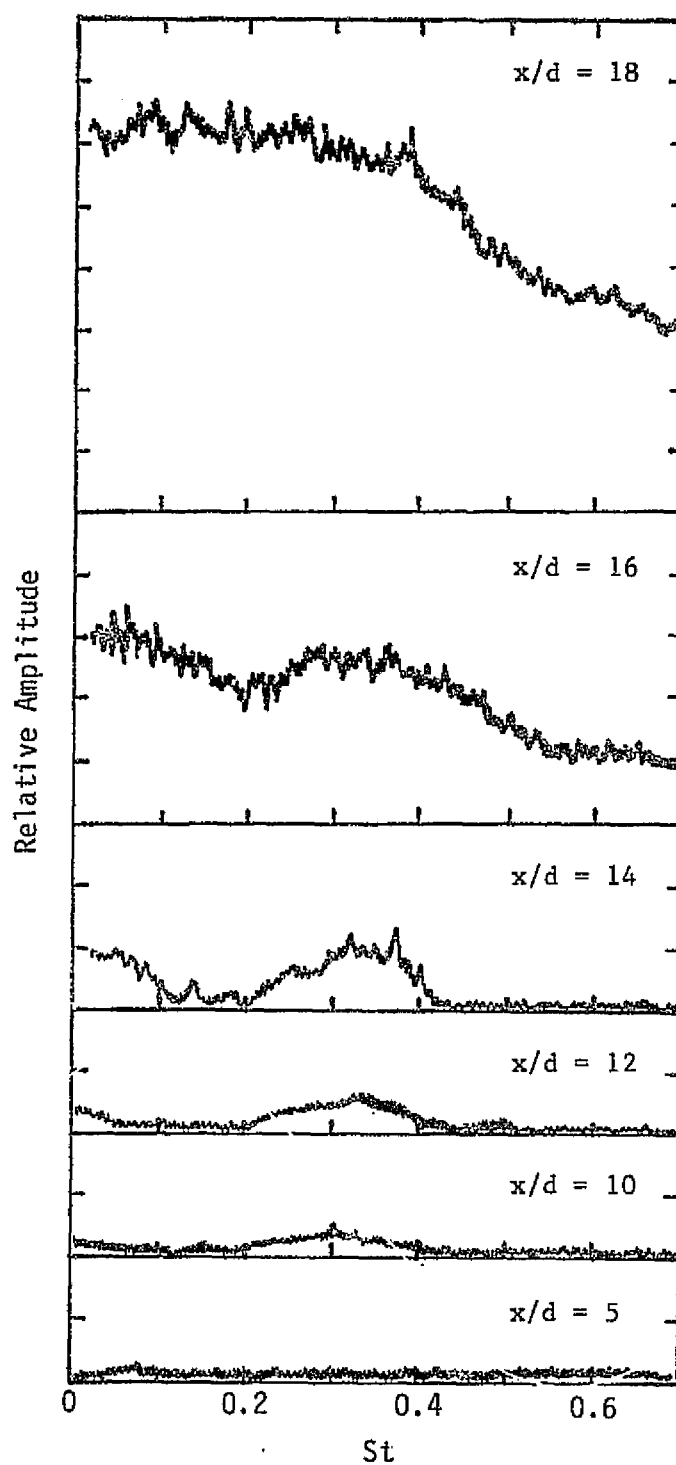


Figure 19. Momentum Transport,  $(\rho u)'v'$ ,  
Spectra in the Jet Shear  
Layer, Unexcited  $M = 2.5$

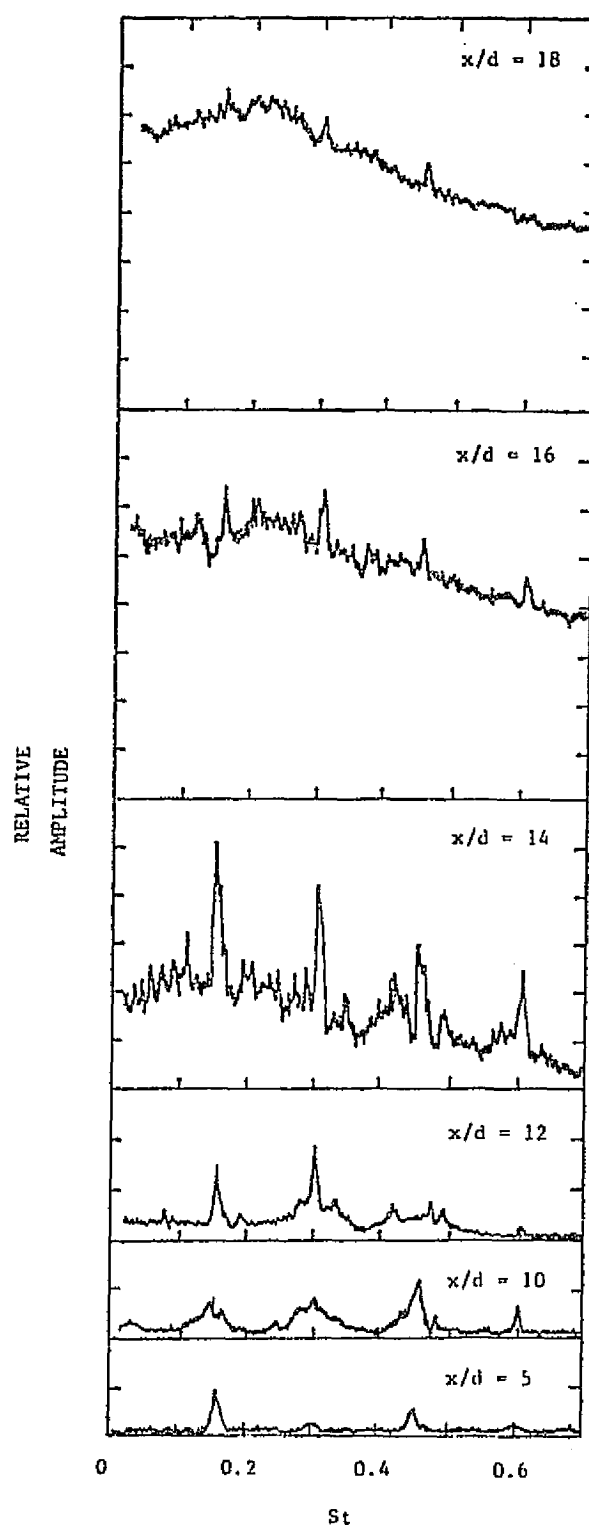


Figure 20. Momentum Transport,  $(\rho u)'v'$ , Spectra in the Jet Shear Layer, Excited  $M = 2.5$

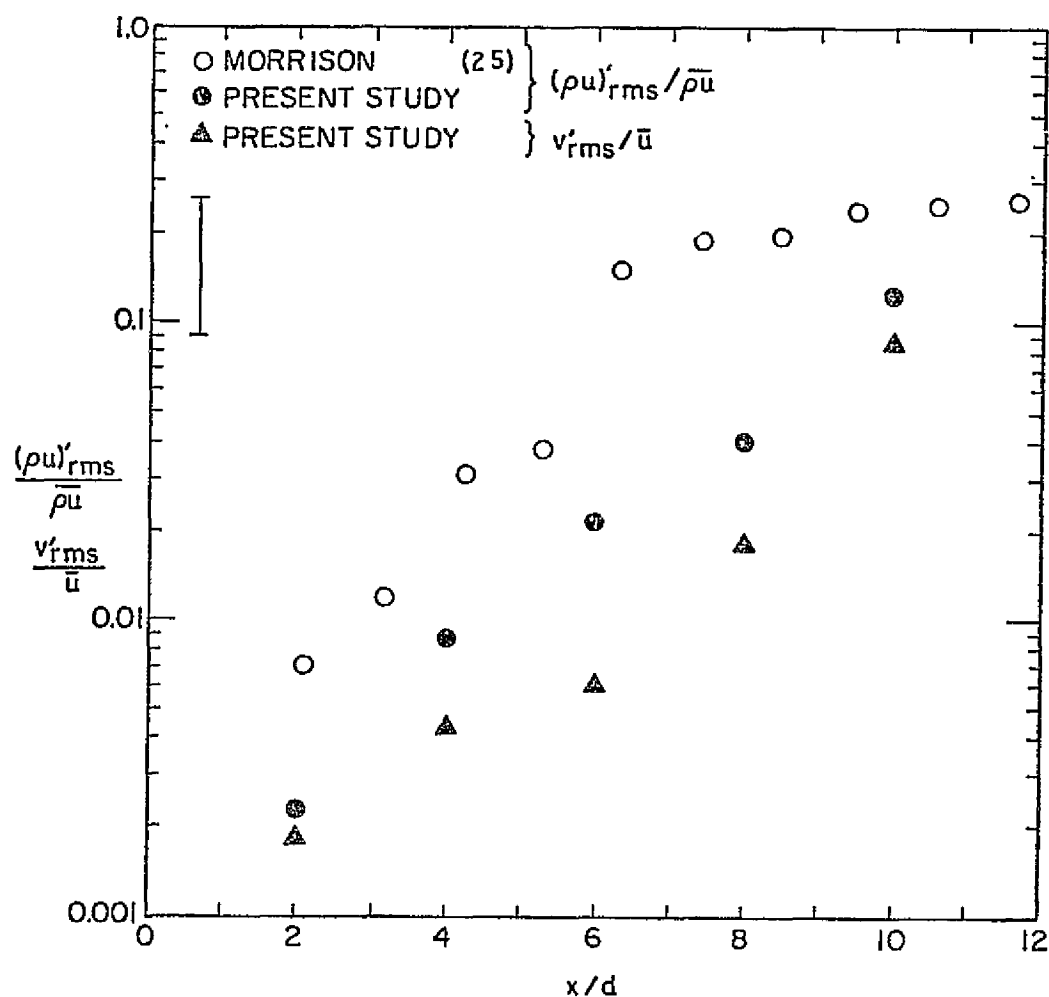


Figure 21. Axial Distributions of Peak Mass Velocity and Peak Radial Velocity Fluctuations,  $M = 2.1$

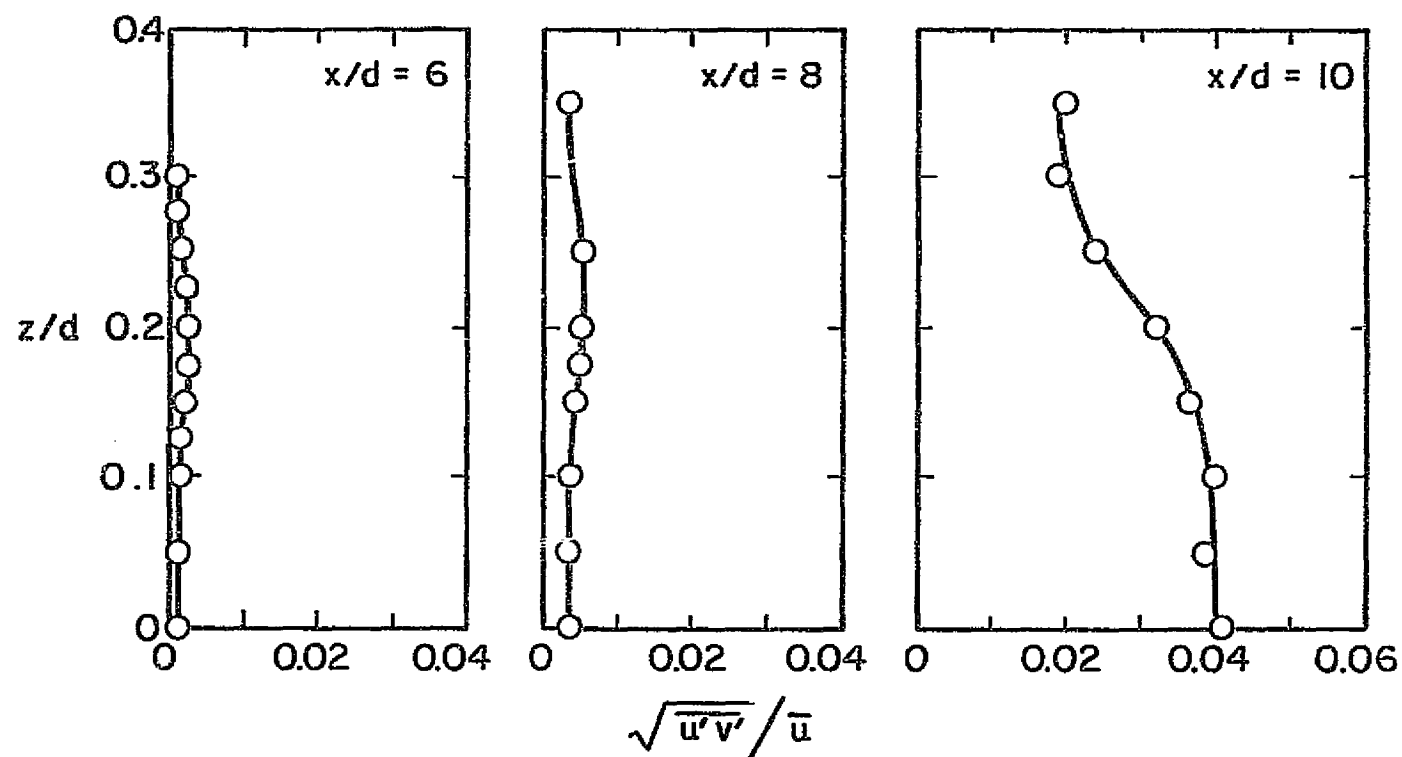


Figure 22. Radial Distributions of Velocity Covariance,  $\sqrt{u'v'}/\bar{u}$ ,  $M = 2.1$

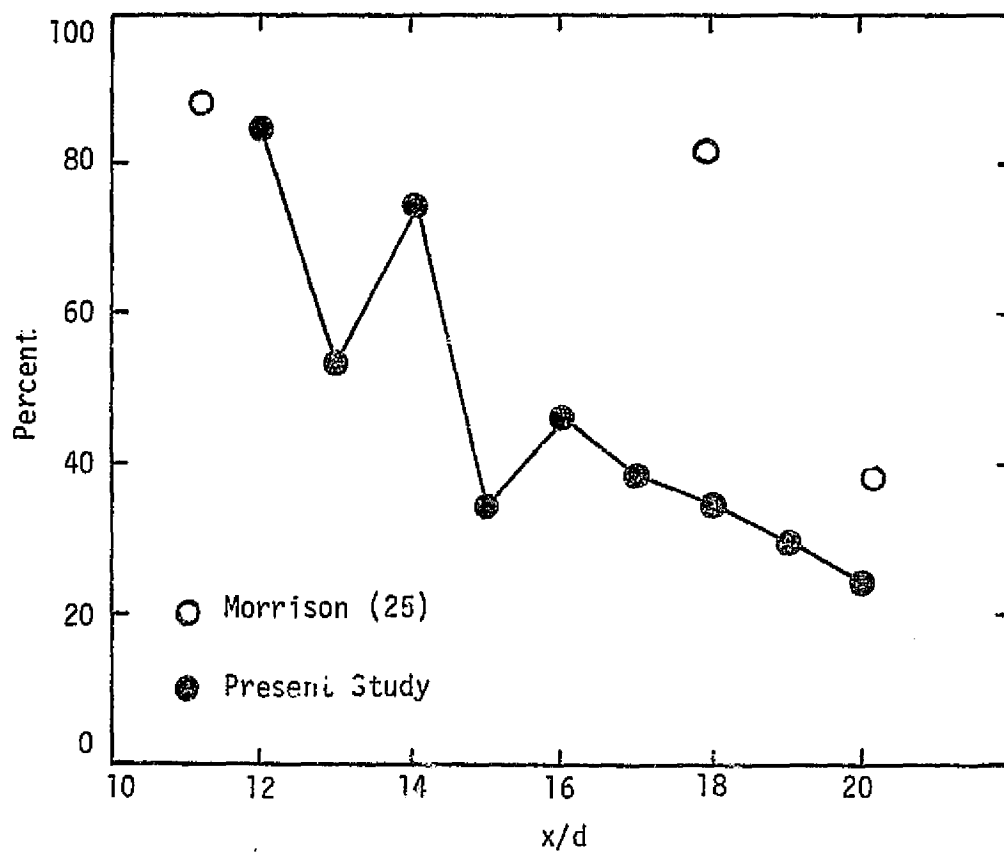


Figure 23. Axial Distribution of Percent Coherent Structure,  $\langle(\rho u)'\rangle_{\text{rms}}/(\rho u)'\text{rms}$ , in the Mass Velocity Fluctuations,  $M = 2.5$

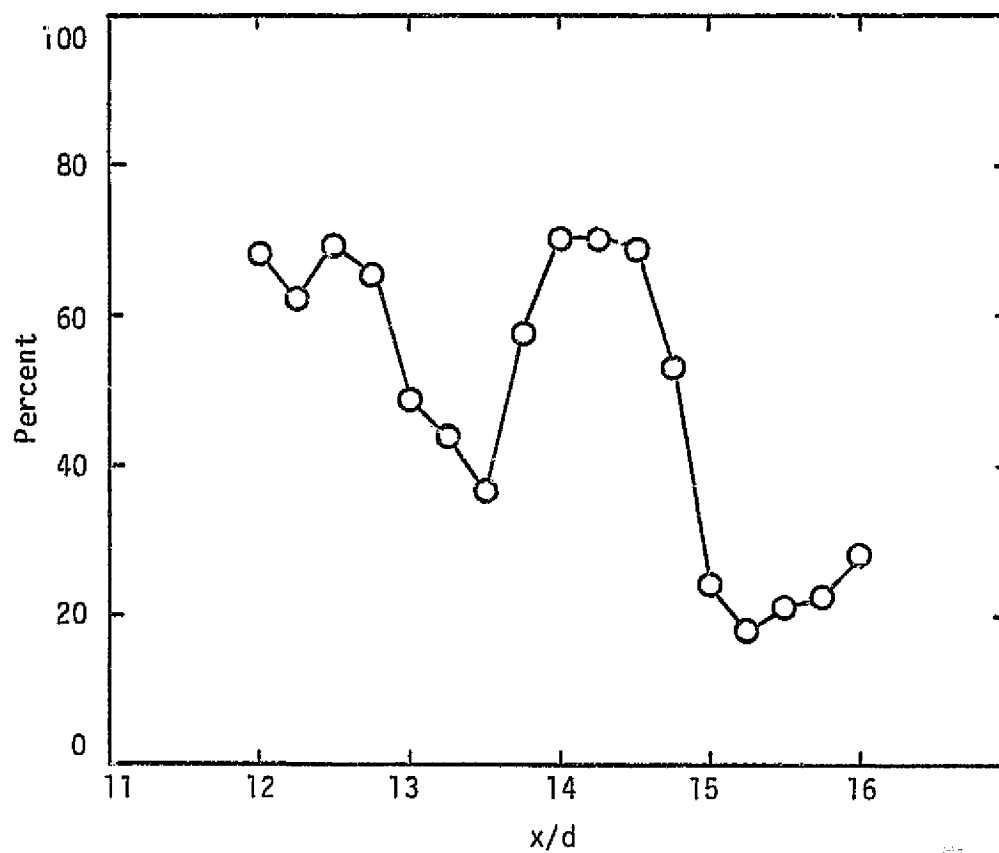


Figure 24. Wavelength Measurement of Axial Coherent Structure Oscillation,  $M = 2.5$

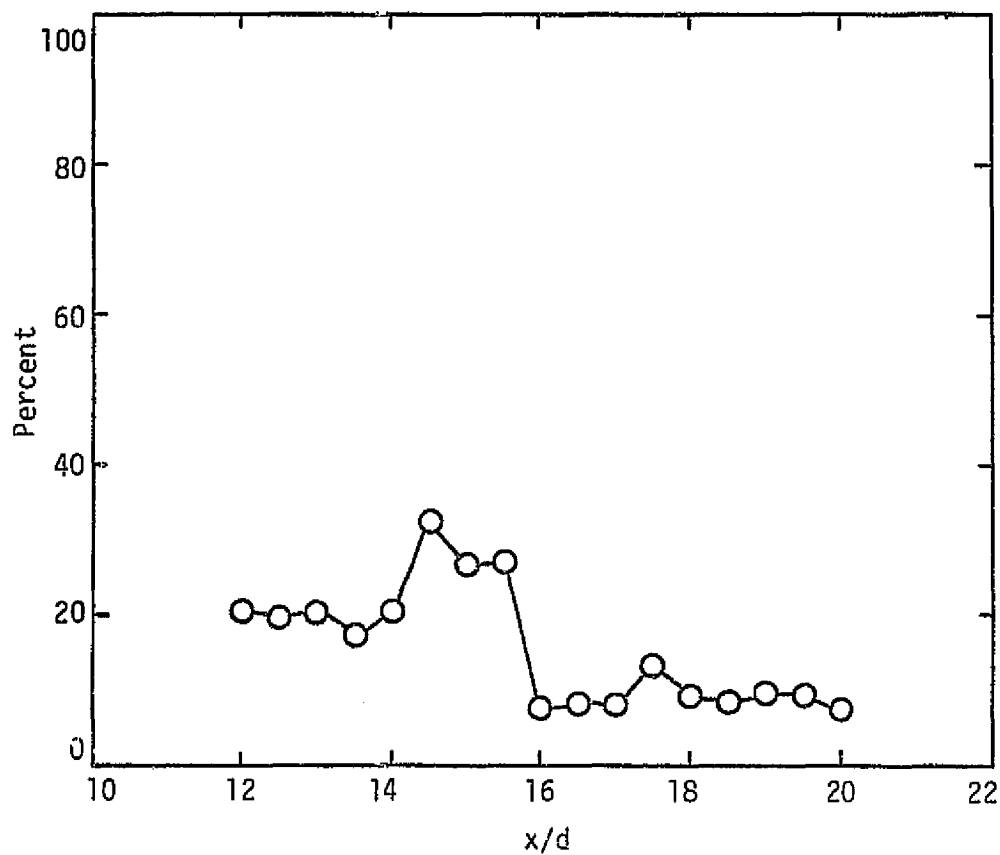


Figure 25. Axial Distribution of Percent Coherent Structure,  $\langle(\rho u)'v'\rangle_{rms}/[(\rho u)'v']_{rms}$ , in the Velocity Covariance,  $M = 2.5$

VITA

Jerry Dale Swearingen

Candidate for the Degree of  
Master of Science

Thesis: **CROSSED HOT-WIRE MEASUREMENTS IN LOW REYNOLDS NUMBER SUPERSONIC  
JETS**

Major Field: Mechanical Engineering

Biographical:

Personal Data:

Education: Graduated from Bishop McGuinness High School in  
Oklahoma City, Oklahoma, in May, 1973; received the Bachelor  
of Science in Mechanical Engineering degree from Oklahoma  
State University, Stillwater, Oklahoma, in December, 1977;  
completed requirements for the Master of Science degree at  
Oklahoma State University in December, 1979.

Honors: American Petroleum Institute Scholarship, Texaco Scholar-  
ship, Continental Oil Company Scholarship, Tau Beta Pi, Pi Tau  
Sigma.

Professional Societies: American Institute of Aeronautics and  
Astronautics, American Society of Mechanical Engineers.